Numéro d'ordre: 016-2010

# UNIVERSITÉ CLAUDE BERNARD (LYON 1)

# HABILITATION À DIRIGER DES RECHERCHES

spécialité : Mathématiques Appliquées

Soutenue publiquement le 3 Juin 2010

par

**Olivier PINAUD**

Titre :

## CONTRIBUTIONS À L'ÉTUDE DE LA PROPAGATION DES ONDES EN MILIEUX ALÉATOIRES ET AU TRANSPORT DANS LES NANOSTRUCTURES

devant le jury composé de

M. Habib Ammari, DR CNRS, ENS Ulm
M. Naoufel Ben Abdallah, Professeur, Université Toulouse III
M. Yves Capdeboscq, Professeur, Université d'Oxford
M. Josselin Garnier, Professeur, Université Paris VII
M. Jérôme Le Rousseau, Professeur, Université d'Orléans
M. Florian Méhats, Professeur, Université Rennes 1
Mme Michelle Schatzman, DR CNRS, Université Lyon 1

après avis favorables de

Habib Ammari
Josselin Garnier
Lenya Ryzhik, Professeur, Université de Stanford

# Remerciements

Mes premiers remerciements iront à mes rapporteurs Habib Ammari, Josselin Garnier et Lenya Ryzhik. C'est un honneur qu'ils aient accepté de porter un jugement sur cette habilitation. Leurs nombreux travaux font référence dans le domaine des problèmes inverses et de la propagation d'ondes dans les milieux aléatoires.

Merci de même à Yves Capdeboscq et Jérôme Le Rousseau, c'est un grand plaisir de les compter parmi les membres du jury.

Pour son soutien, sa confiance, ses conseils précieux et sa présence à la soutenance, je remercie sincèrement Michelle Schatzman.

Un merci tout particulier à Naoufel Ben Abdallah et Florian Méhats pour leur participation au jury mais aussi et surtout pour avoir été de formidables directeurs de thèse, tant par leur caractère humain que leurs qualités scientifiques. Je mesure encore plus aujourd'hui la chance que j'ai eue de débuter dans la recherche dans de si bonnes conditions et je suis ravi de continuer à travailler avec eux.

Je tiens de plus à temoigner mes vives amitié et admiration à Guillaume Bal qui m'a fait découvrir le sujet passionnant des ondes en milieux aléatoires. Il est une source d'inspiration inépuisable et cette habilitation lui doit beaucoup. J'ai appris énormément et apprends continuellement à son contact, c'est une grande chance de collaborer avec lui, je lui en suis très reconnaissant.

De peur d'oublier des noms et de m'attirer des ennuis, je me contenterai de saluer tous mes très appréciés collègues de l'ICJ, appliqués ou non, anciens ou nouveaux, ce fut une joie de passer ces quatre dernières années avec eux dans cette belle ville de Lyon (et d'y faire la tournée des restaus avec certains qui se reconnaîtront).

Merci à ma famille et mes amis pour leur soutien.

Last, but not least bien sûr, Brookie, let's kick it!

# Contents

# Introduction

Ce mémoire d'habilitation regroupe les différents travaux effectués depuis la thèse. Il s'articule autour de deux grandes thématiques, la propagation d'ondes en milieux aléatoires et le transport quantique dans les nanostructures. Il est remarquable que ces domaines, en apparence très éloignés et dont les phénomènes physiques sous-jacents se manifestent à des échelles foncièrement différentes, présentent néanmoins de nombreuses similarités. L'équation fondamentale de la mécanique quantique, l'équation de Schrödinger, décrit aussi bien la dynamique d'un électron dans un semi-conducteur que l'amplitude d'une onde électromagnétique collimatée se propageant dans un milieu d'indice de réfraction donné. La justification d'une telle relation procède de la dualité onde-corpuscule de la physique quantique, un électron est aussi bien une onde qu'une particule, tout dépend de comment et à quelle échelle il est observé. La réciproque est aussi vraie concernant les ondes : dans certains régimes, notamment ceux hautes fréquences considérés dans ce document, l'énergie portée par une onde acoustique dans un milieu aléatoire peut être décrite par une équation de la mécanique classique couramment utilisée en dynamique des gaz par exemple, l'équation de Boltzmann. Un des fils conducteurs de cette habilitation est donc l'équation de Schrödinger que l'on retrouvera sous diverses formes, au chapitre deux dans le contexte des ondes en régime paraxial, aux chapitres quatre et cinq dans le cadre des semiconducteurs, voire même au chapitre trois si identifiée à l'équation de Helmholtz. Un autre est la constante recherche de modèles "macroscopiques" à partir d'une description "microscopique" du problème physique. Dans bien des cas, la dynamique microscopique est trop riche pour offrir des modèles dont le coût de résolution numérique serait abordable. On cherche donc à construire des modèles approchés, décrivant un nombre d'inconnues réduit, capturant au mieux les caractéristiques dominantes des phénomènes microscopiques. La principale technique utilisée pour cela dans le mémoire est l'analyse haute-fréquence, en particulier dans les chapitres un et deux de la première partie où l'on construit des modèles de transport à partir de modèles ondulatoires. Dans le chapitre quatre de la deuxième partie, on obtient des estimations uniformes pour cette étude asymptotique. Les travaux présentés dans le chapitre cinq concernent aussi ce passage micro-macro mais sous un aspect différent.

Plus précisément, dans la première partie :

– On s'intéresse dans le chapitre un à la reconstruction d'inclusions dissimulées dans un milieu complexe dont les caractéristiques microscopiques sont inconnues. On dispose pour cela d'une source émettant une onde acoustique en direction du milieu à sonder, et d'un détecteur où sont effectuées des mesures. Le milieu n'étant pas connu en détails, des hypothèses sur sa structure sont nécessaires : on suppose que l'on peut distinguer y une composante à variations lentes, considérée comme connue, d'une autre à variations rapides mais de faible amplitude. La partie rapide est modélisée par un *milieu aléatoire* dont certaines caractéristiques macroscopiques sont connues ou à déterminer. On suppose de plus que l'onde est dans le régime des hautes fréquences et que les variations de la composante rapide du milieu se font à l'échelle de la longueur d'onde. Dans ce cadre, la dynamique microscopique est caractérisée par l'équation des ondes suivante : pour $\mathbf{x} \in \mathbb{R}^d$,

$$\frac{\partial^2 p^\varepsilon}{\partial t^2} = c_\varepsilon^2 \Delta p^\varepsilon, \qquad p^\varepsilon(t=0,\mathbf{x}) = p_0\left(\frac{\mathbf{x}}{\varepsilon}\right), \qquad \frac{\partial p^\varepsilon}{\partial t}(t=0,\mathbf{x}) = p_1\left(\frac{\mathbf{x}}{\varepsilon}\right),$$

où la vitesse est donnée par $c_\varepsilon(\mathbf{x}) = (\rho_0 \kappa^\varepsilon(\mathbf{x}))^{-1/2}$, pour une densité constante $\rho_0$ et une compressibilité $\kappa^\varepsilon(\mathbf{x})$ de la forme

$$\kappa^\varepsilon(\mathbf{x}) = \kappa_0(\mathbf{x}) + \sqrt{\varepsilon}\kappa_1\left(\frac{\mathbf{x}}{\varepsilon}\right),$$

$\kappa_1$ étant un processus stationnaire homogène de moyenne nulle. On substitue alors le problème inverse de localisation basé sur une description microscopique par un problème inverse résolu à l'aide de modèles macroscopiques reposant sur l'équation de transfert radiatif, ou équation de Boltzmann linéaire. Ces modèles sont obtenus formellement par une asymptotique haute-fréquence de l'équation des ondes et décrivent aussi bien l'énergie de l'onde que la corrélation du champ acoustique en présence d'inclusions et du champ en absence d'inclusions, la distinction se faisant au niveau des conditions au limites à imposer sur l'inclusion. Nous analysons en détails ces modèles et montrons leur capacité à reconstruire un objet avec précision. Nous discutons également de l'intérêt d'utiliser le retournement temporel pour de tels problèmes. Ce chapitre est un résumé des articles [2, 7, 9, 10], travaux en collaboration avec G. Bal.

– Dans le chapitre deux, on effectue une analyse précise de la convergence vers les modèles macroscopiques dans le cadre de l'approximation paraxiale. Dans ce contexte, l'amplitude de l'onde est décrite par une équation de Schrödinger aléatoire de la forme

$$\left(i\eta\frac{\partial}{\partial t} + \frac{\eta^2}{2}\Delta_{\mathbf{x}} + \sqrt{\eta}V\left(\frac{\mathbf{x}}{\eta}, t\right)\right)\psi_\eta(t,\mathbf{x}) = 0, \quad t > 0, \quad \mathbf{x} \in \mathbb{R}^d.$$

On considère deux régimes : dans le premier, les variations du potentiel aléatoire $V$ par rapport à $t$ sont très rapides, et l'on peut alors le remplacer formellement par un bruit blanc suivant la variable $t$ pour obtenir l'équation d'*Itô-Schrödinger*. Dans le second, les variations par rapport au temps sont supposées être suffisamment lentes pour pouvoir considérer le potentiel comme indépendant du temps. L'outil utilisé pour l'étude asymptotique est la *transformée de Wigner*, notée $W_\eta$, qui peut être interprétée comme une densité d'énergie dans l'espace des phases. Sous certaines hypothèses, il est bien connu que l'espérance de la transformée de Wigner $\mathbb{E}\{W_\eta\}$ converge faiblement vers la solution de l'équation de transfert radiatif. Nous nous intéressons ici à la question de la *stabilité statistique*, c'est-à-dire l'étude de la convergence de la variable aléatoire $W_\eta$ et de la différence à la limite entre $W_\eta$ et sa moyenne $\mathbb{E}\{W_\eta\}$. La stabilité statistique est une propriété fondamentale quant à l'utilisation des modèles macroscopiques du chapitre précédent et leur limitation majeure. Nous utilisons pour l'étude la covariance de $W_\eta$, appelée aussi fonction de scintillation, qui vérifie un système fermé d'équations dans le régime d'Itô-Schrödinger et un système approché dans le cas indépendant du temps. Le système est décrit par une équation de transport à coefficients fortement oscillants dont une analyse fine permet d'obtenir le taux de convergence optimal en fonction de certains paramètres du problème, comme la dimension du domaine sur lequel les mesures sont effectuées ou la régularité des conditions initiales. Dans le régime d'Itô-Schrödinger, nous caractérisons de plus la propagation des instabilités en obtenant une équation de transport pour le correcteur d'ordre un de la scintillation. Ce chapitre est un résumé des articles [3, 6], travaux en collaboration avec G. Bal, et de [5], en collaboration avec G. Bal et I. Langmore.

– Le chapitre trois traite du problème classique de la reconstruction de défauts (de conductivité pour l'équation de Laplace ou d'indice pour l'équation de Helmholtz) à partir de mesures au bord. Pour le problème de conductivité (ou de diffusion), on a par exemple :

$$\begin{cases} \nabla \cdot D^\varepsilon \nabla u^\varepsilon = 0, & \text{dans } \Omega, \\ D^\varepsilon \dfrac{\partial u^\varepsilon}{\partial \mathbf{n}} = g, & \text{sur } \partial\Omega, \qquad \displaystyle\int_{\partial\Omega} u^\varepsilon d\sigma = 0, \end{cases}$$

où $\Omega$ est un domaine borné de dimension $d$ quelconque, $\varepsilon$ est le rapport des dimensions caractéristiques du défaut et du domaine, $g$ est une donnée et $D^\varepsilon$ le coefficient de conductivité perturbé localement par une ou plusieurs inclusions. On l'écrit sous la forme $D^\varepsilon(\mathbf{x}) = D_0(\mathbf{x}) + D_1(\frac{\mathbf{x}-\mathbf{x}_0}{\varepsilon})$, où $D_0$ est le coefficient non perturbé et $D_1$ correspond au défaut localisé autour de $\mathbf{x}_0$. Dans les travaux références [21, 45] (la liste est loin d'être exhaustive), un

développement asymptotique de la solution $u^\varepsilon$ en fonction de $\varepsilon$ sur $\partial\Omega$ est proposé. Son intérêt est de rendre le problème inverse de la reconstruction bien posé et de préciser de manière quantitative l'influence de l'inclusion sur les mesures, notamment au premier ordre par l'intermédiaire d'un tenseur de polarisation. Ces formules asymptotiques sont bien connues dans la littérature dans les cadres suivants, parmi d'autres : soit l'opérateur non perturbé est le Laplacien (et donc $D_0$ est constant) et $D_1$ est constant et l'on trouve dans [21] un développement à un ordre arbitraire pour $d$ quelconque ; soit $d \leq 3$, $D_0$ et $D_1$ varient et [45] par exemple offre un développement au premier ordre (qui est ici $\varepsilon^d$, la fraction de volume de l'inclusion). On propose dans ce chapitre un développement asymptotique de $u^\varepsilon$ jusqu'à l'ordre $\varepsilon^{2d}$ et ce pour des coefficients $D_0$ et $D_1$ quelconques, constants ou non, et $d$ arbitraire. Il est naturel ici de s'arrêter à l'ordre $\varepsilon^{2d}$ car au-delà des inclusions de même fraction volumique ne peuvent plus être considérées comme indépendantes. Il y a de même des effets géométriques qui alourdissent nettement les développements aux ordres supérieurs. Nous montrons également qu'il existe des inclusions dont l'effet est nul au premier ordre, phénomène absent lorsque lorsque $D_1$ est constant. Nous comparons enfin les développements asymptotiques issus des équations de Laplace et de Helmholtz et montrons qu'ils sont équivalents pour une inclusion sans saut ($D_1$ régulier) en utilisant le changement de variables classique de Liouville. Ce chapitre est un résumé de [4] réalisé en collaboration avec G. Bal.

Dans la seconde partie sur le transport dans les nanostructures :

– On s'intéresse dans le chapitre quatre au système de Schrödinger-Poisson en domaines ouverts, c'est-à-dire un problème non-linéaire dont les conditions aux limites sont non nulles à l'infini et traduisent l'injection d'électrons dans la structure. Il est classique dans ce contexte de restreindre le domaine d'étude à un domaine borné en introduisant des conditions aux limites transparentes sur des interfaces bien choisies. Une possibilité de contrôler que ces conditions aux limites modélisent correctement la physique est de passer à la limite semi-classique (limite haute-fréquence) et de vérifier que les conditions obtenues correspondent aux conditions classiques d'injection pour l'équation de Vlasov. Ceci requière des estimations sur les solutions indépendantes de la constante de Planck réduite. En réalisant une étude précise des conditions aux limites transparentes, de telles bornes uniformes sont obtenues. Nous montrons également que le système de Schrödinger-Poisson en domaines ouverts admet des solutions au sens faible alors que l'existence n'avait été démontŕee dans la littérature que dans un sens fort. Ce chapitre est un résumé de [8].

– On étudie dans le chapitre cinq le problème quantique des moments suivant : se

donnant une entropie $s$, un Hamiltonien $H$ positif et une densité $n(x)$ positive, existe-t-il un opérateur densité $\varrho$, c'est-à-dire un opérateur auto-adjoint positif de trace égale à un minimisant l'énergie libre quantique

$$F(\varrho) = \mathrm{Tr}\, s(\varrho) + \mathrm{Tr}\, \sqrt{H}\varrho\sqrt{H},$$

où Tr signifie la trace, sous la contrainte de densité locale $\rho(x,x) = n(x)$ avec $\rho(x,y)$ noyau intégral de l'opérateur $\varrho$ ? Nous répondons à la question pour un domaine borné de dimension un et des conditions aux limites périodiques dans le cas de l'entropie de Boltzmann $s(x) = x\log x - x$. Nous caractérisons de plus la solution et montrons que celle-ci s'écrit en utilisant le calcul fonctionnel

$$\varrho = e^{-(H+A)},$$

où $A(x)$ est un potentiel chimique, paramètre de Lagrange associé à la contrainte de densité locale. Ce chapitre est un résumé de [1], réalisé en collaboration avec F. Méhats.

**English summary.** The present memoir gathers works done since the PhD thesis, on two differents topics, wave propagation in random media and quantum transport in nanostructures. The first part contains three chapters:

- Chapter one is a summary of the articles [2, 7, 9, 10] and deals with the imaging of buried inclusions in complex unknown media. The unknown medium is probed with acoustic waves and is modeled as a particular realization of a random medium. Within the high-frequency limit, the inverse problem of localization based on a microscopic wave description is replaced by an inverse problem solved with macroscopic transport equations depending only on some general characteristics of the medium and not on its local details. We study those asymptotic models and show their imaging capabilities. We also discuss the interest in using time reversal in such a context. Jointwork with G. Bal.

- Chapter two deals with the high-frequency limit of random Schrödinger equations, within two regimes: the Itô-Schrödinger (white noise) regime, and a regime where the potential is independent of time. The asymptotics is performed by means of Wigner transforms. We address the question of statistical stability, that is whether the limiting random Wigner function is deterministic or not. We give optimal rates of convergence according to some parameters of the problem as the regularity of the initial conditions or the size of the detector where waves are measured, and characterize the instabilities by computing the first-order corrector to the covariance function of the Wigner transform. This chapter is jointwork with G. Bal, and partly with I. Langmore, and a summary of the articles [3, 5, 6].

– We are interested in chapter three in the influence at the domain boundary of small volume inclusions on the solutions of diffusion or Helmholtz equations of the form $\nabla \cdot D^\varepsilon \nabla u^\varepsilon = 0$ or $(-\Delta + q^\varepsilon)u^\varepsilon = 0$ with prescribed Neumann conditions. We extent previous results to the case of non-constant coefficients in arbitrary dimensions. Besides, we compare the expansions for the diffusion and Helmholtz equations and their relationship via the classical Liouville change of variables. That chapter is a summary of [4], jointwork with G. Bal.

In part two:

– We deal in chapter four with the open Schrödinger-Poisson system, that is a non-linear problem posed on an unbounded domain with non-vanishing conditions at the infinity. It is customary in such a context to introduce transparent boundary conditions to reduce the resolution to a bounded domain. A possibility to validate such boundary conditions is to perform the semi-classical analysis of the system to recover the standard inflow boundary conditions for transport equations. This requires the derivation of uniform bounds with respect to the reduced Planck constant. Such estimates are obtained here thanks to a careful analysis of the non-local transparent boundary conditions. We also give existence and uniqueness of weak solutions while they were defined in a strong sense in the literature. This chapter is a summary of [8].

– We are interested in chapter five in the following problem: for an entropy $s$, an Hamiltonian $H$ and a positive density $n(x)$, can we find a density operator $\varrho$ minimizing the quantum free energy

$$F(\varrho) = \operatorname{Tr} s(\varrho) + \operatorname{Tr} \sqrt{H}\varrho\sqrt{H},$$

under the constraint of local density $\rho(x,x) = n(x)$ where $\rho(x,y)$ is the integral kernel of $\varrho$ ? We give a positive answer to that question and characterize the solution. This chapter is a summary of [1], jointwork with F. Méhats.

# Part I

# Wave propagation in random media, applications to imaging

# Chapter 1

# Imaging models and reconstructions

This chapter gathers works on the reconstruction of inclusions in highly heterogeneous unknown media. The medium is probed by using classical acoustic waves. When fluctuations become too strong, inversion methodologies based on a microscopic description of wave propagation become strongly dependent on the unknown details of the medium. In some situations, it is therefore preferable to use a macroscopic model for a quantity that is quadratic in the wave fields. Here, such macroscopic models take the form of radiative transfer equations. We then replace an inverse problem based on the microscopic wave equation by an inverse problem based on the macroscopic transport equations. In particular:

- We show that transport and diffusion equations indeed accurately describe the propagation of the energy of high-frequency waves in a random medium and correctly captures the presence of an inclusion. A stress is put on the statistical stability, that is how much the energy depends on the realizations of the random medium [9].

- Imaging models based on the wave energy, or on the correlation of the wavefield in presence of an inclusion and the wavefield in absence of an inclusion are constructed. We also discuss the effect of small inclusions on the data [7].

- It is shown that time reversal measurements enjoy a larger signal-to-noise ratio in the presence of background noise than do direct energy measurements [10].

- We perform reconstructions of inclusions in several settings, in particular one for which the inclusion is hidden behind a blocker with no line-of-sight [2].

## 1.1 Introduction

This chapter deals with the reconstruction of inclusions embedded in complex media. The problem of imaging in highly heterogeneous environments arises in many important applications such as biomedical imaging, seismic exploration in geophysics [48] and non-destructive testing of materials [107]. One standard imaging technique consists in probing a medium by sending acoustic, electromagnetic, or elastic waves depending on the applications from a localized source and by collecting the echos on an array of detectors.

Reconstructions then depend on whether the heterogeneous medium is known a priori or not. In the somewhat unlikely event that it is, several classical techniques are available such as e.g. the time reversal methods, which perform well for the localization of buried inclusions: in the context of acoustic waves, the measured field at the detector is time-reversed, which consists in changing the sign of the velocity and sending back first the signal that has been recorded last, and will peak at the location of the most diffractive inclusion. Back-propagation is possible in this configuration because the medium is *known*. These striking refocusing properties, often referred as *super resolution*, are enhanced since propagation occurs in a highly heterogeneous medium rather than in a homogeneous medium, as it has been observed in many physical settings [56, 59, 68, 86]. Time reversal has been extensively analyzed mathematically in various regimes of wave propagation, such as layered media, waves guides, paraxial approximation, white noise, see for instance [34, 49, 40, 99, 75, 71] for a few references. For applications of time reversal to imaging, see e.g. [42, 41].

When the heterogeneous medium is not known, the imaging problem is different. The unknown medium of propagation may then be modeled as a particular realization of a random medium. The average (slow) part of the medium may be assumed to be known while the local fluctuations are rapid and unknown. The imaging method then depends on the strength of the random heterogeneities and on the relation between the wavelength and the scale at which the medium varies, i.e., the correlation length of the random medium.

When the strength of the heterogeneities is weak, interferometry methods are efficient, see e.g. [43]: since the fluctuations are weak, the wave is only slightly scattered by the medium, so that coherent information is available. Such information propagating in the homogeneous (average) known medium, the technique consists in back-propagating available measurements (e.g. time and space correlations of the field) in the homogeneous medium to observe a peak at the inclusion location.

When the fluctuations are strong, scattering can no longer be neglected and thus needs to be modeled. Scattering is mostly generated by heterogeneities at the same scale as the propagating waves. We thus consider the situation where the wavelength

and the correlation length in the random medium are comparable. In such a regime, the dynamics of the wave energy is well described by radiative transfer equations, whose constitutive parameters depend on the statistics of the random medium. The energy density of high-frequency waves propagating in highly heterogeneous media has long been modeled by radiative transfer equation in many fields: quantum waves in semiconductors, electromagnetic waves in turbulent atmospheres and plasmas, microwaves in aerial communication, underwater acoustic waves, elastic waves in the Earth's crust. The derivation of such kinetic models may either be phenomenological or based on first principles for the wave fields; see e.g. [46, 106, 88, 105]. The presence of an inclusion is then seen as a perturbation of the constitutive parameters of the radiative transfer equations, or of its approximation in the diffusion regime. We then replace an inverse problem based on the microscopic wave equation by an inverse problem based on the macroscopic transport equations. We thus abandon the physically accurate microscopic wave model because it is too sensitive to the heterogeneities of the underlying medium, and replace it by a macroscopic model, whose role is precisely to average out the unimportant fluctuations of the medium and keep only its effective macroscopic features.

The imaging problem thus consists in solving an inverse transport problem. Imaging is based on fulfilling three main conditions. Firstly, we need to make sure that the macroscopic model is indeed an accurate description of the physical process for the high-frequency limit. Secondly, we need to estimate the macroscopic statistical properties of the random medium (typically the cross-section for transport regime, or the diffusion coefficient for the diffusion regime). Note that this is a much easier task than reconstructing for instance the velocity field of an heterogeneous medium. Thirdly, we need to ensure that the macroscopic model is statistically stable, and this is the main limitation of transport models. Transport equations are deterministic and model the ensemble average of the energy density. Available measurements typically correspond to one realization of the random medium and thus are not averaged over realizations and are considered as random. It turns out that self-averaging effects allow us to show that the energy density of the waves becomes asymptotically independent of the realization of the random medium as the wavelength tends to zero, which should be seen as an application of the law of large numbers. Therefore, it is expected that the deterministic transport equations are indeed an accurate description of the random wave energy within the high-frequency limit. For the transport models to accurately predict the presence of an inclusion, its effect must be larger than the statistical instabilities due to the finiteness of the frequency, self-averaging occuring only at the limit. The questions of statistical stability and rigorous derivation of transport equations will be addressed in the next chapter within the so-called paraxial approximation. We will assume here, and show numerically as well, that self-averaging holds for our regime of interest.

Time reversal can also be useful in the imaging procedure even though the heterogenous medium is unknown. This is related to signal-to-noise ratio considerations. We will see that time-reversed waves, thanks to their refocusing properties, are less affected by background noise than direct wave measurements. The advantage of time reversal is therefore to provide less noisy measurements for the resolution of the inverse transport problem.

We recall that we deal here with an active source problem for imaging. It is also possible in some situations to localize inclusions without knowing the location of the source using cross-correlated signals, see for instance [74, 76] and the references therein.

We consider time-dependent acoustic waves. We refer to [33] for instance for time-harmonic acoustic waves. Our objectives are the following:

(i) Verify numerically the validity of transport equations (including diffusion models) modeling the propagation of the *energy density* of high-frequency waves in random media as well as the *correlation* of the wave fields in the *presence* and in the *absence* of an inclusion. Constructing such a correlation assumes that both fields (with and without the inclusion) can be measured while energy measurements only require measurements in the presence of the inclusion. In particular, we will verify the transport models accurately capture the presence of an inclusion.

(ii) Evaluate the statistical stability according to some physical parameters of the problem, such as the domain of measurements or the size of the support of the initial conditions.

(iii) Discuss several imaging scenarios according to the different types of available measurements and assess for instance which observables between the energy and the correlation should preferably be used and in which situation.

(iv) Demonstrate the imaging capabilities of the transport models by performing reconstructions and quantifying the sensitivity of the reconstructions with respect to the statistical instabilities.

The rest of the chapter is structured as follows: in section 1.2, we present the transport models for the wave energy density and field-field correlations, as well as a basic result about time reversal. In section 1.3, we present some numerical simulations validating the transport models and show some results about statistical stability. In section 1.4, we explain what are the advantages of time reversal for our imaging problem, discuss different imaging scenarios according to the type of available measurements and finally perform some reconstructions of inclusions. In particular, we locate an inclusion hidden behind a blocker with no line of sight.

## 1.2 Transport models

In this section, we present the transport equations verified by the wave energy densities and field-field correlations in the high frequency regime, and recall important results about time reversal.

### 1.2.1 High-frequency waves

The propagation of acoustic waves is described by the following scalar wave equation for the pressure $p$:

$$\frac{\partial^2 p}{\partial t^2} = \kappa^{-1}(\mathbf{x})\nabla \cdot \rho^{-1}(\mathbf{x})\nabla p, \qquad \mathbf{x} \in \mathbb{R}^d, \quad t > 0, \tag{1.1}$$

supplemented with initial conditions $p(t = 0, \mathbf{x})$ and $\frac{\partial p}{\partial t}(t = 0, \mathbf{x})$. Here, $d$ is dimension and $\rho$ and $\kappa$ are density and compressibility of the underlying medium, respectively. For simplicity, we assume that $\rho(\mathbf{x}) := \rho_0$ is constant. Generalizations to non-constant densities are not difficult. The compressibility $\kappa$ is of the form

$$\kappa(\mathbf{x}) = \kappa_0(\mathbf{x}) + \sigma_0 \kappa_1 \left(\frac{\mathbf{x}}{l_c}\right),$$

where $\kappa_0$ is the background compressibility (supposed to be known and smooth) and $\kappa_1$ accounts for random fluctuations of strength $\sigma_0$ and correlation length $l_c$. $\kappa_1$ is a mean zero, homogeneous stationary random field with correlation function

$$\mathbb{E}\{\kappa_1(\mathbf{x})\kappa_1(\mathbf{y})\} = R(\mathbf{x} - \mathbf{y}). \tag{1.2}$$

Above, $\mathbb{E}\{\cdot\}$ denotes ensemble average over the different realizations of the random medium. $R$ is assumed to decay fast enough so as to avoid long-range interaction effects. We suppose the initial condition has both slow and rapid variations (corresponding to a typical length $\lambda$, e.g. a wavelength or a support size) so that

$$p(t = 0, \mathbf{x}) = p_0\left(\mathbf{x}, \frac{\mathbf{x}}{\lambda}\right), \qquad \frac{\partial p}{\partial t}(t = 0, \mathbf{x}) = p_1\left(\mathbf{x}, \frac{\mathbf{x}}{\lambda}\right).$$

We consider initial conditions oscillating at the frequency $\lambda^{-1} \gg 1$ with support of order one compared to $\lambda$.

In the regime of *weak coupling* [46, 106], it is assumed that the strength of the fluctuations $\sigma_0$ is weak and that the correlation length of the medium $l_c$ and the typical length of the initial condition $\lambda$ are same order. Considering stronger fluctuations would possibly yield a stochastic behavior of the wave energy in the high frequency limit, see [71] for instance. This is not the regime we are interested here

since one of our objectives is to quantify the statistical stability of the reconstructions, that is how much some reconstructed parameters depend on the realization of the random medium. The stochastic homogeneization case $\lambda \gg l_c$ leads to waves propagating in an effective medium, see [28], while the case $\lambda \ll l_c$ leads in the paraxial approximation to random Liouville equations [29]. Following the above discussion, we then set

$$l_c = \lambda = \sigma_0^2 = \varepsilon \ll 1.$$

The fact that $\sigma_0 = \sqrt{\varepsilon}$ insures the random medium has an effect of order $\mathcal{O}(1)$ at the macroscopic level. We recast the scalar wave equation as a first-order hyperbolic system and introduce the acoustic field $\mathbf{u}^\varepsilon = (\mathbf{v}^\varepsilon, p^\varepsilon)$, where $\mathbf{v}^\varepsilon$ is velocity and obtain the following system:

$$\rho_0 \frac{\partial \mathbf{v}^\varepsilon}{\partial t} + \nabla p^\varepsilon = 0, \qquad \kappa^\varepsilon \frac{\partial p^\varepsilon}{\partial t} + \nabla \cdot \mathbf{v}^\varepsilon = 0, \tag{1.3}$$

augmented with initial conditions $p^\varepsilon(t=0,\mathbf{x}) = p_0\left(\mathbf{x}, \frac{\mathbf{x}}{\varepsilon}\right)$ and $\mathbf{v}^\varepsilon(t=0,\mathbf{x}) = \nabla\varphi^\varepsilon(\mathbf{x})$ where the pressure potential $\varphi^\varepsilon$ is obtained by solving $\Delta\varphi^\varepsilon = -\kappa_0 \frac{\partial p^\varepsilon}{\partial t}(t=0,\cdot)$. The sound speed is given by $c_\varepsilon(\mathbf{x}) = (\rho_0 \kappa^\varepsilon(\mathbf{x}))^{-1/2}$ with $\kappa^\varepsilon(\mathbf{x}) = \kappa_0(\mathbf{x}) + \sqrt{\varepsilon}\kappa_1\left(\frac{\mathbf{x}}{\varepsilon}\right)$.

### 1.2.2 Transport equations

The high frequency limit may be obtained by using Wigner transforms (see chapter 2 and [80, 94]), which provides a phase space description of the propagation of the wave energy. The wave energy satisfies transport equations whose constitutive parameters are deduced from the microscopic sound speed $c_\varepsilon$ [105]. We consider two fields: $\mathbf{u}_1^\varepsilon$, which corresponds to waves propagating in a medium *without inclusion*, and $\mathbf{u}_2^\varepsilon$ corresponding to waves propagating a medium *with an inclusion*. We denote by $\Omega$ the domain of the inclusion. Assuming there are no random fluctuations at its location, the inclusion is typically modeled as a jump of the constitutive parameters of the medium, namely the density and compressibility. For the two fields $\mathbf{u}_i^\varepsilon$, the Wigner transform is defined as the following matrix-valued function:

$$W^\varepsilon[\mathbf{u}_i^\varepsilon, \mathbf{u}_j^\varepsilon](t,\mathbf{x},\mathbf{k}) = \frac{1}{(2\pi)^d}\int_{\mathbb{R}^d} e^{i\,\mathbf{k}\cdot\mathbf{y}}\, \mathbf{u}_i^\varepsilon(t,\mathbf{x}-\frac{\varepsilon\mathbf{y}}{2}) \otimes \mathbf{u}_j^\varepsilon(t,\mathbf{x}+\frac{\varepsilon\mathbf{y}}{2})\, d\mathbf{y}.$$

We introduce the notations $W_1^\varepsilon = W^\varepsilon[\mathbf{u}_1^\varepsilon, \mathbf{u}_1^\varepsilon]$, $W_2^\varepsilon = W^\varepsilon[\mathbf{u}_2^\varepsilon, \mathbf{u}_2^\varepsilon]$ and $W_{12}^\varepsilon = W^\varepsilon[\mathbf{u}_1^\varepsilon, \mathbf{u}_2^\varepsilon]$. Let $\mathcal{E}^\varepsilon$ be the energy in absence of inclusion, $\mathcal{E}_{\text{inc}}^\varepsilon$ be the energy in presence of inclusion and let $\mathcal{C}^\varepsilon$ be the correlation of the two fields $\mathbf{u}_1^\varepsilon$ and $\mathbf{u}_2^\varepsilon$. They are respectively

defined as

$$\begin{aligned}
\mathcal{E}^\varepsilon(t,\mathbf{x}) &= \frac{1}{2}\left(\kappa^\varepsilon(\mathbf{x})(p_1^\varepsilon(t,\mathbf{x}))^2 + \rho_0|\mathbf{v}_1^\varepsilon(t,\mathbf{x})|^2\right), \\
\mathcal{E}^\varepsilon_{\rm inc}(t,\mathbf{x}) &= \frac{1}{2}\left(\kappa^\varepsilon(\mathbf{x})(p_2^\varepsilon(t,\mathbf{x}))^2 + \rho_0|\mathbf{v}_2^\varepsilon(t,\mathbf{x})|^2\right), \\
\mathcal{C}^\varepsilon(t,\mathbf{x}) &= \frac{1}{2}\left(\kappa^\varepsilon(\mathbf{x})p_1^\varepsilon(t,\mathbf{x})p_2^\varepsilon(t,\mathbf{x}) + \rho_0\mathbf{v}_1^\varepsilon(t,\mathbf{x})\cdot\mathbf{v}_2^\varepsilon(t,\mathbf{x})\right).
\end{aligned}$$

It is shown in [105] that in the limit $\varepsilon \to 0$, the expectation of the Wigner transform $\mathbb{E}\{W_1^\varepsilon\}$ tends to a measure $W_1$ admitting the following decomposition:

$$W_1(t,\mathbf{x},\mathbf{k}) = a_1^+(t,\mathbf{x},\mathbf{k})\,\mathbf{b}^+(\mathbf{x},\mathbf{k})\otimes\mathbf{b}^+(\mathbf{x},\mathbf{k}) + a_1^-(t,\mathbf{x},\mathbf{k})\,\mathbf{b}^-(\mathbf{x},\mathbf{k})\otimes\mathbf{b}^-(\mathbf{x},\mathbf{k}),$$

where we have defined

$$\mathbf{b}^\pm(\mathbf{x},\mathbf{k}) = \frac{1}{\sqrt{2\rho_0}}\begin{pmatrix}\hat{\mathbf{k}}\\ \pm\rho_0 c_0^{-1}(\mathbf{x})\end{pmatrix}, \qquad c_0(\mathbf{x}) := (\rho_0\kappa_0(\mathbf{x}))^{-1/2}, \qquad \hat{\mathbf{k}} := \frac{\mathbf{k}}{|\mathbf{k}|}.$$

The absence of vortical modes in the latter expression follows from the form of initial condition $\mathbf{u}_1^\varepsilon(t=0,\cdot) = (\nabla\varphi^\varepsilon, p^\varepsilon(t=0,\cdot))$. In the absence of an inclusion and when the average velocity $c_0 = (\rho_0\kappa_0)^{-1/2}$ is independent of position, the amplitude of the propagating mode $a_1^+$ solves the following radiative transfer equation:

$$\frac{\partial a_1^+}{\partial t} + c_0\,\hat{\mathbf{k}}\cdot\nabla_{\mathbf{x}} a_1^+ + \Sigma(\mathbf{k})\,a_1^+ = \mathcal{Q}(a_1^+), \qquad \mathbf{x}\in\mathbb{R}^d, \tag{1.4}$$

augmented with prescribed initial conditions $a_1^+(0,\mathbf{x},\mathbf{k})$, where $\mathcal{Q}$ and $\Sigma^{-1}$ denote the collision operator and mean free time, respectively, and are given by:

$$\mathcal{Q}(a) = \int_{\mathbb{R}^d} a(t,\mathbf{x},\mathbf{p})\sigma(\mathbf{k},\mathbf{p})\delta(c_0|\mathbf{p}|-c_0|\mathbf{k}|)d\mathbf{p}, \qquad \Sigma(\mathbf{k}) = \int_{\mathbb{R}^d}\sigma(\mathbf{k},\mathbf{p})\delta(c_0|\mathbf{p}|-c_0|\mathbf{k}|)d\mathbf{p}.$$

The cross section $\sigma(\mathbf{k},\mathbf{p})$ appearing in these expressions is given by

$$\sigma(\mathbf{k},\mathbf{p}) = \frac{\pi c_0^2|\mathbf{k}|^2}{2(2\pi)^d}\hat{R}(\mathbf{k}-\mathbf{p}), \qquad \hat{R}(\mathbf{k}) = \int_{\mathbb{R}^d} e^{-i\mathbf{x}\cdot\mathbf{k}}R(\mathbf{x})d\mathbf{x}.$$

A similar expression is obtained for $a_1^-(t,\mathbf{x},\mathbf{k}) = a_1^+(t,\mathbf{x},-\mathbf{k})$. The expectation of the physical energy density is then derived from the phase-space energy density by averaging out the $\mathbf{k}$ variable: formally,

$$\lim_{\varepsilon\to 0}\mathbb{E}\{\mathcal{E}^\varepsilon\}(t,\mathbf{x}) = \int_{\mathbb{R}^d} a_1^+(t,\mathbf{x},\mathbf{k})d\mathbf{k}. \tag{1.5}$$

The question of the statistical stability of the limit, that is determining whether the random variable $W_1^\varepsilon$ converges to its average $\mathbb{E}\{W_1^\varepsilon\}$ (and therefore to $W_1$) in the

high-frequency limit, is addressed in the next chapter in the paraxial approximation. Regarding $W_2^\varepsilon$ and $W_{12}^\varepsilon$, we have for $\mathbf{x} \in \mathbb{R}^d \backslash \overline{\Omega}$, $i = 2, 12$,

$$W_i(t, \mathbf{x}, \mathbf{k}) = a_i^+(t, \mathbf{x}, \mathbf{k})\, \mathbf{b}^+(\mathbf{x}, \mathbf{k}) \otimes \mathbf{b}^+(\mathbf{x}, \mathbf{k}) + a_i^-(t, \mathbf{x}, \mathbf{k})\, \mathbf{b}^-(\mathbf{x}, \mathbf{k}) \otimes \mathbf{b}^-(\mathbf{x}, \mathbf{k}),$$

where $a_2^\pm$ and $a_{12}^\pm$ satisfy the transport equation (1.4) in $\mathbb{R}^d \backslash \overline{\Omega}$. As (1.5), the limits of the expectations of $W_2^\varepsilon$ and $W_{12}^\varepsilon$ are obtained from the densities $a_2^+$ and $a_{12}^+$ by averaging out the momentum. The boundary conditions on $\partial\Omega$ will be precised later on.

**Diffusion regime.** It is well known that solutions of radiative transfer equations in the small mean free path regime are well approximated by solutions to diffusion equations [92]. Let us define the mean free path $l = c_0 \Sigma^{-1}$. The diffusive regime arises when $\eta = l/L \ll 1$, where $L$ is the typical distance of wave propagation. Rescaling time and space as $t \to t/\eta^2$ and $\mathbf{x} \to \mathbf{x}/\eta$, we find in the limit $\eta \to 0$ that $a_\pm^1(t, \mathbf{x}, \mathbf{k})$ becomes independent of the angular variable $\hat{\mathbf{k}} = \mathbf{k}/|\mathbf{k}|$:

$$a_1^\pm(t, \mathbf{x}, \mathbf{k}) \approx U^1(t, \mathbf{x}, |\mathbf{k}|),$$

and more precisely that $U^1$ satisfies the following diffusion equation [105] in the two dimensional setting $d = 2$ for instance:

$$\begin{aligned} &\frac{\partial U^1}{\partial t} - D_0(|\mathbf{k}|)\Delta U^1 = 0, \qquad \mathbf{x} \in \mathbb{R}^2 \\ &U^1(0, \mathbf{x}, |\mathbf{k}|) = \frac{c_0}{4\pi|\mathbf{k}|^2} \int_{\mathbb{R}^2} a_1^\pm(0, \mathbf{x}, \mathbf{p}) \delta(c_0(|\mathbf{k}| - |\mathbf{p}|)) d\mathbf{p}. \end{aligned} \tag{1.6}$$

The diffusion coefficient and anisotropy factor are defined as

$$D_0(|\mathbf{k}|) = \frac{c_0^2}{2[\Sigma(|\mathbf{k}|) - \lambda(|\mathbf{k}|)]} \quad ; \quad \lambda(|\mathbf{k}|)\hat{\mathbf{k}} = \frac{c_0^2|\mathbf{k}|^2}{(4\pi)^2} \int_{\mathbb{R}^2} \hat{R}(\mathbf{p} - \mathbf{k})\hat{\mathbf{p}} \delta(c_0(|\mathbf{k}| - |\mathbf{p}|)) d\mathbf{p}.$$

In the sequel, we denote by $U^2$ and $U^{12}$ the diffusion limits of $a_2^\pm$ and $a_{12}^\pm$.

**Modeling of the inclusion.** Dealing with reflection-transmission phenomena within the high-frequency regime is a difficult task and few rigorous mathematical results are avaiblable, see [70, 96]. Formally, the wave energy satisfies the Snell law at the inclusion boundary. Here, we simplify the analysis by assuming that the inclusion is a sound soft inclusion, which is equivalent to setting an infinite sound speed within it. This leads to vanishing Dirichlet conditions for the pressure $p^\varepsilon$ on $\partial\Omega$. At the transport level, the energy is specularly reflected since the inclusion is non-penetrable, and $a_2^\pm$ therefore satisfies specular boundary conditions on $\partial\Omega$. Regarding the correlation $\mathcal{C}^\varepsilon$, it is shown in [7] that it must verify vanishing Dirichlet

conditions on $\partial\Omega$ since the two wave fields $\mathbf{u}_1^\varepsilon$ and $\mathbf{u}_2^\varepsilon$ satisfy different dispersion relations inside the inclusion. We thus prescribe the following boundary conditions for the energy and correlation amplitudes $a_2^+$ and $a_{12}^+$:

$$\begin{aligned} a_2^+(t,\mathbf{x},\mathbf{k}) &= a_2^+(t,\mathbf{x},\mathbf{k}-2\mathbf{k}\cdot\mathbf{n}(\mathbf{x})\mathbf{n}(\mathbf{x})), \quad \mathbf{x}\in\partial\Omega, \\ a_{12}^+(t,\mathbf{x},\mathbf{k}) &= 0, \qquad \mathbf{x}\in\partial\Omega,\ \mathbf{k}\cdot\mathbf{n}(\mathbf{x})>0. \end{aligned}$$

Above, $\mathbf{n}(\mathbf{x})$ is the outward normal to the boundary $\partial\Omega$ at $\mathbf{x}\in\partial\Omega$. In the diffusive regime, the boundary conditions turn into Neumann and still Dirichlet boundary conditions, see [7]:

$$\frac{\partial U^2}{\partial \mathbf{n}} = 0, \qquad U^{12}=0, \qquad \mathbf{x}\in\partial\Omega. \tag{1.7}$$

### 1.2.3 Time reversal

See [34] for a mathematical presentation of time reversal in the context of acoustic waves. We denote by $\mathbf{u}^B(\boldsymbol{\xi})$ the refocused wave field around the initial condition location $\mathbf{x}=\mathbf{0}$. $\mathbf{u}^B(\boldsymbol{\xi})$ is obtained after the following procedure: the initial field propagates for a time $T$ according to (1.3); at time $t=T^-$ it is time-reversed at a detector located at $\mathcal{D}$, i.e., the sign of the velocity is changed keeping that of the pressure fixed; and finally at $t=T^+$, the time-reversed field is back-propagated in the medium to yield the field $\mathbf{u}^B(\boldsymbol{\xi})$ around the origin. An important result is the following: in the limit $\varepsilon\to 0$, the back-propagated field $\mathbf{u}^B$ verifies

$$\mathbf{u}^B(\boldsymbol{\xi}) = \big(\hat{F}_+(T,\mathbf{0},\cdot)*\mathbf{S}_+\big)(\boldsymbol{\xi}) + \big(\hat{F}_-(T,\mathbf{0},\cdot)*\mathbf{S}_-\big)(\boldsymbol{\xi}), \tag{1.8}$$

where $\mathbf{S}_\pm$ are the decompositions of the rescaled initial condition $\mathbf{S}=(\mathbf{v}^{\varepsilon=1}(t=0,\cdot),p^{\varepsilon=1}(t=0,\cdot))$ on the vectors $\mathbf{b}^\pm$ defined in the preceding section, and $\hat{F}_\pm$ are the Fourier transforms of amplitudes $F_\pm(T,\mathbf{0},\mathbf{k})$ with respect to the variable $\mathbf{k}$, solutions to a transport equation of the form (1.4) with an initial condition given by the indicator function of the detector $\mathbb{1}_{\mathcal{D}}$. The effect of time reversal can thus be asymptotically seen as a convolution of the initial conditions with a filter solution to a radiative transfer equation, the main difference with the energy density of the preceding section being the initial condition. In practice, the value of the filter is obtained by measuring the amplitude of the refocused signal $\mathbf{u}^B(\boldsymbol{\xi})$ and that of the initial condition and by forming

$$F_\pm(T,\mathbf{0},\mathbf{k}) = \frac{A\hat{\mathbf{u}}^B(\mathbf{k})\cdot\mathbf{b}_\pm(\mathbf{0},\mathbf{k})}{A\hat{\mathbf{S}}_\pm(\mathbf{k})\cdot\mathbf{b}_\pm(\mathbf{0},\mathbf{k})},$$

where the matrix $A$ is defined by $A=\mathrm{Diag}(\rho_0,\rho_0,\rho_0,\kappa_0)$. We will see that time reversal measurements enjoy a better signal-to-noise ratio than energy measurements.

## 1.3 Validation of transport models

We present here numerical simulations validating the transport models for the energy and the field-field correlations. We describe first the numerical setting; secondly, we compare the energies given by the wave, transport and diffusion equations, and evaluate as well the perturbation due to an inclusion in these three regimes; we then show that correlations are indeed accurately described by a transport equation with Dirichlet boundary conditions at the inclusion boundary and we finally present some results about the statistical stability of the wave energy.

**Numerical setting.** The numerical setting for wave propagation is detailed in [9, 7]. We recall here its main characteristics. The wave equation is solved in two-space dimensions as a mixed finite-difference discretization of the equations (1.3). The computational domain is surrounded by a classical perfectly matched layer. We use a second order centered scheme for the discretization in time so that the overall scheme is second order both in time and space. The code is parallelized using the PETSc library, which allows for simulations on large domains. The initial condition is chosen so that only one frequency $|\mathbf{k}_0|$ is present at the transport level, at least approximately. More precisely, we choose:

$$\mathbf{u}_0(\mathbf{x}) = \left(\mathbf{0}, C_0 \exp\left(\frac{-|\mathbf{x}-\mathbf{x}_0|^2}{2\sigma^2}\right) J_0(|\mathbf{k}_0||\mathbf{x}-\mathbf{x}_0|)\right)^t = (\mathbf{0}, p_0)^t$$

where $J_0$ is the zero-th order Bessel function of the first kind. This initial condition exhibits an oscillatory behavior at the frequency $\mathbf{k}_0$ and is localized in the vicinity of the point $\mathbf{x}_0$. The constant $C_0$ is chosen so that the energy associated to $\mathbf{u}_0$ is equal to one. The exponential term is chosen here to localize the source term. However, it has sufficiently slow variations in order not to interfere with the highly oscillatory Bessel function. Here, $\sigma$ is chosen to be on the order of ten wavelengths so that the frequency content of $\mathbf{u}_0$ is primarily that of a single wavenumber $|\mathbf{k}_0|$.

In the simulations, we assume that

$$\rho_0 = 1, \quad \kappa^\varepsilon(\mathbf{x}) = 1 + \sqrt{\varepsilon}\kappa_1\left(\frac{\mathbf{x}}{\varepsilon}\right),$$

where $\kappa_1$ is a stationary mean-zero random variable. The average sound speed is thus normalized to $c_0 = 1$. The fluctuations of the compressibility $\kappa_1(\mathbf{x})$ are carefully modeled in the Fourier domain to satisfy prescribed power spectra in (1.2). The transport equations are solved by a Monte Carlo method using a variance reduction technique, and the diffusion equation by a standard finite elements scheme. The initial condition at the transport level is

$$a_0(\mathbf{x}, \mathbf{k}) = \delta(\mathbf{x}-\mathbf{x}_0)\delta(|\mathbf{k}| - |\mathbf{k}_0|)|\mathbf{k}_0|^{-1}.$$

The power spectrum $\hat{R}$ is chosen isotropic and of the form

$$\hat{R}(r) = \begin{cases} \hat{R}_0 & \text{for} \quad r < M, \\ 0 & \text{for} \quad r > M, \end{cases}$$

where $M$ is a given parameter such that $M \geq 2|\mathbf{k}_0|$. See [9] for anisotropic power spectra. The parameter $\hat{R}_0$ controls the strength of the fluctuations. When we say a medium has fluctuations of $x\%$, we mean $\sqrt{R_0} = x\%$, with the relation $(2\pi)^2 R_0 = \pi M^2 \hat{R}_0$. We introduce the following notations, for a detector $\mathcal{D} \subset \mathbb{R}^2$:

$$\mathcal{E}^\varepsilon(t) = \int_{\mathcal{D}} \mathcal{E}^\varepsilon(t,\mathbf{x}) d\mathbf{x}, \qquad \mathcal{E}^\varepsilon_{\text{inc}}(t) = \int_{\mathcal{D}} \mathcal{E}^\varepsilon_{\text{inc}}(t,\mathbf{x}) d\mathbf{x}, \qquad \mathcal{C}^\varepsilon(t) = \int_{\mathcal{D}} \mathcal{C}^\varepsilon(t,\mathbf{x}) d\mathbf{x},$$
$$\mathcal{A}_i(t) = \int_{\mathcal{D}} \int_{\mathbb{R}^2} a_i^+(t,\mathbf{x},\mathbf{k}) d\mathbf{x}\, d\mathbf{k} = \int_{\mathcal{D}} \int_{S^1} a_i^+(t,\mathbf{x},\hat{\mathbf{k}}|\mathbf{k}_0|) 2\pi|\mathbf{k}_0| d\mathbf{x}\, d\hat{\mathbf{k}}, \qquad i = 1, 2, 12,$$
$$\mathcal{U}_i(t) = \int_{\mathcal{D}} U^i(t,\mathbf{x},|\mathbf{k}_0|) d\mathbf{x}, \qquad i = 1, 2,$$

for wave, transport and diffusion predictions.

**Energies.** We show here that the energy for the wave regime is well approximated by that of transport and diffusion, and that the presence of an inclusion is accurately captured. The wavelengh is assumed to be one so that $|\mathbf{k}_0| = 2\pi$. Since the diffusion regime holds for large time scales, we perform simulations on a fairly large domain of size $600 \times 300$, see figure 1.1. The fluctuations are set to $\sqrt{R_0} = 5\%$. The first step of the simulation is to reconstruct the transport and diffusion parameters, namely the mean free path since the cross-section is isotropic and the diffusion coefficient. The numerical value of $\Sigma^{-1}(|\mathbf{k}_0|)$ is obtained by minimizing the quantity $\|\mathcal{E}^\varepsilon - \mathcal{A}_1\|_{L^2(0,T)}$, where $T = 3000$, *for one realization of the random medium.* The numerical value of the diffusion coefficient $D(|\mathbf{k}_0|)$ is estimated by minimizing $\|\mathcal{E} - \mathcal{U}\|_{L^2(t_0,T)}$, where $t_0$ is a parameter that accounts for the fact that the diffusion limit is not a correct approximation for short times. We set $M = 2|\mathbf{k}_0|$. The found numerical estimation $\Sigma^{-1}_{\text{num}} = 88.5$, see figure 1.2. The relative error on the energies is 1.8%. The theoretical value with $c_0 = 1$ is given by $\Sigma^{-1}_{\text{th}} = 83.0$. However corrected for the slower speed of propagation caused by the discretization, see [9], we find a "theoretical value" (for the discrete waves) of $\Sigma^{-1}_{\text{th}} = 86.9$, which fits extremely well (by 2%) to the numerical estimation.

For the diffusion regime, we set $t_0 = 400$ and obtain for the best fit $D_{\text{num}} = 43.2$. This is to be compared to the theoretical values $D_{\text{th}} = c_0^2(2\Sigma)^{-1} = 39.6$ after correction for the sound speed $c_{\text{num}} = 0.95$. The relative residual error between $\mathcal{E}$ and $\mathcal{U}$ is about 2.0%. The error between the estimated and theoretical values is thus around 8% for $D$. This gives a relatively accurate description of the diffusion coefficient knowing that the computational domain is less than 7 mean free paths

large in the horizontal direction and less than 4 mean free paths large in the vertical direction.

On figure 1.2, right, are represented the quantities $\mathcal{E}^\varepsilon - \mathcal{E}_{\text{inc}}$, $\mathcal{A}_1 - \mathcal{A}_2$ and $\mathcal{U}_1 - \mathcal{U}_2$ capturing the influence of a spherical inclusion of radius $\mathsf{R} = 40$ on the energies. The transport models fits extremely well the wave results, while diffusion models do not. This is related to the fact that there are not enough mean free paths between the source and the inclusion. It is shown in [9], by increasing the strength of the fluctuations that diffusion can also accurately describe the presence of an inclusion in an adequate range of parameters. See also [9] for different types of inclusions or smaller detectors.

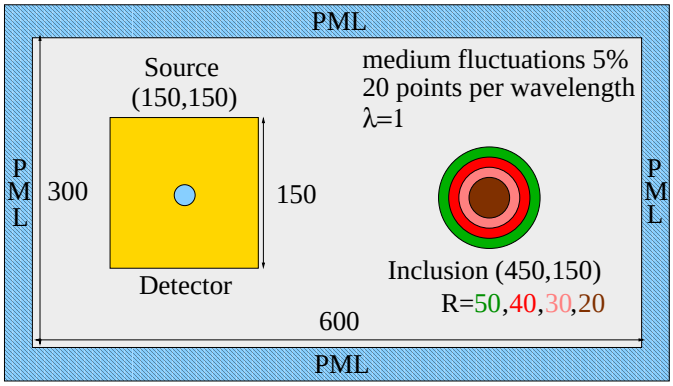


Figure 1.1: Geometry of the problem.

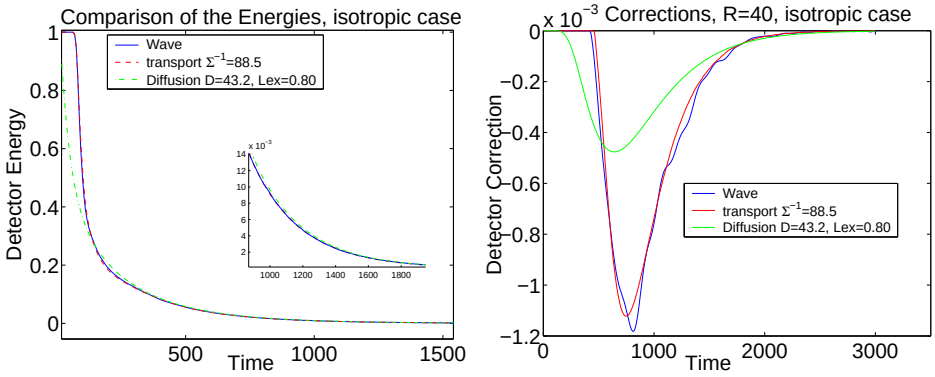


Figure 1.2: Left: representation of $\mathcal{E}^\varepsilon$, $\mathcal{A}_1$ and $\mathcal{U}_1$; Right: Perturbation due to a perfectly reflecting inclusion, representation of $\mathcal{E}^\varepsilon - \mathcal{E}_{\text{inc}}$, $\mathcal{A}_1 - \mathcal{A}_2$ and $\mathcal{U}_1 - \mathcal{U}_2$.

**Correlations.** We show that the correlation $\mathcal{C}^\varepsilon$ is accurately described by its transport approximation with Dirichlet boundary conditions at the inclusion boundary.

Since we are not be interested in the diffusion regime here, we reduce the size of the computational domain to lower the simulation cost. We also increase the fluctuations to $\sqrt{R_0} = 8\%$ so as to obtain a mean free path around 40. The results are represented in figure 1.3, and exhibit a very good agreement between the wave and transport descriptions.

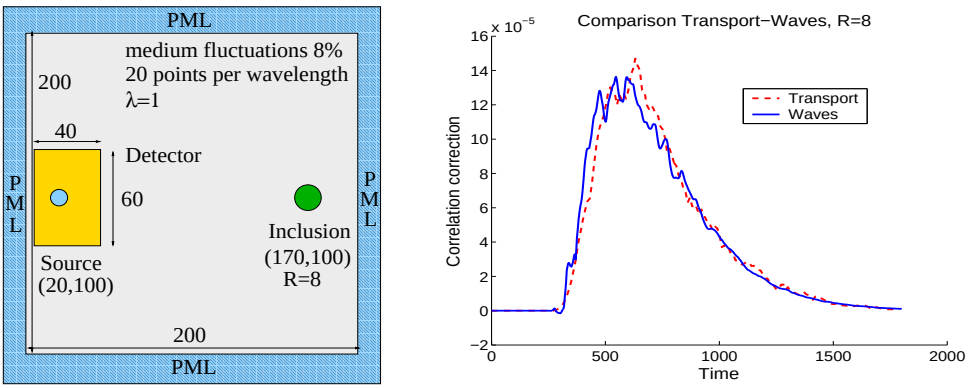


Figure 1.3: Left: domain of computation; Right: representation of $\mathcal{E}^\varepsilon - \mathcal{C}^\varepsilon$ and $\mathcal{A}_1 - \mathcal{A}_{12}$.

**Statistical stability.** We address here the question of how far is $\mathcal{E}^\varepsilon$ from its statistical average $\mathbb{E}\{\mathcal{E}^\varepsilon\}$. Statistical stability of the energy measurements is a crucial component for detection and imaging as was already mentioned earlier. How unstable measurements of $\mathcal{E}^\varepsilon$ depends on several parameters: of course, the level of disorder $R_0$ as well as, as it is shown in chapter 2 for the paraxial approximation, the size of the detector $\mathcal{D}$ or the size of the support of the initial conditions. We will only investigate here the dependence with respect to the support, see [10, 9] for an analysis related to the domain of measurements. As an indicator of the instabilites, we consider the relative standard deviation

$$S(t) = \frac{\sigma\{\mathcal{E}^\varepsilon\}(t)}{\mathbb{E}\{\mathcal{E}^\varepsilon\}(t)},$$

where $\sigma$ denotes standard deviation. The average and the standard deviation are computed over 20 realizations of the random medium and the measurements are performed over an array of size $80 \times 80$ centered at the point $(100, 100)$, see figure 1.4. The initial condition is a zero-th order Bessel function of the first kind localized by a Gaussian function with standard deviation $\sigma = 3, 6, 9, 12$. Figure 1.4, left panel, shows the relative standard deviation $S(t)$ in that configuration. The results are coherent with the theory presented in chapter 2 for the paraxial approximation, meaning the instabilities are stronger as the support gets smaller. The instabilites

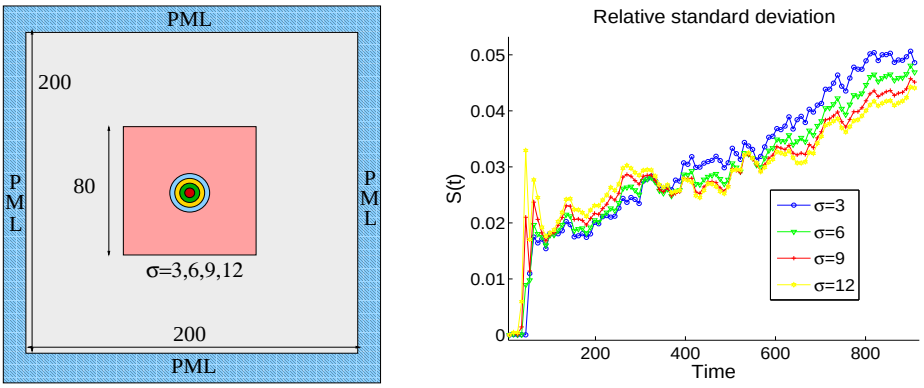


Figure 1.4: Left: domain of computation to evaluate the statistical stability according to the size of the support of the initial condition. Right: relative standard deviation of the energy computed over 20 realizations for the four different sizes of the support.

have typically a magnitude about a few percent of the energy value. In the case where only measurements in presence of an inclusion are available, it is thus required for accurate reconstructions that the inclusion has an influence on the measurements larger than the few percents of the instabilites.

## 1.4 Inverse problem and reconstructions

In this section, we explain what could be the advantages of time reversal compared to direct energy or correlation measurements, we discuss the different imaging scenarios according to the type of available measurements, and finally present some reconstruction results.

### 1.4.1 Time reversal vs direct measurements

We address here the question of the advantages of time reversal. As was seen in section 1.2.3, the time reversal operation is asymptotically described by a filter solution to a radiative transfer equation, as much as the energy density do. The initial conditions for both the filter and the energy being qualitatively equivalent (morally an indicator function for the filter and a Dirac measure for the energy), it is legitimate to wonder how time reversal could be useful in our context, if it is, since time reversal is a more expensive procedure than direct measurements. Energy measurements only require one step (emission then measure), while time reversal requires two steps (emission, measure with time reveral + backpropagation). It is

related to signal-to-noise ratio considerations. For simplicity, we assume $t$, $\mathbf{x}$ and $\mathbf{k}$ are fixed. We distinguish three types of noise:

- Noise $n_{\mathrm{m}}$, with zero mean and variance $\sigma_{\mathrm{m}}$, caused on the transport solutions by the random fluctuations in the underlying medium.
- Noise $\mathbf{n}_{\mathrm{b}}(\mathbf{x})$, with zero mean and variance $\sigma_{\mathrm{b}}$ independent of $\mathbf{x}$, caused on the measured fields at the recording array (assumed additive to model background noise).
- Noise $n_{\mathrm{f}}$, with zero mean and variance $\sigma_{\mathrm{f}}$, caused on the measured filter (assumed multiplicative to model detector defects) at the source location.

The last two noises are classical and merely correspond to errors in the measured data. The first error models the accuracy of the asymptotic transport models. Three mechanisms contribute to the latter error. Firstly, the asymptotic limit is derived in the limit $\varepsilon \to 0$ whereas $\varepsilon$ is finite in practice. Secondly, the estimate on the transport or diffusion parameters may not be perfect and thirdly, the transport models may often be valid only for the statistical average (with respect to the realizations of the random medium). The measured field at the detector is

$$\tilde{\mathbf{u}}^{\varepsilon}(t,\mathbf{x}) = \mathbf{u}^{\varepsilon}(t,\mathbf{x}) + \mathbf{n}_{\mathrm{b}}(\mathbf{x}). \tag{1.9}$$

Assuming the field $\mathbf{u}^{\varepsilon}$ and the noise $\mathbf{n}_{\mathrm{b}}$ are independent, that $\mathbf{n}_{\mathrm{b}}(\mathbf{x})$ and $\mathbf{n}_{\mathrm{b}}(\mathbf{y})$ for two different detectors points at $\mathbf{y} \neq \mathbf{x}$ are weakly correlated to simplify, as well as $\mathbf{u}^{\varepsilon}(\mathbf{x})$ and $\mathbf{u}^{\varepsilon}(\mathbf{y})$, and that the detector $\mathcal{D}$ is sufficiently large so that the law of large numbers applies, we obtain formally

$$\overline{\mathcal{E}}^{\varepsilon}(t) = \mathcal{E}^{\varepsilon}(t) + \sigma_{\mathrm{eb}}^2, \qquad \sigma_{\mathrm{eb}}^2 = \frac{1}{2}|\mathcal{D}|\,\sigma_{\mathrm{b}}^2\,\operatorname{Tr} A, \qquad A = \operatorname{Diag}(\rho_0,\rho_0,\rho_0,\kappa_0),$$

where $\overline{\mathcal{E}}^{\varepsilon}(t)$ is the integrated measured energy on the detector, and $\mathcal{E}^{\varepsilon}(t)$ is the unperturbed integrated data. As $\varepsilon \to 0$, we have $\mathcal{E}^{\varepsilon}(t) \approx \mathcal{A}(t)$, where $\mathcal{A}$ is defined in section 1.3, which we recast as $\mathcal{E}^{\varepsilon}(t) = (1+n_{\mathrm{m}})\mathcal{A}(t)$ to take into account the noise related to the random fluctuations, so that we have finally $\overline{\mathcal{E}}^{\varepsilon}(t) = (1+n_{\mathrm{m}})\mathcal{A}(t)+\sigma_{\mathrm{eb}}^2$. This is the error model for the energy. Regarding the filter $F_{\pm}(T,\mathbf{0},\mathbf{k})$, we recall the initial condition has the form $\mathbf{S}(\mathbf{x}/\varepsilon)$, so that for the energy to be of order one in $d$ dimensions, the initial condition needs to be rescaled as $\varepsilon^{-d/2}\mathbf{S}(\mathbf{x}/\varepsilon)$. The filter is obtained by backpropagating (1.9) for a time $T$. The noise signal $\mathbf{n}_{\mathrm{b}}(\mathbf{x})$ has amplitude and energy of order $\mathcal{O}(1)$ and is not correlated to the true signal $\mathbf{u}^{\varepsilon}(t,\mathbf{x})$. Its amplitude will therefore remain of order $\mathcal{O}(1)$ after back-propagation. In contrast, the true signal $\mathbf{u}^{\varepsilon}(t,\mathbf{x})$ will backpropagate to give a signal of order

$F_+\varepsilon^{-d/2}\hat{\mathbf{S}}_+$, i.e. of order $\varepsilon^{-d/2}$ in the vicinity of $\mathbf{0}$. We can thus model the measured filter $F_\pm$ as

$$\overline{F}_\pm = (1 + n_\mathrm{f} + n_\mathrm{m})F_\pm + \varepsilon^{3/2} n_\mathrm{bb},$$

where $n_\mathrm{bb}$ is obtained by backpropagating $\mathbf{n}_\mathrm{b}(\mathbf{x})$ through the random medium for a time $T$. Thanks to the powerful refocusing property of time reversed waves, the amplitude of the back-propagated measured signal is of order $\varepsilon^{-d/2}$. This implies that the signal-to-noise ratio $F/n_\mathrm{bb} \sim \varepsilon^{-d/2}$, which renders legitimate the assumption that the errors performed in the measurements are multiplicative rather than additive, since the additive noise can be neglected. The only advantage of time reversal measurements over energy measurements is therefore that they enjoy a better signal-to-noise ratio at the price of a higher technological cost.

### 1.4.2 Imaging scenarios

The goal of this section is to compare the measurements of the energy $\mathcal{E}^\varepsilon_\mathrm{inc}$ and the correlation $\mathcal{C}^\varepsilon$. We mention three possible scenarios and give their advantages and disadvantages. We leave alone time reversal knowing the scenarios are identical and that the only difference is the strength of the background noise.

(i) In the first scenario, we are only able to measure $\mathcal{E}^\varepsilon_\mathrm{inc}$. We do not have access to measurements in the *absence* of the inclusion and thus cannot form $\mathcal{E}^\varepsilon_\mathrm{inc} - \mathcal{E}^\varepsilon$, let alone $\mathcal{C}^\varepsilon - \mathcal{E}^\varepsilon$.

(ii) In the second scenario, we can estimate energy densities $\mathcal{E}^\varepsilon$ and $\mathcal{E}^\varepsilon_\mathrm{inc}$ and thus can form the difference $\mathcal{E}^\varepsilon_\mathrm{inc} - \mathcal{E}^\varepsilon$. We may not be able to measure wave fields accurately enough to form $\mathcal{C}^\varepsilon$.

(iii) In the last scenario, we can measure $\mathbf{u}^i_\varepsilon$ for $i = 1, 2$ accurately and thus can form $\mathcal{E}^\varepsilon$, $\mathcal{E}^\varepsilon_\mathrm{inc}$, and $\mathcal{C}^\varepsilon$ as well as the differences $\mathcal{E}^\varepsilon_\mathrm{inc} - \mathcal{E}^\varepsilon$ and $\mathcal{C}^\varepsilon - \mathcal{E}^\varepsilon$.

These scenarios are increasingly constraining technologically and practically. Imaging is hardest in the first scenario. The reason is that the measurements are inevitably noisy because the random wave energy density becomes deterministic only at the limit $\varepsilon \to 0$ so that it is statistically stable (independent of the realization of the random medium) only up to a certain point. The influence of the inclusion, modeled by $a^1_+ - a^2_+$ in the transport regime and by $U^1 - U^2$ in the diffusive regime, thus has to be larger than the noise level coming from our lack of knowledge of the specific realisation of the random medium.

Imaging is much simplified in scenarios (ii) and (iii) because we can form differential measurements: i.e., the difference of measurements in the absence and in the

presence of the inclusion. Scenario (ii) requires energy measurements only, which ideally may be performed at a more macroscopic level than the wavelength, and are thus technologically less demanding than the measurements required in scenario (iii) to form accurate correlations.

Both scenarios (ii) and (iii) allow us to remove a substantial amount of noise coming from our lack of knowledge of the specific realization of the random medium. The reason is simple: path emanating from the source term and reaching the array of detectors without hitting the inclusion are not known exactly. They generate considerable noise in scenario (i). However, they cancel in scenarios (ii) and (iii) when we form the differences $\mathcal{E}^\varepsilon_{\rm inc} - \mathcal{E}^\varepsilon$ and $\mathcal{C}^\varepsilon(t,\mathbf{x}) - \mathcal{E}^\varepsilon$. In the latter two measurements, noise has to be proportional to the *product* of the size of the inclusion with our lack of knowledge of the random medium. Such a product is therefore quite small, see [2] for a formal analysis.

To compare scenarios (ii) and (iii), we assume the inclusion is a ball of radius $\mathsf{R}$ with small volume fraction compared to the overall domain. We showed in [7] that the influence of the inclusion of the energy and on the correlation are at the transport level

$$\mathbb{E}\{\mathcal{E}^\varepsilon\} - \mathbb{E}\{\mathcal{E}^\varepsilon_{\rm inc}\} \approx \mathcal{O}(\mathsf{R}^{d-1}) \qquad ; \qquad \mathbb{E}\{\mathcal{E}^\varepsilon\} - \mathbb{E}\{\mathcal{C}^\varepsilon\} \approx \mathcal{O}(\mathsf{R}^{d-1}).$$

Therefore, both differences are same order. In the light of this, we may thus think there is not interest in using correlations if the effect of the inclusion is same order on both observables. Nevertheless, taking into account the statistical instabilites, that determine how close is for instance $\mathcal{E}^\varepsilon - \mathcal{E}^\varepsilon_{\rm inc}$ from its average $\mathbb{E}\{\mathcal{E}^\varepsilon\} - \mathbb{E}\{\mathcal{E}^\varepsilon_{\rm inc}\}$, we showed formally in [2], and validated numerically as well, that $\mathcal{E}^\varepsilon - \mathcal{C}^\varepsilon$ is more stable than the energy difference so that there is still an interest in using correlations in the transport regime if they are available. This fact is illustrated in figure 1.5, where $\mathcal{E}^\varepsilon - \mathcal{E}^\varepsilon_{\rm inc}$ and $\mathcal{E}^\varepsilon - \mathcal{C}^\varepsilon$ are represented for three differents realizations of the random medium for the configuration of figure 1.6.

The situation is different in the diffusive regime. For the correlations, because of increasing scattering, more and more paths reach the inclusion where they are absorbed since the correlation satisfies Dirichlet boundray conditions at the inclusion boundary. The net effect of the inclusion on measurements is therefore stronger. Regarding the energy, it is conserved at the boundary of the inclusion because of the Neumann conditions (specular reflection in the transport regime), and some symmetries render the correction proportional to $\mathsf{R}^d$. We thus find, see [7] and also chapter 3, for $d \geq 3$,

$$\mathbb{E}\{\mathcal{E}^\varepsilon\} - \mathbb{E}\{\mathcal{E}^\varepsilon_{\rm inc}\} \approx \mathcal{O}(\mathsf{R}^{d}) \qquad ; \qquad \mathbb{E}\{\mathcal{E}^\varepsilon\} - \mathbb{E}\{\mathcal{C}^\varepsilon\} \approx \mathcal{O}(\mathsf{R}^{d-2}).$$

When scattering is strong, correlations of the form $\mathcal{C}^\varepsilon$ provide more signal to detect and image small volume inclusions than do energy measurements. Scenario

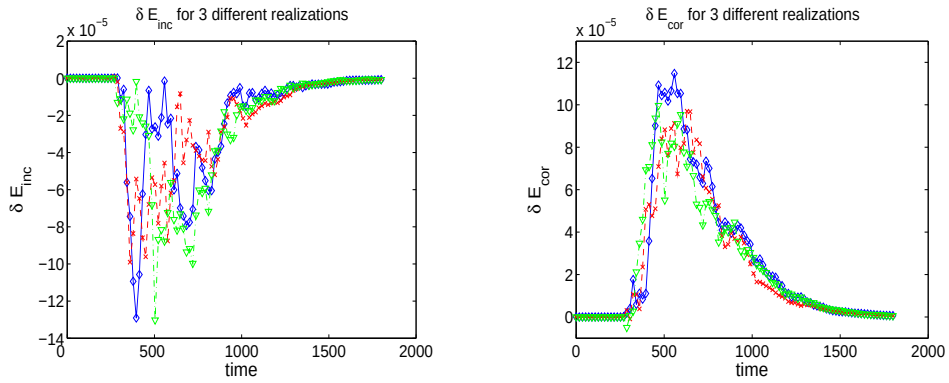


Figure 1.5: Representation of $\delta\mathcal{E}_{\rm inc} = \mathcal{E}^\varepsilon - \mathcal{E}^\varepsilon_{\rm inc}$ and $\delta\mathcal{E}_{\rm cor} = \mathcal{E}^\varepsilon - \mathcal{C}^\varepsilon$ for three different realizations of the random medium and a ball of radius 8.

(iii) becomes optimal among the three considered scenarios.

### 1.4.3 Reconstructions

We present here the procedure we use to reconstruct the inclusion. We are interested in fairly strong medium fluctuations with significantly small mean free paths. In this setting, available data are primarily incoherent, that is the fraction of the wave that has been scattered by the random medium is dominant. The coherent part of the waves is damped by the fluctuations and becomes negligible compared to the incoherent part. Imaging in this configuration is difficult and is possible essentially in two cases, as claimed in the preceding section; (i) either the inclusion is large enough to overcome statistical instabilities and reconstructions can be performed from knowledge of the energy in presence of inclusion $\mathcal{E}^\varepsilon_{\rm inc}$; or (ii) the inclusion's influence on the data is smaller and in this case differential measurements are needed, that is we need to measure the energies both in the presence and in the absence of the inclusion. In the latter case, the measurements are $\mathcal{E}^\varepsilon_{\rm inc} - \mathcal{E}^\varepsilon$ and the statistical instabilities are reduced since they are now proportional to the size of the inclusion. For computational purposes, we consider the setting where measurements are available both in the presence and the absence of the inclusion since it requires smaller computational domains. We also assume that measurements can be performed at the wavelength scale so that we have access to the wave fields $\mathbf{u}^\varepsilon_1$ and $\mathbf{u}^\varepsilon_2$ and the correlation $\mathcal{C}^\varepsilon$ can be computed.

Consider therefore that we know from wave measurements the quantities $\mathcal{E}^\varepsilon_{\rm inc} - \mathcal{E}^\varepsilon$ and $\mathcal{C}^\varepsilon - \mathcal{E}^\varepsilon$. The imaging procedure then consists of finding the transport predictions $a_2^+ - a_1^+$ and $a_{12}^+ - a_1^+$, which depend on the inclusion, that best fit the measurements $\mathcal{E}^\varepsilon_{\rm inc} - \mathcal{E}^\varepsilon$ and $\mathcal{C}^\varepsilon - \mathcal{E}^\varepsilon$. This requires in the first place that we estimate

the power spectrum $\hat{R}$ and the mean free time $\Sigma^{-1}$ that characterize the transport equation (1.4). Once these parameters are known, an inverse transport problem is solved to find the inclusion location.

Some examples of obtained results are the following. We define first the influence of the inclusion on the measurements by $\delta\mathcal{E}_{\rm inc} = \mathcal{E}^\varepsilon - \mathcal{E}^\varepsilon_{\rm inc}$ for the wave fields and $\delta\mathcal{A}_{\rm inc} = \mathcal{A}_1 - \mathcal{A}_2$ for transport quantities. The influence of the inclusion on the correlations is denoted by $\delta\mathcal{E}_{\rm cor} = \mathcal{E}^\varepsilon - \mathcal{C}^\varepsilon$ for the wave fields and by $\delta\mathcal{A}_{\rm cor} = \mathcal{A}_1 - \mathcal{A}_{12}$ for transport. We suppose the inclusion is a ball centered at $(X, Y)$ with radius $\mathsf{R}$. The data $\delta\mathcal{E}_{\rm inc}$ and $\delta\mathcal{E}_{\rm cor}$ are smoothed out by a Gaussian filter $G$ to lower the statistical instabilities, see [2]. To estimate the set of parameters $\mathcal{S} = (X, Y, \mathsf{R}) \subset \mathbb{R}^3_+$, we minimize for $i = 1, \cdots, 20$ realizations of the random medium the quantities

$$\frac{\|G * \delta\mathcal{E}^i_{\rm inc} - \delta\mathcal{A}_{\rm inc}[\mathcal{S}]\|_{L^2(0,T)}}{\|\mathcal{E}^\varepsilon_i\|_{L^2(0,T)}} \quad \text{and} \quad \frac{\|G * \delta\mathcal{E}^i_{\rm cor} - \delta\mathcal{A}_{\rm cor}[\mathcal{S}]\|_{L^2(0,T)}}{\|\mathcal{E}^\varepsilon_i\|_{L^2(0,T)}}$$

for the energy and the correlation, respectively. $G * \delta\mathcal{E}^i_{\rm inc}$ and $G * \delta\mathcal{E}^i_{\rm cor}$ are the regularized versions of $\delta\mathcal{E}^i_{\rm inc}$ and $\delta\mathcal{E}^i_{\rm cor}$. We then obtain two distributions of the estimated parameters $\hat{S}^i_{\rm inc}$ and $\hat{S}^i_{\rm cor}$, $i = 1, \cdots, 20$. The time $T$ is set to 1800. We consider the two configurations depicted in figure 1.6 for 8% of fluctuations and a wavelength equal to one. The inclusion is located at $(170, 160)$, has a radius $\mathsf{R} = 8$ in configuration 1, and $\mathsf{R} = 20$ in configuration 2 with the particularity that it is hidden behind a blocker with no line-of-sight. No coherent information is therefore available, and it is typically in that situation that interferometry methods would fail for instance.

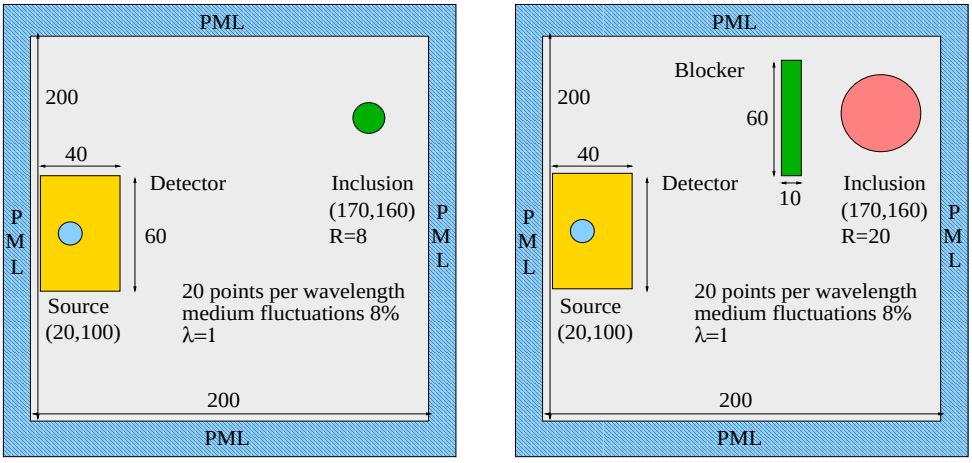


Figure 1.6: Configuration 1 on the left for an inclusion of radius $\mathsf{R} = 8$, and configuration 2 on the right with blocker for an inclusion of radius $\mathsf{R} = 20$.

The results of the reconstructions are gathered in table 1.1 below and are depicted in figure 1.7 for configuration 1 and in 1.8 for configuration 2. We give the

averaged values over 20 realizations of $X$, $Y$ and $\mathsf{R}$, as well as the standard deviations $\Delta X$, $\Delta Y$ and $\Delta\mathsf{R}$. We remark that in both configurations, the results are very close to the exact location of the inclusion, even though $\varepsilon$ is small but not zero ($\varepsilon = \frac{1}{200}$) and the fact we used an elementary second order in time and space numerical scheme for the acoustic wave equation.

| | Conf. 1 ($\mathsf{R} = 8$) | | Conf. 2 with blocker ($\mathsf{R} = 20$) | |
|---|---|---|---|---|
| | energy | correlation | energy | correlation |
| $\mathsf{R}$ | 8.10 | 6.67 | 18.28 | 19.49 |
| $\Delta\mathsf{R}$ | 1.87 | 1.54 | 2.44 | 1.75 |
| $X$ | 169.20 | 167.84 | 161.78 | 160.46 |
| $\Delta X$ | 10.65 | 5.70 | 17.76 | 12.90 |
| $Y$ | 162.64 | 156.45 | 160.70 | 161.58 |
| $\Delta Y$ | 12.12 | 4.11 | 11.97 | 7.67 |

Table 1.1: Reconstruction results. The exact location of the inclusion is $(X, Y) = (170, 160)$ with radii $\mathsf{R} = 8$ or $\mathsf{R} = 20$. Statistics are performed over 20 realizations.

For configuration 1, averaged results are accurate by around 2% on the position for both energy and correlation measurements. Regarding the radius, averaged reconstructions using correlations are a bit less accurate than with energies, $\mathsf{R} = 6.67$ to be compared with $\mathsf{R} = 8.10$ for instance, but are more stable. Indeed, we observe a standard deviation on the position $X$ of about 6% for energies with half this value for the correlations, and of 7.5% on $Y$ for energies with 2.5% for correlations. Standard deviations are comparable for the radius. The larger error on the radius is likely due to the fact that radiative transfer is less precise close to the inclusion and that interference effects need to be accounted for. In such a configuration, the statistical instabilities have a fairly important influence on the reconstructions since the correction due to the inclusion is rather weak so that the signal-to-noise ratio is lower than for cases where the radius is larger, see for instance results for $\mathsf{R} = 20$ in [2]. As we have mentioned in section 1.4.2, noise is larger for energies than correlations, which explains the more stable reconstructions of the position of the center of the inclusion. Without the convolution with the filter $G$ that smoothes out high-frequency statistical instabilities, the amount of noise would have been much larger on the energies and reconstructions would have been more difficult, if even possible.

For configuration 2, we remark that the average value of the radius is close to the exact value by about 9% and 2.5% using energies and correlations, respectively. The corresponding standard deviations are about 12.2% and 8.7%. The average of the $X$ coordinates fits the exact value by about 6% for both energies and correlations, with

standard deviations of 10% for the energy and 7.5% for the correlation. The average of the $Y$ coordinates fits the exact value by less than 1%, with standard deviations of 7.5% for the energy and 4.8% for the correlation. Within this configuration, correlations yield a stability about 50% better than that of energies for the radius and the $Y$ coordinates. The slight increase in statistical instabilities compared to configuration 1 is due to the presence of the blocker, which renders the measurements more faint and therefore more sensitive to the random fluctuations even though the size of the ball has been augmented.

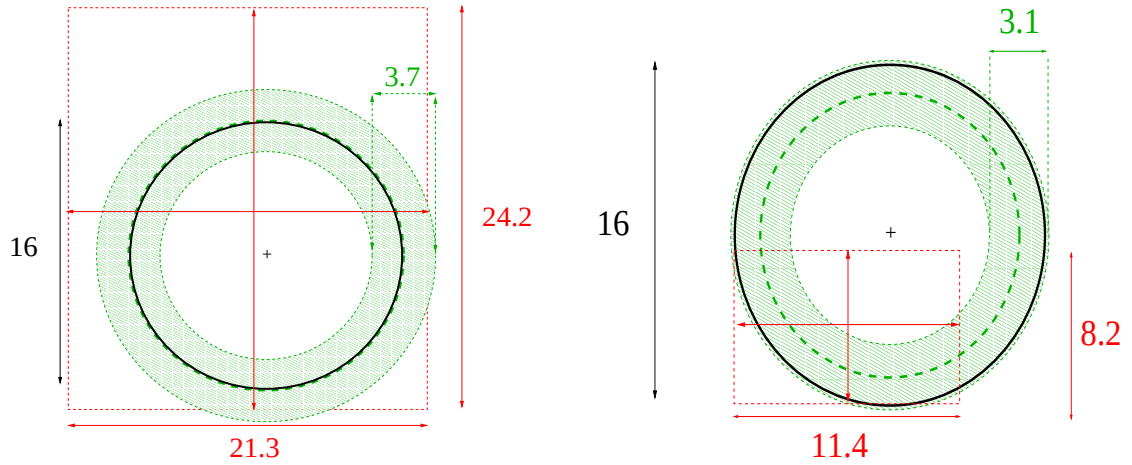


Figure 1.7: Reconstructions for configuration 2 (R=8) using energies (left) and correlations (right). The black circle represents the exact radius and the cross the exact location of the ball center. The dashed circle corresponds to the average reconstructed radius R, and the shaded zone around circles of radii $\mathsf{R} \pm \Delta\mathsf{R}$. The center of the dashed rectangle is the average reconstructed ball center $(X, Y)$ and its dimensions are $2\Delta X \times 2\Delta Y$.

## 1.5 Conclusion and perspectives

In this chapter, we derived imaging models based on radiative transfer equations to reconstruct an inclusion embedded in a random medium with sufficiently strong disorder that methods based on wave propagation in a homogeneous medium are inaccurate. We also considered the case of time reversal and showed its only advantage here is an increase of signal-to-noise ratio. From wave measurements, the position and the radius of a spherical inclusion were estimated by solving an inverse transport problem, the presence of the inclusion being seen as a perturbation of the transport parameters. Two different observables were considered as inputs for the inverse problem: the wave energy and the correlation between the wavefield in

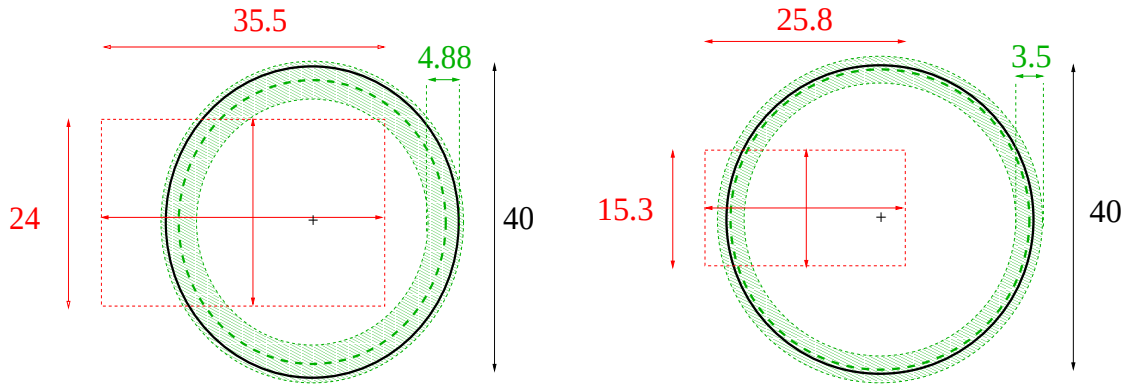


Figure 1.8: Reconstructions for configuration with blocker (R=20) using energies (left) and correlations (right). The black circle represents the exact radius and the cross the exact location of the ball center. The dashed circle corresponds to the average reconstructed radius R, and the shaded zone around circles of radii $\mathsf{R} \pm \Delta\mathsf{R}$. The center of the dashed rectangle is the average reconstructed ball center and its dimensions are $2\Delta X \times 2\Delta Y$.

the presence of the inclusion and the wavefield without an inclusion. Such reconstructions are possible since energy and correlation are statistically stable quantities in the limit of vanishing wavelength. Using the scattering properties of the random medium, we have also reconstructed inclusions hidden behind a blocker that prevents any coherent information from being measured at the array of detectors.

Different paths can be taken to improve or extent this work. The enhancement of the reconstructions accuracy cannot be done without a better understanding of the statistical instabilities that are the major limitations of the transport models. Models for such instabilities are not available at the present time for the random wave equation. They could be derived by characterizing the first-order corrector to transport. This is done in chapter 2 in the *Itô-Schrödinger regime* for the variance of the corrector only. In the recent work [91], a stochastic equation for the corrector has been obtained for a particular type of initial conditions within the same regime. Doing so for to the random wave equation seems so far out of reach, yet it is likely an equation for the simple scattering contribution of the corrector can be derived. By simple scattering, we mean the fraction of the wave that has interacted only once with the medium. Even though this would not thoroughly characterize the instabilities, taking the simple scattering corrector into account in the models would presumably lower the statistical instabilities and subsequently improve the accuracy of the reconstructions. Also, it is well-known in a one dimensional setting, see e.g. [71], that the statistical stability is strongly related to the possibility of summing over frequency. This would require here to solve independent transport equations for each fixed frequency and would possibly yield more stable results.

We considered here random media with *short-range* correlations, while phenomena with long distance dependence are ubiquitous in nature, e.g. in turbulent atmosphere, plasmas, geophysics of biology. They have to be included in the imaging procedure to model physics as precisely as possible. Long-range correlations will modify the cross-section so as to render it singular near the origin. This raises many difficulties: the concept of solutions of the related transport equations is unclear for such cross-sections and designing a convenient numerical method of resolution is not straightforward; besides, does statistical stability still hold true for such media? This is paramount for imaging theory, and it is shown in chapter 2 in a particular setting that instabilites are higher in such a context; also, is there a smooth transition between short-range and long-range regimes? All these questions may be answered by following the same route we did for media with short-range correlations.

A thorough comparison of transport-based imaging and interferometry methods still remains to be done. We already mentioned these last ones perform well when the medium fluctuations are moderate since they are based on back-propagation of cross-correlated fields in a homogeneous medium supposed to model the true medium. This is not quite accurate for highly heterogeneous media. Nevertheless, in a work in progress with G. Bal not detailed in this document, we show that if the offsets of the cross-correlations are well chosen, then the corresponding correlations are indeed propagating in an homogeneous medium. The method thus amounts to filtering some correlations to propagate only the right ones. The practical computation of the offsets is extremely difficult and still needs to be worked out. In spite of that, using the method with approximated offsets exhibits fairly interesting results and an increase of the signal-to-noise ratio.

# Chapter 2

# Asymptotics and statistical stability

In this chapter, we are intererested in the high-frequency asymptotics of waves propagating in random media within the *paraxial approximation*. Depending on the physical setting, several models can be derived. The ones we deal with here are described by either a *Itô-Schrödinger equation* or by a *Schrödinger equation with time-independent random potential*. The asymptotic analysis is performed by means of Wigner transforms that may be seen as a phase space decomposition of the energy density. It is well known that the ensemble average of the Wigner function satisfies at the limit a *radiative transfer equation* with a scattering cross-section depending on some statistical properties of the random potential. Much less is known about the limit of the *whole process* related to the Wigner transform and not only its average. We present here some results of statistical stability, that is situations where the whole process converges to its average. An appropriate tool for the analysis is the scintillation function, which is the covariance function of the Wigner transform and whose convergence to zero implies the convergence in probability. In particular:

- We obtain optimal rates of convergence according to some physical parameters of the problem, as the domain of measurements or the regularity of the initial conditions. For instance, if $\eta \ll 1$ is the dimensionless transversal wavelength, statistical stability is observed in the Itô-Schrödinger regime for smooth initial conditions as soon as the Wigner function is averaged over a spatial domain of typical size $\eta^{1-s_1}$, for $s_1 > 0$ [6].

- We characterize the statistical instabilities by computing the first-order corrector for the Itô-Schrödinger regime scintillation, and obtain for instance that

the instabilities come from either simple of double scattering, that is the fraction of the wave that has interacted once or twice with the medium, but not from higher scattering events [3].

- For the Schrödinger equation with time-independent random potentials with long-range correlations, we consider the simple scattering contribution to the scintillation and show by computing the first-order scintillation corrector that statistical stability occurs for any dimension and any decay of the correlation function provided the power spectrum of the fluctuations is integrable [5].

## 2.1 Introduction

We are interested here in the asymptotic analysis of the classical random scalar wave equation for the pressure $p(t, \mathbf{x}, z)$, where $t$ is time, $\mathbf{x} \in \mathbb{R}^d$, $z \in \mathbb{R}$, (so that the overall spatial dimension is $d+1$), that reads, for a random sound speed $c(\mathbf{x}, z)$ :

$$\frac{\partial^2 p}{\partial t^2}(t, \mathbf{x}, z) = c^2(\mathbf{x}, z) \left(\Delta_{\mathbf{x}} + \Delta_z\right) p(t, \mathbf{x}, z), \qquad t > 0,$$

equipped with appropriate initial conditions. We will assume that the wave has a privileged direction of propagation (here $z$) and backscattering effects can be neglected so that the regime of *paraxial approximation* holds. See for instance [77] and subsequent papers for situations where backscattering is significant. To precise the physical setting, let $L_x$ and $L_y$ be the typical distances of propagation in the directions $\mathbf{x}$ and $z$, and let $\delta_x$ and $\delta_y$ be the typical lengths (correlation lengths) at which the random sound speed fluctuates. Since it is assumed that the beam mainly propagates in the $z$ direction, the pressure $p$ is sought under the form

$$p(t, \mathbf{x}, z) = \frac{1}{2\pi} \int_{\mathbb{R}} e^{ik(z - c_0 t)} \psi(z, \mathbf{x}, k) c_0 dk,$$

where $\psi(z, \mathbf{x}, k)$ is the amplitude associated to the wavenumber $k$ and $c_0$ is the statistical average of the random sound speed $c$, supposed to be constant for simplicity. Plugging that expression into the wave equation, it comes

$$\frac{\partial^2 \psi}{\partial z^2} + 2ik \frac{\partial \psi}{\partial z} + \Delta_{\mathbf{x}} \psi + k^2 (n^2 - 1) \psi = 0,$$

where $n(\mathbf{x}, z) = c_0 / c(\mathbf{x}, z)$ is the refraction index. Introducing

$$(n^2 - 1)(\mathbf{x}, z) = V_0 V \left( \frac{\mathbf{x}}{l_x}, \frac{z}{l_z} \right), \qquad V_0 \in \mathbb{R},$$

and rescaling $\mathbf{x}$, $z$ as $L_x \mathbf{x}$, $L_z z$, we find

$$-\frac{i}{2kL_z} \frac{\partial^2 \psi}{\partial z^2} + \frac{\partial \psi}{\partial z} - \frac{iL_z}{2kL_x^2} \Delta_{\mathbf{x}} \psi - \frac{ikL_z V_0}{2} V \left( \frac{L_x \mathbf{x}}{l_x}, \frac{L_z z}{l_z} \right) \psi = 0.$$

Starting from the equation above, many asymptotic regimes can be derived, see for instance [78, 100] for a thorough survey. For the ones we are interested here, we define the following dimensionless parameters, with $k := \frac{2\pi}{\lambda}$, $\lambda$ being a typical wavelength of the problem:

$$\varepsilon = \frac{\lambda}{4\pi L_x} \quad ; \quad \eta = \frac{l_x}{L_x} \quad ; \quad \delta = \frac{l_z}{L_z} \quad ; \quad \gamma = \frac{L_x}{L_z} \quad ; \quad \alpha = \frac{l_z}{\lambda}.$$

We have consequently,

$$-i\varepsilon\gamma\frac{\partial^2\psi}{\partial z^2}+\frac{\partial\psi}{\partial z}-\frac{i\varepsilon}{2\gamma}\Delta_{\mathbf{x}}\psi-\frac{i\pi V_0\alpha}{\delta}V\left(\frac{\mathbf{x}}{\eta},\frac{z}{\delta}\right)\psi=0. \tag{2.1}$$

We consider two regimes: *the Itô-Schrödinger regime* in which the variations of the sound speed in the $z$ direction are faster than anything else in the problem and lead to some averaging thanks to the central limit theorem; a second regime somehow opposite to the first one in which the variations of the sound speed in the $z$ direction are so slow that the sound speed can be considered as independent of $z$. This regime is modeled by a *random Schrödinger equation* and is often encountered in quantum physics when describing the motion of a particule in a random time-independent potential.

**The Itô-Schrödinger regime.** It is assumed that

- $\alpha \ll 1$ (fast $z$ variations of the sound speed compared to the wavelength),
- $\varepsilon \ll 1$ (high frequencies),
- $\eta \ll 1$, $\delta \ll 1$ (small correlation lengths),
- $\gamma \ll 1$ (small angle of propagation),

with the following relations between the parameters, $\delta \ll \eta$, $\varepsilon = \eta\,\gamma$, $\pi V_0\alpha = \sqrt{\delta}$. Then (2.1) can be recast as

$$-i\varepsilon\gamma\frac{\partial^2\psi}{\partial z^2}+\frac{\partial\psi}{\partial z}-\frac{i\eta}{2}\Delta_{\mathbf{x}}\psi-\frac{i}{\sqrt{\delta}}V\left(\frac{\mathbf{x}}{\eta},\frac{z}{\delta}\right)\psi=0.$$

Formally neglecting the term $\varepsilon\gamma\frac{\partial^2\psi}{\partial z^2}$ and assuming that $V$ is a mean-zero process with sufficiently short-range correlations, the central limit theorem leads to the *Itô-Schrödinger equation*, written in Itô form:

$$d\psi(z,\mathbf{x})=\frac{1}{2}\big(i\eta\Delta_{\mathbf{x}}-R(\mathbf{0})\big)\psi(z,\mathbf{x})dz+i\psi(z,\mathbf{x})B\Big(\frac{\mathbf{x}}{\eta},dz\Big). \tag{2.2}$$

Here, $B(\mathbf{x},dz)$ is a standard (infinite dimensional) Wiener measure, whose statistics are described by

$$\mathbb{E}\{B(\mathbf{x},z)B(\mathbf{y},z')\}=R(\mathbf{x}-\mathbf{y})z\wedge z', \tag{2.3}$$

where $\mathbb{E}$ is mathematical expectation with respect to the measure of an abstract probability space $(\Omega,\mathcal{F},\mathbb{P})$ on which $B(\mathbf{x},dz)$ is defined, $z\wedge z'=\min(z,z')$ and $R$ is the correlation function of the random medium. A rigorous passage from the wave equation to (2.2) is a difficult task and some results can be found in [25] when $d=2$ and in stratified media, see also [79].

**The random Schrödinger equation.** We still make the hypotheses $\varepsilon \ll 1$, $\eta \ll 1$ and $\gamma \ll 1$, with now $\delta \gg 1$, modeling slow variations of the sound speed in the $z$ direction, and assume the following relations, $\varepsilon = \eta\,\gamma$, $\frac{\pi V_0 \alpha}{\delta} = \sqrt{\eta}^{-1}$. Neglecting formally again the term $\varepsilon\gamma\frac{\partial^2\psi}{\partial z^2}$, one finds *the random Schrödinger equation:*

$$\left(i\eta\frac{\partial}{\partial z} + \frac{\eta^2}{2}\Delta_{\mathbf{x}} + \sqrt{\eta}V\left(\frac{x}{\eta}, 0\right)\right)\psi(z,\mathbf{x}) = 0, \quad z > 0, \quad x \in \mathbb{R}^d. \tag{2.4}$$

**High-frequency asymptotics and radiative transfer equations.** The high-frequency asymptotics of (2.2) or (2.4) leads to radiative transfer equations. The appropriate tool in the analysis of such equations is the *Wigner transform* [110] of the wavefunction defined as

$$W_\eta[\psi_\eta](z,\mathbf{x},\mathbf{k}) = W_\eta(z,\mathbf{x},\mathbf{k}) = \frac{1}{(2\pi)^d}\int_{\mathbb{R}^d} e^{i\mathbf{k}\cdot\mathbf{y}}\psi_\eta\Big(z, \mathbf{x} - \frac{\eta\mathbf{y}}{2}\Big)\overline{\psi_\eta}\Big(z, \mathbf{x} + \frac{\eta\mathbf{y}}{2}\Big)d\mathbf{y}, \tag{2.5}$$

where the solution to (2.2) or (2.4) is now denoted by $\psi_\eta$ and $\overline{\psi_\eta}$ is the complex conjugate of $\psi_\eta$. The Wigner transform $W_\eta$ is real-valued and $\int_{\mathbb{R}^d} W_\eta(t,\mathbf{x},\mathbf{k})d\mathbf{k} = |\psi_\eta(\mathbf{x},t)|^2$ by inverse Fourier transform so that $W_\eta$ may be seen as a phase space (microlocal) decomposition of the energy density, even though it is not always positive. We refer the reader to [94, 80] for an extensive study of Wigner transforms with applications to high-frequency limit of hyperbolic or Schrödinger equations.

The rigorous derivations of radiative transfert equations that can be found in the literature depend very much on the structure of the random potential and whether or not it depends on the $z$ variable, and at which scale. Such a $z$ dependence usually provides additional averaging that helps passing to the limit. We refer for instance to [31, 32, 102] where $V$ is Markovian with respect to time or has with finite-range time correlations, or to [65, 66, 67]. See also the recent paper [30] for an analysis of the phase of the wavefunction. On the contrary, when $V$ is independent of $z$, the derivation is much more involved, see [64, 109], and extensively uses diagrammatic expansions of the solution. One can refer to [63, 62] for a direct limit from a Schrödinger equation to a diffusion equation.

The typical obtained result is the following: under appropriate conditions on the initial condition $\psi_\eta^0 := \psi_\eta(t=0,\cdot)$, the *ensemble average* of the Wigner transform $a_\eta := \mathbb{E}\{W_\eta\}$ converges weakly in an adapted functional setting to the solution $a$ of the following radiative transfer equation (or linear Boltzmann equation):

$$\Big(\frac{\partial}{\partial z} + \mathbf{k}\cdot\nabla_{\mathbf{x}} + R_0 - \mathcal{Q}\Big)a(z,\mathbf{x},\mathbf{k}) = 0, \qquad a(0,\mathbf{x},\mathbf{k}) = a_0(\mathbf{x},\mathbf{k}), \tag{2.6}$$

where $a_0$ is the limit of the ensemble average of the Wigner transform of the initial

condition $\psi_\eta^0$, and the scattering operator $\mathcal{Q}$ and $R_0$ read

$$(\mathcal{Q}a)(z,\mathbf{x},\mathbf{k}) \;=\; \int_{\mathbb{R}^d} \sigma(\mathbf{k},\mathbf{k}')a(z,\mathbf{x},\mathbf{k}')d\mathbf{k}', \quad R_0(\mathbf{k}) = \int_{\mathbb{R}^d} \sigma(\mathbf{k},\mathbf{k}')d\mathbf{k}'.$$

The scattering cross section $\sigma$ depends on the structure of the random potential $V$. For instance, when $V$ is independent of $z$, $\sigma(\mathbf{k},\mathbf{k}') = \hat{R}(\mathbf{k}-\mathbf{k}')\delta(|\mathbf{k}|^2 - |\mathbf{k}'|^2)$, where $\delta$ is the Dirac distribution and $\hat{R}$ denotes the Fourier transform of $R$ with the convention $\hat{R}(\mathbf{k}) = \mathcal{F}R(\mathbf{k}) = \int_{\mathbb{R}^d} e^{-i\mathbf{k}\cdot\mathbf{x}}R(\mathbf{x})d\mathbf{x}$. Since $R(\mathbf{x})$ is a correlation function, $\hat{R}(\mathbf{k})$ is non-negative by Bochner's theorem. $\hat{R}$ is called the power spectrum of the random medium. For the Itô-Schrödinger regime, one has $\sigma(\mathbf{k},\mathbf{k}') = \hat{R}(\mathbf{k}-\mathbf{k}')$.

The derivation of (2.6) from the Itô-Schrödinger equation (2.2) is immediate since moments of the wavefunction satisfy closed-form equations. Starting from (2.2) and writing the stochastic equation for the Wigner transform, a direct application of the Itô calculus yields that $a_\eta$ solves (2.6) with an initial condition $a_{\eta 0} := \mathbb{E}\{W_\eta[\psi_\eta^0]\}$, see for instance [100]. It then suffices to pass to the limit in the initial condition to obtain the convergence of $a_\eta$ to $a$.

Whereas the limit of $\mathbb{E}\{W_\eta\}$ can be characterized in various settings, much less is known about the limit of the whole process $W_\eta$. It is proved in [32], under additional hypotheses on the Wigner transform (basically it is given by a mixed state so as to obtain $L^2$ estimates), that $W_\eta[\psi_\eta]$ converges weakly and in probability to its average $\mathbb{E}\{W_\eta[\psi_\eta]\}$, that is

$$\mathbb{P}\Big(|\langle W_\eta(z),\varphi\rangle - \langle a_\eta(z),\varphi\rangle| \geq \delta\Big) \to 0, \qquad \text{uniformly on compact intervals.}$$

Above, $\varphi$ is a test function in the Schwarz space $\mathcal{S}(\mathbb{R}^{2d})$ and $\langle\cdot,\cdot\rangle$ denotes the $\mathcal{S}'-\mathcal{S}$ duality product, where $\mathcal{S}'$ is the space of tempered distributions. The latter result means that the Wigner transform is *self-averaging*. This is an important property for instance in the analysis of the refocusing properties of time-reversed waves [32, 34, 99, 69] for which it is shown that the quality of refocusing is independent of the local fluctuations of the random medium and hence only depends on macroscopic characteristics. The statistical stability of waves is also a fundamental requirement for applications to imaging or detection in complex media as claimed in the previous chapter: a heterogeneous medium with unknown local variations is often modeled as a particular realization of a random medium with given macroscopic quantities (which are known or to be estimated). The inverse problem of the reconstruction of an inclusion embedded in the medium is then done using a radiative transfer equation derived from ensemble averages of observables and not from a single realization; see [9, 7, 33]. It is thus important that these observables do not differ significantly for two different realizations of the random medium. Note that for the particular form of the initial conditions $W_\eta(z=0,\mathbf{x},\mathbf{k}) = \delta(\mathbf{x})f(\mathbf{k})$, where $f$ is a regular function,

the limit in distribution of the random corrector in $W_\eta$ was recently investigated in [91].

Our main motivation here is the analysis of the convergence of the whole process $W_\eta$ in the Itô-Schrödinger regime and for the random Schrödinger equation with $z$-independent potentials, and to quantify the statistical stability according to some parameters of the problem such as the regularity of the initial conditions or the size of the averaging domain (typically the size of the support of the test function $\varphi$ above).

In the *Itô-Schrödinger regime*, the convergence of $W_\eta$ to its average can be made precise so as to obtain information on the rate of convergence, see e.g. [27, 100]. This is rendered possible by the fact that the *scintillation function* $J_\eta$ (or covariance function), defined as

$$J_\eta(z,\mathbf{x},\mathbf{k},\mathbf{y},\mathbf{p}) = \mathbb{E}\{W_\eta(z,\mathbf{x},\mathbf{k})W_\eta(z,\mathbf{y},\mathbf{p})\} - \mathbb{E}\{W_\eta(z,\mathbf{x},\mathbf{k})\}\mathbb{E}\{W_\eta(z,\mathbf{y},\mathbf{p})\}, \tag{2.7}$$

solves a closed-form equation. The weak convergence of $J_\eta$ to zero implies convergence of $W_\eta$ in probability thanks to the Chebyshev inequality

$$\mathbb{P}\Big(|\langle W_\eta(z),\varphi\rangle - \langle a_\eta(z),\varphi\rangle| \geq \delta\Big) \leq \frac{1}{\delta^2}\langle J_\eta(z),\varphi\otimes\varphi\rangle,$$

with $(\varphi\otimes\varphi)(\mathbf{x},\mathbf{k},\mathbf{y},\mathbf{p}) := \varphi(\mathbf{x},\mathbf{k})\varphi(\mathbf{y},\mathbf{p})$. The asymptotic analysis of $J_\eta$ is carried out in section 2.2 where we will the present the results of [6] and [3] in the context of random medium with short-range correlations. Understanding how fast the scintillation function converges to zero is a difficult and complicated problem. It is difficult because the algebra is never straightforward and it is complicated because it depends in a non-trivial way on quite a few physical parameters such as the regularity of the wave initial condition and on the power spectrum of the random fluctuations in the underlying medium.

In the regime where the *random potential does not depend on the z variable*, the problem is largely more complex and only partial results regarding the statistical stability exist. Indeed, in this case the scintillation function does not statisfy a closed-form equation and a complete analysis has still be to carried out. In section 2.3, we present the results of [5] in which the contribution of the single scattering to the scintillation function is investigated. By single scattering, we mean the following. The scintillation function can formally be written as an infinite expansion with terms corresponding to increasing orders of interaction of the waves with the underlying medium. The first non-trivial term in the scintillation function is the one that is linear in the power spectrum $\hat{R}$, and all other terms are at least quadratic in the power spectrum or, when the random fluctuations are not modeled as Gaussian processes, depend on higher order statistics of the fluctuations. When scattering is relatively weak, the linear term in the power spectrum will then presumably be the

dominant contribution in the scintillation function. We referred to this term as the single scattering contribution to scintillation.

To complete the introduction, one should mention that the case of discrete models on lattices has been investigated in [47] for the Schrödinger equation and in [95] for the wave equation.

## 2.2 The Itô-Schrödinger regime

### 2.2.1 Setting of the problem

We assume in this section that $d \geq 2$. The scintillation function $J_\eta$ solves the closed-form equation

$$\Big(\frac{\partial}{\partial z} + \mathcal{T}_2 + 2R_0 - \mathcal{Q}_2 - \mathcal{K}_\eta\Big) J_\eta = \mathcal{K}_\eta a_\eta \otimes a_\eta, \tag{2.8}$$

equipped with vanishing initial conditions $J_\eta(0, \mathbf{x}, \mathbf{k}, \mathbf{y}, \mathbf{p}) = 0$ when the initial condition of the Schrödinger equation is deterministic. Here, we have defined

$$\begin{aligned}
\mathcal{T}_2 &= \mathbf{k} \cdot \nabla_{\mathbf{x}} + \mathbf{p} \cdot \nabla_{\mathbf{y}}, \\
\mathcal{Q}_2 h &= \int_{\mathbb{R}^{2d}} \Big(\hat{R}(\mathbf{k} - \mathbf{k}')\delta(\mathbf{p} - \mathbf{p}') + \hat{R}(\mathbf{p} - \mathbf{p}')\delta(\mathbf{k} - \mathbf{k}')\Big) h(\mathbf{x}, \mathbf{k}', \mathbf{y}, \mathbf{p}') d\mathbf{k}' d\mathbf{p}', \\
\mathcal{K}_\eta h &= \sum_{\epsilon_i, \epsilon_j = \pm 1} \epsilon_i \epsilon_j \int_{\mathbb{R}^{2d}} \hat{R}(\mathbf{u}) e^{i\frac{(\mathbf{x}-\mathbf{y})\cdot\mathbf{u}}{\eta}} h\left(\mathbf{x}, \mathbf{k} + \epsilon_i \frac{\mathbf{u}}{2}, \mathbf{y}, \mathbf{p} + \epsilon_j \frac{\mathbf{u}}{2}\right) d\mathbf{u}.
\end{aligned} \tag{2.9}$$

Equation (2.8) is obtained by computing the fourth moment of the wave function, see [27]. The analysis of (2.8) and of the highly oscillating operator $\mathcal{K}_\eta$ will show that $J_\eta$ converges weakly to zero.

To be consistent with the usual notation for the time-dependent Schrödinger equation, we relabel the variable $z$ as $t$. We assume that the initial condition $\psi_\eta^0$ of the Itô-Schrödinger equation (2.2) is deterministic (i.e., independent of the random medium) and uniformly bounded with respect to $\eta$ in $L^2(\mathbb{R}^d)$. We assume that our random medium has sufficiently short range correlations so that $\hat{R} \in L^1(\mathbb{R}^d) \cap L^\infty(\mathbb{R}^d)$. In such a setting, it is proved in [50] that (2.2) admits a unique solution $\psi_\eta(t, \mathbf{x}, \omega) \in \mathcal{C}^0([0, \infty), L^2(\mathbb{R}^d))$, $\mathbb{P}$ a.s.. Moreover, $\psi_\eta$ admits moments of arbitrary order so that its Wigner transform and related scintillation function are well-defined. Let $a_{\eta 0} := \mathbb{E}\{W_\eta[\psi_\eta^0]\} = W_\eta[\psi_\eta^0]$, where $W_\eta$ is defined in (2.5) and let $\mathcal{F}a_{\eta 0}$ be the Fourier transform of $a_{\eta 0}$ and $\mathcal{F}_{\mathbf{x}} a_{\eta 0}$ (resp. $\mathcal{F}_{\mathbf{k}} a_{\eta 0}$) be its partial Fourier transform with respect to $\mathbf{x}$ (resp. $\mathbf{k}$). Two important quantities are the $L^1$ norms of $\mathcal{F}_{\mathbf{x}} a_{\eta 0}$ and $\mathcal{F}_{\mathbf{k}} a_{\eta 0}$. Denoting by $a \lesssim b$ the inequality $a \leq Cb$, where $C > 0$ is some universal constant, this leads us to make the following hypotheses on $a_{\eta 0}$:

**Hypotheses H:** $\mathcal{F}\nabla_{\mathbf{x}}^p a_{\eta 0} \in L^\infty(\mathbb{R}^{2d})$, $\mathcal{F}_{\mathbf{x}}\nabla_{\mathbf{x}}^p a_{\eta 0} \in L^1(\mathbb{R}^{2d})$, $\mathcal{F}_{\mathbf{k}}\nabla_{\mathbf{x}}^p a_{\eta 0} \in L^1(\mathbb{R}^{2d})$, for $p = 0$ or 1 (with the convention that $\nabla_{\mathbf{x}}^0 a_{\eta 0} := a_{\eta 0}$) with the following estimates, for $(\alpha, \beta) \in \mathbb{R}^2$ verifying $0 \leq \alpha \leq 1$ and $0 \leq \beta \leq 1$:

$$\|\mathcal{F}\nabla_{\mathbf{x}} a_{\eta 0}\|_{L^\infty(\mathbb{R}^{2d})} \lesssim \eta^{-\alpha},$$
$$\|\mathcal{F}_{\mathbf{x}}\nabla_{\mathbf{x}}^p a_{\eta 0}\|_{L^1(\mathbb{R}^{2d})} \lesssim \eta^{-(d+p)\alpha} \quad \text{and} \quad \|\mathcal{F}_{\mathbf{k}}\nabla_{\mathbf{x}}^p a_{\eta 0}\|_{L^1(\mathbb{R}^{2d})} \lesssim \eta^{-d\beta - p\alpha}.$$

The relevance of the above hypothesis is better explained by looking at the following examples.

**Typical initial conditions.** Let us consider initial conditions $\psi_\eta(\mathbf{x}, 0)$ oscillating at frequencies of order $\eta^{-1}$ and with a spatial support of size $\eta^\alpha$ for $0 \leq \alpha \leq 1$. The parameter $\alpha$ quantifies the macroscopic concentration of the initial condition. The simplest example is a modulated plane wave of the form:

$$\psi_\eta^{(1)}(\mathbf{x}) = \frac{1}{\eta^{\frac{d\alpha}{2}}}\chi\Big(\frac{\mathbf{x} - \mathbf{x}_0}{\eta^\alpha}\Big)e^{i\frac{(\mathbf{x}-\mathbf{x}_0)\cdot\mathbf{k}_0}{\eta}}, \tag{2.10}$$

where $\chi \in \mathcal{S}(\mathbb{R}^d)$. The direction of propagation is given by $\mathbf{k}_0$. Note that the above sequence of initial conditions is indeed uniformly bounded in $L^2(\mathbb{R}^d)$, and that the related Wigner transform reads

$$a_{\eta 0}(\mathbf{x}, \mathbf{k}) = \frac{1}{\eta^d} a_0\left(\frac{\mathbf{x} - \mathbf{x}_0}{\eta^\alpha}, \frac{\mathbf{k} - \mathbf{k}_0}{\eta^{1-\alpha}}\right), \tag{2.11}$$

where $a_0(\mathbf{x}, \mathbf{k})$ is the Wigner transform of the rescaled initial condition $\psi_1^{(1)}$. Such an initial condition then verifies hypotheses **H** with $\beta = 1 - \alpha$. The parameter $\alpha$ measures the concentration of the initial conditions in the spatial variables while $\beta$ measures that in the momentum variables. We restrict $\alpha$ and $\beta$ to be less than one to ensure that $\eta^{-1}$ is the highest frequency in the problem. Allowing for higher frequencies while still considering a Wigner transform at the frequency $\eta^{-1}$ will lead to vanishing limiting Wigner transforms and would be of little interest for then energy is lost when passing to the limit, see e.g. [80, 94]. See also [3] for other types of initial conditions.

Since the scintillation function $J_\eta$ is itself oscillatory, the limit depends at which scale it is measured. We thus define localized test functions of the form:

$$\varphi_{\eta, s_1, s_2}(\mathbf{x}, \mathbf{k}) = \frac{1}{\eta^{d(s_1+s_2)}}\varphi\Big(\frac{\mathbf{x}}{\eta^{s_1}}, \frac{\mathbf{k} - \mathbf{k}_1}{\eta^{s_2}}\Big), \tag{2.12}$$

where $(s_1, s_2) \in \mathbb{R}^2$ and $\mathbf{k}_1 \in \mathbb{R}^d$ and $\varphi \in \mathcal{S}(\mathbb{R}^{2d})$.

### 2.2.2 Results

The first result we obtained is the following:

**Theorem 2.2.1** [6] *Let $d \geq 2$ and assume that hypotheses **H** are satisfied. Then, the scintillation function $J_\eta$ verifies the following estimate, uniformly on compact intervals:*

$$\langle J_\eta(t), \varphi_{\eta,s_1,s_2} \otimes \varphi_{\eta,s_1,s_2} \rangle \lesssim \eta^{(\alpha-\beta)\vee 0 - 2ds_2} \left( \eta^{d(1-\alpha-2s_1)} \wedge \eta^{d(1-2\alpha-s_1)} \right). \tag{2.13}$$

*Here, $\langle \cdot, \cdot \rangle$ denotes the $S' - S$ duality product, $a \wedge b = \min(a, b)$, $a \vee b = \max(a, b)$ and $(\varphi \otimes \varphi)(\mathbf{x}, \mathbf{k}, \mathbf{y}, \mathbf{p}) := \varphi(\mathbf{x}, \mathbf{k})\varphi(\mathbf{y}, \mathbf{p})$.*

The rate of convergence given by theorem 2.2.1 is not optimal when the domain of measurement is large, that is when $s_1 = s_2 = 0$, except when $\alpha = 1 - \beta = 1$ or when $\alpha = 1 - \beta = 0$. The optimal rate will be given in theorem 2.2.2. It is optimal regarding the size of the spatial support of the test function. Indeed, consider the case of an initial condition of the form (2.10) with a large spatial support, which corresponds to $\alpha = 0$, and angularly averaged measurements ($s_2 = 0$) with a very small spatial domain. In this setting, we find that

$$\langle J_\eta, \varphi_{\eta,s_1,0} \otimes \varphi_{\eta,s_1,0} \rangle \lesssim \eta^{d(1-s_1)}. \tag{2.14}$$

This means that the energy density becomes asymptotically statistically stable as soon as it is measured over an area that is large compared to the correlation length of the medium, i.e., $s_1 < 1$. This is an optimal result of self-averaging as we cannot expect the energy density to be statistically stable point-wise, or when averaged over sub-wavelength domains. The above result, which is based on estimating $K_\eta$ in (2.9) in appropriate norms, improves on estimates obtained in [27, 100]. The most stable case corresponds to $\alpha = s_1 = s_2 = 0$, which corresponds to a large support of the initial condition and a large domain of measurements. We find

$$\langle J_\eta(t), \varphi_{\eta,0,0} \otimes \varphi_{\eta,0,0} \rangle \lesssim \eta^d, \tag{2.15}$$

in other words, the scintillation is of order $\mathcal{O}(\eta^d)$. Unsurprisingly, the most stable configuration thus corresponds to situations where both the initial condition and the domain of measurements have large support compared to the wavelength for then the most averaging can occur.

Theorem 2.2.1 can be refined so as to obtain optimal convergence rates, see theorem 2.2.2 below. We can characterize moreover the dynamics of the statistical instabilities by computing the limit of the first-order corrector of $J_\eta$ for practically useful (pure state) initial conditions. This requires us to define a functional setting adapted to Wigner transforms and to a precise analysis of (2.8) and of the oscillating

operator $\mathcal{K}_\eta$. The outcome is a characterization of the propagation of the statistical instabilities. We show in theorem 2.2.3 that their dynamics are driven by a transport equation with a non-vanishing initial condition or source term depending on the singularities of the initial condition of the Schrödinger equation.

**Theorem 2.2.2** *[3] Let $d \geq 2$ and assume that hypotheses **H** are satisfied. Then, the scintillation function $J_\eta$ verifies the following estimate, uniformly on compact intervals:*

$$\langle J_\eta(t), \varphi_{\eta,s_1,s_2} \otimes \varphi_{\eta,s_1,s_2} \rangle \lesssim g_d(\eta),$$

*with $g_d$ given by, for $d \geq 3$ (see [3] for the expression of $g_2$),*

$$g_d(\eta) = \eta^{d(1-\alpha)-2d(s_1+s_2)} \left[\eta^{2(1-\alpha)-s_1-s_1\vee s_2+(\alpha-\beta)\vee 0}\right] \vee \eta^{1-\beta+((\alpha-\beta)\vee 0)\wedge((d-1)(1-\alpha-\beta)+\alpha)}.$$

Contrary to theorem 2.2.1, theorem 2.2.2 is not optimal regarding $s_1$ and $s_2$, that is the size of the support of the test function. It is regarding the parameters of an initial condition of the form (2.11) as will show theorem 2.2.3. Before stating it, we first define, with $[a] = (\mathbf{x}, \mathbf{k}, \mathbf{y}, \mathbf{p})$:

$$\begin{aligned} j^1_\alpha(t,[a]) &= \delta(\mathbf{x}-\mathbf{x}_0-t\mathbf{k})\,\delta(\mathbf{y}-\mathbf{x}_0-t\mathbf{p})(\nabla\delta)^T(\mathbf{k}-\mathbf{k}_0)\,M^\alpha(t)\,(\nabla\delta)(\mathbf{p}-\mathbf{k}_0), \\ j^2_\alpha(t,[a]) &= 2\,\delta(\mathbf{x}-\mathbf{y})\Big(\sigma_\alpha(t,\mathbf{x},\mathbf{k}-\mathbf{k}_0)\delta(\mathbf{p}-\mathbf{k}) - \sigma_\alpha(t,\mathbf{x},\mathbf{p}-\mathbf{p}_0)\delta(\mathbf{k}-\mathbf{k}_0) \\ &\qquad -\sigma_\alpha(t,\mathbf{x},\mathbf{k}-\mathbf{k}_0)\delta(\mathbf{p}-\mathbf{p}_0) + \delta(\mathbf{k}-\mathbf{k}_0)\delta(\mathbf{p}-\mathbf{p}_0)\int_{\mathbb{R}^d}\sigma_\alpha(t,\mathbf{x},\mathbf{k})d\mathbf{k}\Big). \end{aligned}$$

where $M^\alpha$ is a matrix and $\sigma_\alpha$ a cross-section that both depend on the value of $\alpha$ and on the spatial dimension, see [3] for their complete expressions. Their main features is that $M^\alpha$ depends *linearly* on $\hat{R}$ while $\sigma_\alpha$ depends on the *square* of $\hat{R}$.

**Theorem 2.2.3** *[3] Assume the initial condition $\psi^0_\eta$ has the form (2.10). Then under the assumptions **H**, we have, for $0 < \alpha < 1$,*

$$J_\eta = \eta^{(d+2)(1-\alpha)+(2\alpha-1)\vee 0}\, J^1_\alpha + \eta^{d(1-\alpha)+\alpha}(\left[\eta^{2\alpha-1} f_d(\eta)\right] \wedge 1)\, J^2_\alpha + r_\eta,$$

*where $f_d = 1$ when $d \geq 3$ and $f_2 = 1 + |\log \eta^{\alpha-\beta}|$, where $r_\eta$ is negligible compared to the first two terms in the $L^\infty((0,T), \mathcal{S}'(\mathbb{R}^{4d})) - *$ topology, and where we have defined*

$$J_\eta = \eta^d\, J^2_0 + r_\eta \ \text{ when } \alpha = 0, \qquad \text{and} \qquad J_\eta = \eta\, J^1_1 + r_\eta \ \text{ when } \alpha = 1.$$

*Here, $J^1_\alpha \in \mathcal{C}^0([0,T], Z')$ when $\alpha < 1$ and $J^1_1 \in \mathcal{C}^0([0,T], X_\infty)$ and $J^2_\alpha \in \mathcal{C}^0([0,T], X_\infty)$ are distributional solutions to the following 4-transport equations,*

$$\Big(\frac{\partial}{\partial t} + \mathcal{T}_2 + 2R_0 - \mathcal{Q}_2\Big) J^i_\alpha = S^i_\alpha, \qquad J^i_\alpha(t=0,\cdot) = J^{i,0}_\alpha. \tag{2.16}$$

*The spaces $Z'$ and $X_\infty$ are defined later on. For $i = 1, 2$, we have $S^i_\alpha = 0$ when $\alpha > \frac{1}{2}$ and $J^{i,0}_\alpha = 0$ when $\alpha \leq \frac{1}{2}$, and*

$$S^i_\alpha = j^i_\alpha \quad \text{when} \quad 0 \leq \alpha \leq \frac{1}{2} \qquad \text{and} \qquad J^{i,0}_\alpha = j^i_\alpha(0,\cdot) \quad \text{when} \quad \frac{1}{2} < \alpha < 1.$$

Theorem 2.2.2 indicates how the statistical instabilities propagate. Depending on the value of $\alpha$, either the first term or the second term dominates in the decomposition of $J_\eta$. When $d \geq 3$, the critical value of $\alpha$ is $\alpha^\star = \frac{2}{3}$: when $\alpha < \alpha^\star$, then the term involving $J^2_\alpha$ is the leading one, while the term involving $J^1_\alpha$ dominates when $\alpha > \alpha^\star$; when $\alpha = \alpha^\star$, both terms are of the same order. Both $J^1_\alpha$ and $J^2_\alpha$ satisfy a 4-transport equation. Depending on whether $\alpha \leq \frac{1}{2}$ or $\alpha > \frac{1}{2}$, the instabilities are created either by a source term or by an initial condition.

$J^1_\alpha$ is the most singular term as the corresponding data in the transport equation are proportional to delta distributions both in space and momentum (when $\alpha < 1$) whereas the data corresponding to $J^2_\alpha$ are more regular in the momentum variables. This should be related to the fact that $J^1_\alpha$ is linear with respect to the power spectrum $\hat{R}$ while $J^2_\alpha$ is proportional to $\hat{R}^2$ so that $J^1_\alpha$ corresponds to the simple scattering contribution to the scintillation while $J^2_\alpha$ corresponds to the double scattering and is therefore more regular. Moreover, when $\alpha < \alpha^\star$, the double scattering contribution gives the leading order, while it is given by the simple scattering when $\alpha > \alpha^\star$. It can also be noticed that higher order scattering terms are negligible in the limit. Let us now examine the different scenarios depending on the value of $\alpha$.

**Case** $0 < \alpha \leq \frac{1}{2}$. The initial condition $a_{\eta 0}$ is more singular in the momentum variables than in the spatial variables, with comparable singularities when $\alpha = \frac{1}{2}$. The instabilities are created by the ballistic part of the wave through the source term $j^2_\alpha$ supported at the spatial points $\mathbf{x} = \mathbf{y} = \mathbf{x}_0 - t\mathbf{k}_0$ with four configurations for the momentum $\mathbf{k}$ and $\mathbf{p}$: $\mathbf{k} = \mathbf{p}$, $\mathbf{k} = \mathbf{k}_0$, $\mathbf{p} = \mathbf{p}_0$ or $\mathbf{k} = \mathbf{p} = \mathbf{k}_0$. Instabilities are thus created along the wave propagation in the direction of the initial condition $\mathbf{k}_0$ but also in other directions related to $\sigma_\alpha$.

**Case** $\frac{1}{2} < \alpha < 1$. The initial condition $a_{\eta 0}$ is more singular in the spatial variables than in the momentum variables. This results in a stronger localization of the instabilities. They are generated by an initial condition given by $j^1_\alpha(0,\cdot)$ when $\alpha > \alpha^\star$ and $j^2_\alpha(0,\cdot)$ when $\alpha < \alpha^\star$. When $\alpha < \alpha^\star$, instabilities are created at $\mathbf{x} = \mathbf{y} = \mathbf{x}_0$ with the same momentum configuration as the case $0 < \alpha \leq \frac{1}{2}$. When $\alpha > \alpha^\star$, instabilities are still created at $\mathbf{x} = \mathbf{y} = \mathbf{x}_0$ but with momentum $\mathbf{k} = \mathbf{p} = \mathbf{k}_0$. Note that these instabilities are fairly singular since they are defined in this case by gradients of delta distributions.

**Case** $\alpha = 1$. This the *most unstable* case since instabilities are of order $\eta$. Since in this configuration the initial condition $a_{\eta 0}$ is regular with respect to $\mathbf{k}$, instabilities are created at $\mathbf{x} = \mathbf{y} = \mathbf{x}_0$ in all directions, see [3] for the expression of $J^1_1$.

**Case** $\alpha = 0$. This is the most stable case since instabilities are of order $\eta^d$. The initial condition is regular with respect to the spatial variables so that the source term $j_0^2$ is also regular. The situation is essentially the same as the case $0 < \alpha \leq \frac{1}{2}$. The main difference is that the instabilities are created not only at the ballistic position at time $t$ (that is at $\mathbf{x} = \mathbf{x}_0 - \mathbf{k}t$), but on a larger domain related to the spatial support of $a_0$.

### 2.2.3 Outline of the proof

Let us define first the following functional spaces: $X_\infty$, and $Z$ the spaces of tempered distributions $h$ in $\mathcal{S}'(\mathbb{R}^{4d})$ such that

$$\begin{aligned} \|h\|_{X_\infty} &= \sup_{\mathbf{u},\boldsymbol{\zeta},\mathbf{v},\boldsymbol{\xi}\in\mathbb{R}^d} |\mathcal{F}h(\mathbf{u},\boldsymbol{\xi},\mathbf{v},\boldsymbol{\zeta})| < \infty, \\ \|h\|_Z &= (2\pi)^{-4d} \int_{\mathbb{R}^{4d}} \omega(\mathbf{u},\boldsymbol{\xi},\mathbf{v},\boldsymbol{\zeta}) |\mathcal{F}h(\mathbf{u},\boldsymbol{\xi},\mathbf{v},\boldsymbol{\zeta})| d\boldsymbol{\xi} d\mathbf{u} d\mathbf{v} d\boldsymbol{\zeta} < \infty, \\ \omega(\mathbf{u},\boldsymbol{\xi},\mathbf{v},\boldsymbol{\zeta}) &= (1 + |\boldsymbol{\xi}| + |\boldsymbol{\xi}||\mathbf{u}| + |\mathbf{u}|^2)(1 + |\boldsymbol{\zeta}| + |\boldsymbol{\zeta}||\mathbf{v}| + |\mathbf{v}|^2). \end{aligned}$$

Here $|\mathbf{u}|$ is the Euclidean norm of the vector $\mathbf{u}$. We denote by $Z'$ the dual of $Z$. Above, we identified the Fourier transform of the distribution $h$ with the function $\mathcal{F}h$.

The proof starts with the integral formulation of the 4-transport equation (2.8) in terms of the transport semi-group $(\mathcal{G}_t^2\varphi)(\mathbf{x},\mathbf{k},\mathbf{y},\mathbf{p}) = \varphi(\mathbf{x} - t\mathbf{k}, \mathbf{k}, \mathbf{y} - t\mathbf{q}, \mathbf{q})$ and the scattering operator $\mathcal{Q}_2$. It reads

$$J_\eta(t) = \int_0^t e^{-2R_0(t-s)} \mathcal{G}_{t-s}^2 (\mathcal{Q}_2 + \mathcal{K}_\eta) J_\eta(s) ds + \int_0^t e^{-2R_0(t-s)} \mathcal{G}_{t-s}^2 \mathcal{K}_\eta a_\eta \otimes a_\eta(s) ds. \tag{2.17}$$

Defining

$$T^{\mathcal{Q}}\varphi(t) := \int_0^t e^{-2R_0(t-s)} \mathcal{G}_{t-s}^2 \mathcal{Q}_2 \varphi(s) ds \quad ; \quad T_\eta^{\mathcal{K}}\varphi(t) := \int_0^t e^{-2R_0(t-s)} \mathcal{G}_{t-s}^2 \mathcal{K}_\eta \varphi(s) ds,$$

$$T_{2\eta} := T^{\mathcal{Q}} + T_\eta^{\mathcal{K}} \qquad ; \qquad J_\eta^0(t) := \int_0^t e^{-2R_0(t-s)} \mathcal{G}_{t-s}^2 \mathcal{K}_\eta a_\eta \otimes a_\eta(s) ds,$$

we recast (2.17) as $J_\eta = T_{2\eta} J_\eta + J_\eta^0$. It is easy to show that (2.17) admits a unique solution in $X_\infty$. As a consequence, the dynamics of $J_\eta$ is basically driven by that of $J_\eta^0$. Depending on how singular the initial condition $a_{\eta 0}$ is in the variable $\eta$, the behavior of $J_\eta$ as $\eta \to 0$ can be quite different. A first distinction is whether $\beta > 0$ or $\beta = 0$. By analogy with (2.10), the first case corresponds to initial conditions *localized* in the momentum variables while the second corresponds to

*smooth* initial conditions in the momentum variables, regardless of the regularity with respect to the spatial variables. The second case is the easier to treat. The oscillatory term $T_\eta^{\mathcal{K}} J_\eta$ is negligible compared to the other terms in this configuration due to regularization effects and so $J_\eta$ approximately solves $J_\eta \approx T^{\mathcal{Q}} J_\eta + J_\eta^0$. Since the dominant part of the source term $J_\eta^0$ converges in the $X_\infty$ norm and the above equation is stable for the same norm, we can pass to the limit $\eta \to 0$ in it after appropriately rescaling $J_\eta$.

When the initial condition is singular in momentum however, i.e., when $\beta > 0$, then $J_\eta^0$ does not converge in $X_\infty$ but rather in the smaller Fourier weighted space $Z'$. We cannot pass to the limit directly in the equation since it is not stable in $Z'$, the highly oscillating operator $\mathcal{K}_\eta$ having a norm of order $\eta^{-1}$ in $\mathcal{L}(Z')$. The term $T_\eta^{\mathcal{K}} J_\eta$ is no longer negligible in some configurations. We are thus lead to studying the convergence of $J_\eta$ by setting $J_\eta = J_\eta^0 + J_\eta^1$ with $J_\eta^1$ the solution to

$$J_\eta^1 = T_{2\eta} J_\eta^1 + T_{2\eta} J_\eta^0.$$

The convergence of $J_\eta^0$ can be fully characterized in $Z'$. The salient feature of the derivation is that, in most configurations, $J_\eta^0$ is dominated by its ballistic part, denoted by $J_\eta^{00}$, i.e., $J_\eta^0 \approx J_\eta^{00}$.

To analyze $J_\eta^1$, we distinguish in the source term $T_{2\eta} J_\eta^0$ the smooth part $\mathcal{Q}_2$ from the oscillating part $\mathcal{K}_\eta$ by splitting $J_\eta^1$ as $J_\eta^1 = J_\eta^{1,\mathcal{Q}} + J_\eta^{1,\mathcal{K}}$ with

$$J_\eta^{1,\mathcal{Q}} = T_{2\eta} J_\eta^{1,\mathcal{Q}} + T^{\mathcal{Q}} J_\eta^0, \tag{2.18}$$

$$J_\eta^{1,\mathcal{K}} = T_{2\eta} J_\eta^{1,\mathcal{K}} + T_\eta^{\mathcal{K}} J_\eta^0. \tag{2.19}$$

The limit of $J_\eta^1$ also depends on the singularities of the initial condition, which determine whether $J_\eta^{1,\mathcal{Q}}$ or $J_\eta^{1,\mathcal{K}}$ is the leading term. As long as the initial condition remains sufficiently singular in the momentum variables compared to the spatial variables, which is mathematically expressed by the relation $\beta > 2\alpha - 1$ when $d \geq 3$ (so that $\alpha < \alpha^\star = \frac{2}{3}$ when $\beta = 1 - \alpha$), the dominant term in $J_\eta$ is given by $J_\eta^{1,\mathcal{K}}$, that is

$$J_\eta \approx J_\eta^{1,\mathcal{K}}, \text{ when } \beta > 2\alpha - 1,$$

the terms $J_\eta^0$ and $J_\eta^{1,\mathcal{Q}}$ being negligible. This is due to the fact that the initial condition is too singular in the momentum variables for a regularization effect of the singular source term $T_\eta^{\mathcal{K}} J_\eta^0$ of (2.19) to take place. This configuration gives rise to a limiting behavior dominated by the double scattering contribution. The main ideas remain the same in dimension $d = 2$. In the case $\beta < 2\alpha - 1$, the dominant term is $J_\eta^0 + J_\eta^{1,\mathcal{Q}}$, that is $J_\eta \approx J_\eta^0 + J_\eta^{1,\mathcal{Q}}$, when $\beta < 2\alpha - 1$. Here, the initial condition is sufficiently smooth in the momentum variables to render $T_\eta^{\mathcal{K}} J_\eta^0$ negligible compared to $J_\eta^0$ and $J_\eta^{1,\mathcal{Q}}$. Such a configuration gives rise to a limiting behavior dominated

by the single scattering contribution. When $\beta = 2\alpha - 1$, both dynamics are of the same order and coexist.

Knowing now which term between $J_\eta^{1,\mathcal{K}}$ and $J_\eta^0 + J_\eta^{1,\mathcal{Q}}$ is dominant, it remains to analyze their limit. A distinction is whether $\alpha > \beta$ or not, that is whether the initial condition is more singular in the spatial variables than in the momentum variables. When $\alpha \leq \beta$, the source of scintillation is given by a source term in the limiting equation for the rescaled $J_\eta$. When $\alpha > \beta$, it is given by an initial condition. All cases can be treated within similar frameworks.

Regarding the limit of $J_\eta^{1,\mathcal{K}}$, consider first the source term $T_\eta^{\mathcal{K}} J_\eta^0$ in equation (2.19): when the initial condition is singular in the spatial variables, i.e., $\alpha > 0$, we show that the dominant term in $T_\eta^{\mathcal{K}} J_\eta^0$ (which will be denoted by $T_\eta^{\mathcal{K}} J_\eta^{00}$) is induced by the ballistic part of $a_\eta$, so that $T_\eta^{\mathcal{K}} J_\eta^0$ can be replaced by $T_\eta^{\mathcal{K}} J_\eta^{00}$ for the $X_\infty$ strong topology in the equation (2.19) solved by $J_\eta^{1,\mathcal{K}}$. This requires the analysis of a *double* application of the operator $\mathcal{K}_\eta$. When the initial condition is regular in the spatial variables, that is $\alpha = 0$, the ballistic and scattered parts in $J_\eta^0$ are of the same order so the full $T_\eta^{\mathcal{K}} J_\eta^0$ has to be considered. Regarding the operator term $T_{2\eta} J_\eta^{1,\mathcal{K}} := T^{\mathcal{Q}} J_\eta^{1,\mathcal{K}} + T_\eta^{\mathcal{K}} J_\eta^{1,\mathcal{K}}$ in (2.19), we show that $T_\eta^{\mathcal{K}} J_\eta^{1,\mathcal{K}}$ is higher order in $X_\infty$ so that the dominant term in $J_\eta^{1,\mathcal{K}}$ basically solves a 4-transport equation with $\mathcal{K}_\eta := 0$ and a source term $T_\eta^{\mathcal{K}} J_\eta^{00}$ (or $T_\eta^{\mathcal{K}} J_\eta^0$ for the particular case $\alpha = 0$), that is $J_\eta^{1,\mathcal{K}} \approx T^{\mathcal{Q}} J_\eta^{1,\mathcal{K}} + T_\eta^{\mathcal{K}} J_\eta^{00}$. It then suffices to compute the limit of the source term in $X_\infty$ and pass to the limit in the equation.

Regarding the limit of $J_\eta^{1,\mathcal{Q}}$, consider first the source term $T^{\mathcal{Q}} J_\eta^0$ in (2.18): as $J_\eta^0$ will be seen to converge in $Z'$, $T^{\mathcal{Q}} J_\eta^0$ converges in $Z'$ and not in $X_\infty$. It is then not directly possible to pass to the limit in (2.18) in $Z'$ due to the presence of the operator $\mathcal{K}_\eta$ which is not bounded in $\mathcal{L}(Z')$. Nevertheless, writing $T_{2\eta} J_\eta^{1,\mathcal{Q}} = T^{\mathcal{Q}} J_\eta^{1,\mathcal{Q}} + T_\eta^{\mathcal{K}} J_\eta^{1,\mathcal{Q}}$, we take advantage of the regularizing properties of the $\mathcal{G}_t^2 \mathcal{Q}_2$ operator in the source term $T^{\mathcal{Q}} J_\eta^0$ to prove that $J_\eta^{1,\mathcal{Q}}$ has enough regularity so that $T_\eta^{\mathcal{K}} J_\eta^{1,\mathcal{Q}}$ is found to be of higher order and can thus be neglected. This step is not possible when considering the term $J_\eta^0$ without the regularization of $T^{\mathcal{Q}}$ as $T^{\mathcal{Q}} J_\eta^0$ and then $J_\eta^{1,\mathcal{Q}}$ would not be sufficiently regular. Hence, the operator $T_{2\eta}$ can be replaced by $T^{\mathcal{Q}}$ and $J_\eta^{1,\mathcal{Q}}$ is a morally a solution to $J_\eta^{1,\mathcal{Q}} \approx T^{\mathcal{Q}} J_\eta^{1,\mathcal{Q}} + T^{\mathcal{Q}} J_\eta^0$, which is stable in $Z'$ so that we can pass to the limit in the equation.

## 2.3 The single scattering regime for random Schrödinger equations

### 2.3.1 Settings

We consider in this section equation (2.4), and recast the variable $z$ as $t$ and $V\left(\frac{x}{\eta},0\right)$ as $V\left(\frac{x}{\eta}\right)$ to find

$$\left(i\eta\frac{\partial}{\partial t}+\frac{\eta^2}{2}\Delta_{\mathbf{x}}+\sqrt{\eta}V\left(\frac{x}{\eta}\right)\right)\psi_\eta(t,\mathbf{x})=0,\quad t>0,\quad x\in\mathbb{R}^d, \tag{2.20}$$

augmented with a *deterministic* initial condition $\psi_\eta(t=0,\mathbf{x})$ uniformly bounded in $L^2(\mathbb{R}^d)$ with respect to $\eta$, for $d\geq 1$. Here, $V$ is a mean-zero homogeneous stationary random field with autocorrelation $R(\mathbf{x}):=\mathbb{E}\{V(\mathbf{x}+\mathbf{y})V(\mathbf{y})\}$ and is time-independent. The symbol $\mathbb{E}$ denotes the ensemble average with respect to a given probability space $(\Omega,\mathcal{F},\mathbb{P})$ on which $V$ is defined. The Wigner transform $W_\eta$ of $\psi_\eta$ is defined as in (2.5) and satisfies the stochastic Wigner equation

$$\frac{\partial}{\partial t}W_\eta+\mathbf{k}\cdot\nabla_{\mathbf{x}}W_\eta=A_\eta W_\eta, \tag{2.21}$$

with

$$\begin{aligned}(A_\eta W_\eta)(\mathbf{x},\mathbf{k}) &:= \int_{\mathbb{R}^d} f_\eta(\mathbf{x},\mathbf{k}-\mathbf{q})W_\eta(\mathbf{x},\mathbf{q})d\mathbf{q},\\ f_\eta(\mathbf{x},\boldsymbol{\xi}) &:= \frac{i}{\sqrt{\eta}\pi^d}\left[\hat{V}(-2\boldsymbol{\xi})e^{-i2\boldsymbol{\xi}\cdot\mathbf{x}/\eta}-\hat{V}(2\boldsymbol{\xi})e^{i2\boldsymbol{\xi}\cdot\mathbf{x}/\eta}\right].\end{aligned}$$

The initial condition of (2.21), denoted by $W_\eta^0(\mathbf{x},\mathbf{k})$, is the Wigner transform of $\psi_\eta(0,\cdot)$. Let $a_\eta:=\mathbb{E}\{W_\eta\}$ be the ensemble average of $W_\eta$. For sufficiently rapidly decaying correlation function $R$, $a_\eta$ converges in a proper functional setting to the solution $a_0$ of a radiative transfer equation as mentioned in the introduction.

**Long range correlations.** Here, we are interested in random fields with possibly *long range* interactions, which can be modeled with slowly decaying autocorrelations that do not belong to $L^1(\mathbb{R}^d)$. Assuming $R(\mathbf{x})\sim_{|\mathbf{x}|\to\infty}\mathbf{x}^{\delta-d}$, with $0<\delta<d$, some standard rescaling arguments show that $\hat{R}$ is singular at the origin and behaves like $|\mathbf{k}|^{-\delta}$. This leads us to consider correlation functions with singular Fourier transforms near the origin of the form

$$\hat{R}(\mathbf{k})=\frac{S(\mathbf{k})}{|\mathbf{k}|^\delta},\quad 0<\delta<d, \tag{2.22}$$

with $S$ bounded and continuous at zero. Since, $0 < \delta < d$, $\hat{R}$ is locally integrable. Physically realizable media will also have $\int \hat{R}(\mathbf{k})d\mathbf{k} = (2\pi)^d R(\mathbf{0}) < \infty$. Short-range correlations correspond to integrable $R$. In this case $\hat{R}$ is bounded so we may take $\delta = 0$ in (2.22).

**Scintillation and single scattering.** Unlike the Itô-Schrödinger regime, the scintillation function of the above Wigner function *does not* satisfy a closed-form equation. We will therefore follow a perturbative approach and only consider the scintillation created by single scattering, that is after only one interaction with the random potential, assuming scattering is weak enough so that multiple interactions can be neglected. Doing so, we can obtain an exact expression of the scintillation and fully characterize its limit. Such expression follows from a multiple scattering expansion of $W_\eta$: introducing first the free transport semigroup $J$, $Jh(t, \mathbf{x}, \mathbf{k}) := h(\mathbf{x} - t\mathbf{k}, \mathbf{k})$, and the operator

$$D^{-1}h(t, \mathbf{x}, \mathbf{k}) := \int_0^t h(t - s, \mathbf{x} - s\mathbf{k}, \mathbf{k})ds,$$

then (2.21) can be recast as an integral equation whose solution can be decomposed formally as the multiple scattering expansion:

$$(I - D^{-1}A_\eta)W_\eta = JW_\eta^0, \qquad ; \qquad W_\eta = \sum_{j=0}^{\infty} (D^{-1}A_\eta)^j JW_\eta^0.$$

Retaining only the terms $j \leq 1$ in the latter decomposition, we have

$$\begin{aligned} J_\eta(t, \mathbf{x}, \mathbf{k}, \mathbf{y}, \mathbf{p}) &\approx \mathbb{E}\left\{(JW_\eta^0 + D^{-1}A_\eta JW_\eta^0)(t, \mathbf{x}, \mathbf{k})(JW_\eta^0 + D^{-1}A_\eta JW_\eta^0)(t, \mathbf{y}, \mathbf{p})\right\} \\ &\quad -\mathbb{E}\left\{(JW_\eta^0 + D^{-1}A_\eta JW_\eta^0)(t, \mathbf{x}, \mathbf{k})\right\}\mathbb{E}\left\{(JW_\eta^0 + D^{-1}A_\eta JW_\eta^0)(t, \mathbf{y}, \mathbf{p})\right\}, \\ &= \mathbb{E}\left\{D^{-1}A_\eta JW_\eta^0)(t, \mathbf{x}, \mathbf{k})(D^{-1}A_\eta JW_\eta^0)(t, \mathbf{y}, \mathbf{p})\right\}, \\ &:= \mathbb{E}\{\mathcal{W}_{11}^\eta(t, \mathbf{x}, \mathbf{k}, \mathbf{y}, \mathbf{p})\}. \end{aligned}$$

Above, we used the facts that $V$ is mean-zero and the initial condition is assumed to be deterministic.

**Initial conditions.** We slightly generalize the condition (2.11) by considering initial condition of the form

$$W_\eta^0(\mathbf{x}, \mathbf{k}) = \frac{1}{\eta^{d(\alpha+\beta)}} a_0\left(\frac{\mathbf{x}}{\eta^\alpha}, \frac{\mathbf{k} - \mathbf{k}_0}{\eta^\beta}\right), \tag{2.23}$$

The parameter $\alpha$ measures the concentration of the initial conditions in the spatial variables while $\beta$ measures that in the momentum variables. The most physical case

is when $\alpha+\beta = 1$ as in (2.11). This is related to the Heisenberg uncertainty principle, which states that waves cannot be localized both in space and momentum. The case $\alpha + \beta > 1$ can be treated mathematically in the same fashion as the physical case and so we present it for completeness. The case $\alpha + \beta < 1$ corresponds to mixtures of states and can be obtained by averaging of $a_0(\cdot, \cdot; \zeta)$ with respect to an additional measure in the $\zeta$ variable in order to regularize the initial conditions; see e.g. [32]. We assume in the sequel that $|k_0| \neq 0$ with $|k_0|$ of order one compared to $\eta$.

### 2.3.2 Results

Let $\varphi \in \mathcal{S}(\mathbb{R}^{2d})$ be a real valued test function and let $W_{11}^\eta$ be the expectation of $\mathcal{W}_{11}^\eta$, $W_{11}^\eta := \mathbb{E}\{\mathcal{W}_{11}^\eta\}$. We denote by $w^\eta$ the quantity

$$w^\eta(t) := \int_{\mathbb{R}^{2d}} W_{11}^\eta(t, \mathbf{x}, \mathbf{k}, \mathbf{y}, \mathbf{p})\, \varphi(\mathbf{x}, \mathbf{k})\, \varphi(\mathbf{y}, \mathbf{p}) d\mathbf{x} d\mathbf{y} d\mathbf{k} d\mathbf{p}.$$

The main result is theorem 2.3.1 below, which states that the scintillation corresponding to single scattering is of order $\eta^{(d-\delta)(1-\alpha)+1-\alpha\wedge\beta}$.

When $\delta = 0$, which corresponds to the case of an integrable correlation function $R(x)$, we find in the physical case $\alpha + \beta = 1$ that scintillation is maximal when $\beta = 0$ and $\alpha = 1$. In this case it is proportional to $\eta$. This corresponds to highly localized initial conditions in space and is consistent with the results obtained in the Itô-Schrödinger regime in the preceding section. The unphysical case $\alpha = \beta = 1$ predicts scintillation of order $\mathcal{O}(1)$. This is consistent with the results obtained in [27] for initial conditions of the form $\delta$ in space and $\delta$ in wavenumbers. However, we repeat that the case $\alpha = \beta = 1$ is not a physical description of initial conditions for the Schrödinger equation that are square integrable.

When long range correlations are present, the structure of scintillation is modified. When $\delta$ is close to $d$, which corresponds to the strongest possible long range interactions as the correlation function barely decays, the largest scintillation (in the physical case $\alpha + \beta = 1$) is obtained for $\alpha = \beta = \frac{1}{2}$ and thus gives a scintillation of order close to $\eta^{\frac{1}{2}}$.

These results show that the single scattering contribution of scintillation converges to zero and this is consistent with the fact that the Wigner function is self-averaging. Note however, that in dimension $d = 1$, the above results also predict self-averaging of the Wigner transform since scintillation is always smaller than $\mathcal{O}(\eta^{\frac{1}{2}})$. Yet it is known that waves localize in dimension $d = 1$ and that the deterministic radiative transfer model is replaced by a stochastic limit [71, 90]. In dimension $d = 1$, it turns out that there are larger contributions to scintillation than that given by single scattering. The single scattering contribution is however

dominant in certain regimes and its asymptotic limit is characterized in detail in the following result.

**Theorem 2.3.1** *Assume the initial condition $W_\eta^0$ has the form (2.23) with $a_0 \in \mathcal{S}(\mathbb{R}^{2d})$, $|k_0| \neq 0$, and that the scattering cross section is given by (2.22). Then $\eta^{-(d-\delta)(1-\alpha)-1+\alpha\wedge\beta} w^\eta(t)$ is bounded in $L^\infty((0,T))$, converges pointwise on $(0,T]$ and uniformly on $[t_0,T]$ to $w(t)$, for any $t_0 > 0$ independent of $\eta$. See [5] for the different expressions of $w(t)$ according to the values of $\alpha$ and $\beta$.*

The results of the theorem can be straightforwardly generalized to some particular cases. For instance, when $\alpha = \beta = 0$, which corresponds to choosing smooth initial conditions for the Wigner equation, we can actually consider localized test functions as in the previous section and simple calculations show that the roles of $(\alpha, \beta)$ and $(s_1, s_2)$ are symmetrical. As another example, when $\alpha = s_2 = 0$, the theorem applies with minor changes with $\alpha$ replaced by $s_1$. More precisely, we have the following proposition:

**Proposition 2.3.2** *Assume the initial condition $W_\eta^0$ has the form (2.23) with $a_0 \in \mathcal{S}(\mathbb{R}^{2d})$ and that the scattering cross section is given by (2.22). Assume moreover that the test function $\varphi$ in the definition of $w^\eta$ is replaced by (2.12). Then, there exist two non-identically zero continuous functions $w_1$ and $w_2$ on $[0,T]$, such that, if $\alpha = \beta = 0$,*

$$\eta^{-(d-\delta)(1-s_1)-1+s_1\wedge s_2} w^\eta(t) \to w_1(t),$$

*or if $\alpha = s_2 = 0$,*

$$\eta^{-(d-\delta)(1-s_1)-1+s_1\wedge\beta} w^\eta(t) \to w_2(t),$$

*pointwise on $(0,T]$ and uniformly on $[t_0,T]$, for any $t_0 > 0$ independent of $\eta$.*

According to the proposition, when $\alpha = 0$ and $\beta = 1$, the scintillation is of order $\mathcal{O}(\eta^{(d-\delta)(1-s_1)})$, so that statistical stability occurs as soon as $s_1 < 1$, i.e., as soon as the array of detectors is large compared to the wavelength, as we expect physically. When $s_1 = 1$, scintillation is an $\mathcal{O}(1)$. These results are consistent with the ones obtained in the previous section.

**Elements of proof.** The proof is done by deriving an exact expression for $w^\eta$ and by passing to the limit in it. The expression is given by, see [5] for the details:

$$\begin{aligned} w^\eta(t) &= \frac{\eta^{(d-\delta)(1-\alpha)-1}}{(2\pi)^d} \int d\mathbf{k}\, \frac{S(\mathbf{k}\eta^{1-\alpha})}{|\mathbf{k}|^\delta} \\ &\qquad \times \left| \int_0^t e^{-i\eta^{-\alpha} s \mathbf{k}_0\cdot\mathbf{k}} \mathcal{F}(f_s^\eta a_0)(k, \eta^{\beta-\alpha}s\mathbf{k}, \eta^{1-\alpha}\mathbf{k}) ds \right|^2, \\ f_s^\eta(\mathbf{x},\mathbf{q},\mathbf{k}) &:= \sum_\pm \mp\varphi(\mathbf{x}\eta^\alpha + t\mathbf{q}\eta^\beta + t\mathbf{k}_0 \pm (t-s)\mathbf{k}/2,\, \mathbf{q}\eta^\beta + \mathbf{k}_0 \pm \mathbf{k}/2). \end{aligned}$$

We then perform Taylor expansions of the function $f_s^\eta$ defined above and carefully estimate the growth of the remainders according to the different variables. This allows to recast $w^\eta$ as a leading term and a negligible one and the different expressions of the limiting $w^\eta$ follow from a passage to the limit in the leading order.

## 2.4 Perspectives

Several directions are to be investigated. Regarding the Itô-Schrödinger regime, the case $d = 1$ remains to be treated in the context of the chapter. The analysis is slightly different than when $d \geq 2$, but still interesting so as to compare with the time-independent potential case for which it is known that localization appears in $d = 1$, see for instance [71]. Long-range correlations have also to be taken into account into the model, to figure whether or not statistical stability still occurs: long-distance correlations in the transverse directions lead to a singular power spectrum, as in section 2.3; in the direction of propagation, they lead to a fractional Brownian motion instead of a classical one. Such analysis of statistical stability has not been done yet.

Concerning the time-independent potential case, the convergence of the Wigner transform for the complete problem including all scattering orders is an open problem. As mentioned earlier, it is known that waves localize in dimension one in such a setting, even with short-range correlations, while the analysis of section 2.3 shows the simple scattering is stable. This means that the instabilities are created by higher order scatterings, which is compatible with the results for the Itô-Schrödinger regime in which double scattering is dominant for a certain range of parameters. Some partial results show the scintillation function of the double scattering is stable for $d \geq 2$ and is unstable when $d = 1$ for a set of initial conditions, and stable for others. This is to be confirmed with numerical simulations.

We considered here only linear models. Non-linear interactions, as a Poisson potentials, can be included in the models. Non-linearity proportional to $|\psi_\eta|^2$ could likely be treated in a relative simple manner since $|\psi_\eta|^2$ is the integral of the Wigner transform with respect to the momentum. The effects of non-linearities on the statistical stability is still to be investigated.

Regarding the full wave equation, the high-frequency asymptotics in the weak coupling regime is an open problem.

# Chapter 3

# Influence of inclusions on boundary measurements for elliptic equations

In this chapter, we are interested in the analysis of the influence of general, small volume, inclusions on the trace at the domain's boundary of the solution to elliptic equations of the form $\nabla \cdot D^\varepsilon \nabla u^\varepsilon = 0$ or $(-\Delta + q^\varepsilon)u^\varepsilon = 0$ with prescribed Neumann conditions. The theory is well-known for instance when the constitutive parameters in the elliptic equation are constant in the background and inside the inclusions, and this leads in this case to high order asymptotic expansions of the trace of the solution at the domain's boundary; or, in dimension less than three, when the background is smooth but not constant, and in this configuration only first order expansions are available, that is of order $\varepsilon^d$ where $d$ is dimension and $\varepsilon$ is the diameter of the inclusion. We generalize the results to varying backgrounds in any dimensions and to the case of arbitrary, and thus possibly rapid, fluctuations of the parameters inside the inclusion and obtain expansions up to an order $\varepsilon^{2d}$. Besides, we construct inclusions whose leading influence is of order at most $\varepsilon^{d+1}$ rather than the expected $\varepsilon^d$. We also compare the expansions for the diffusion and Helmholtz equations and their relationship via the classical Liouville change of variables. That chapter is a summary of [4].

## 3.1 Introduction

Asymptotic expansions for the influence of small volume inclusions for elliptic and other equations is now well-established. We refer to e.g. [21, 26, 44, 45, 72, 85] and their references for a few historic and recent works on the subject. A major advantage of such expansions is that they help us understand what details of the constitutive parameters in the equation may or may not be reconstructed from available boundary measurements. Indeed, in the elliptic equations of interest in this chapter, namely the diffusion or conductivity equation and the Helmholtz equation, the reconstruction of the constitutive parameters $X$ from knowledge of the full Dirichlet-to-Neumann map $\Lambda$, the most general type of information available at the domain's boundary, is an extremely ill-conditioned problem. Available stability estimates for both types of equations predict that the accuracy in the reconstruction is at best logarithmic in the accuracy of the measurements. More precisely, we have [20, 87]

$$\|X_1 - X_2\|_{L^\infty(\Omega)} \leq C \left| \log \|\Lambda_1 - \Lambda_2\|_{\mathcal{L}(H^{\frac{1}{2}}(\partial\Omega), H^{-\frac{1}{2}}(\partial\Omega))} \right|^{-\delta},$$

for a domain $\Omega$ of dimension $d$ and some positive constant $C$ and $\delta \in (0,1)$, where $X_1$ and $X_2$ are two sets of parameters and $\Lambda_1$ and $\Lambda_2$ their corresponding measurements.

For such severely ill-posed problems, only a limited number of degrees of freedom may be reconstructed from even quite accurate measurements. A natural way of limiting the number of degrees of freedom is to assume that the constitutive coefficients are known throughout the domain, except at some locations where unknown inclusions may be present. The asymptotic expansions in the size of the inclusion mentioned above thus provide a very efficient tool to understand what may or may not be reconstructed from data with a given level of noise.

For elliptic equations, the existing works on the subject, see e.g. [21, 44], typically assume the parameters jumps across the interface of the inclusion. One of the main objectives here is to consider the case of more general inclusions whose coefficient may vary at the small scale $\varepsilon$ and need not "jump" from the values of the background parameters. We also want to stress the similarities and differences between expansions for the diffusion equation $\nabla \cdot D^\varepsilon \nabla u^\varepsilon = 0$ and the Helmholtz equation $(-\Delta + q^\varepsilon)u^\varepsilon = 0$ with $q^\varepsilon$ of order $\varepsilon^{-2+\eta}$ for $\eta \in [0,2]$. In both cases of the diffusion equation and the Helmholtz equation when $\eta = 0$, we need to introduce local correctors and obtain a limiting influence at the domain's boundary that is non-linear in the parameters inside the inclusion.

The maximal leading term in the expansion is always of order $\mathcal{O}(\varepsilon^d)$, the volume of the inclusion. We construct expansions up to the order $\varepsilon^{2d}$ for varying backgrounds. Going beyond this order of accuracy requires a more careful analysis of the decay properties of local correctors at infinity than is available here, or the

use of single and double layer potentials as in [21] in the case of constant coefficients inside and outside of the inclusion. Note that the cross-talk between two inclusions of volume $\mathcal{O}(\varepsilon^d)$ is also a term of order $\varepsilon^{2d}$. It seems therefore natural to stop the expansion at the order $\mathcal{O}(\varepsilon^{2d})$ for the influence of any given well-separated inclusions. The $\mathcal{O}(\varepsilon^d)$ leading term in the expansion typically gives access to the location of the perturbation and to the product of its volume and its amplitude. To recover the volume and the amplitude separately, one needs the next order term in the expansion, see e. g., [21, 26]. This is the main motivation for obtaining high order asymptotic formulas.

Because our inclusions are modeled by somewhat arbitrary parameters that need not jump from the local value of the background parameter or are not constant, the limiting polarization tensors need not satisfy any property of positivity or definiteness. On the contrary, we show that the polarization tensors vanish to first order for some types of inclusions, whose influence at the domain's boundary is therefore at most of order $\varepsilon^{d+1}$ rather than $\varepsilon^d$. Although we do not explore this aspect here, the proposed asymptotic expansions may be used to construct inclusions whose influence on the measurements is minimized in a prescribed manner.

## 3.2 The diffusion equation

In this section, we are interested in the analysis of small inclusions in the diffusion or conductivity problem. As we have mentioned in the introduction, the reconstruction of diffusion or conductivity coefficients from boundary measurements is a severely ill-posed problem. One possible way to overcome this difficulty is to assume that the background diffusion coefficient is known and that the unknown part of the coefficient is localized and has small volume.

Under such hypotheses, asymptotic expansions of the perturbed field in the volume of the inclusion have been derived in [72] when the inclusion is perfectly reflecting or insulating. These formulas have then been extended to more general inclusions in [45] for dimensions $d \leq 3$, and to higher orders in the volume and to domain with Lipschitz boundaries in [21] for arbitrary dimensions. In those references, the inclusion is modeled by a jump in the diffusion coefficient so that its first order effect on the boundary measurements is proportional to the inclusion's volume. The so-called polarization tensor contains the information about the inclusion that is available at this level of the asymptotic expansion.

Such a setting for the diffusion coefficient prevents us from using the well-known change of variable $q := \frac{\Delta\sqrt{D}}{\sqrt{D}}$ that allows us to relate the diffusion equation to the Helmholtz or Schrödinger equation. Since one of the objectives here is to show the equivalence of the asymptotic expansions within the diffusion and Helmholtz

frameworks, we consider general inclusions with or without jumps and derive the corresponding asymptotic expansions. We also recover the formulas in [21] in the special case of constant coefficients in the background and the inclusion.

We consider the following system of equations:

$$\nabla \cdot D^\varepsilon \nabla u^\varepsilon = 0, \quad \text{in } \Omega, \quad D^\varepsilon \frac{\partial u^\varepsilon}{\partial \mathbf{n}} = g, \quad \text{on } \partial\Omega, \quad \text{with } \int_{\partial\Omega} u^\varepsilon d\sigma = 0, \tag{3.1}$$

where $\Omega$ is a bounded open domain of dimension $d \geq 2$ with Lipschitz boundary, $\sigma$ is the surface measure on $\partial\Omega$, and $g \in L^2(\partial\Omega)$ such that the following compatibility condition holds $\int_{\partial\Omega} g d\sigma = 0$. It is assumed that $D^\varepsilon$ is bounded from below by a positive constant independent of $\varepsilon$ and that $D^\varepsilon$ satisfies the decomposition $D^\varepsilon(\mathbf{x}) = D_0(\mathbf{x}) + D_1(\frac{\mathbf{x}-\mathbf{x}_0}{\varepsilon})$, where $0 < C_0' \leq D_0 \in \mathcal{C}^\infty(\overline{\Omega})$, $D_1 \in L^\infty(\Omega)$ and $D_1$ vanishing in $\mathbb{R}^d \backslash \overline{B}$, $B$ being a bounded set with Lipschitz boundary. We assume in addition that the domain of the inclusion is located away from the boundary in the sense that there exists $d_0 > 0$ independent of $\varepsilon$ such that $\text{dist}(\partial\Omega, \mathbf{x}_0 + \varepsilon B) > d_0$. The Lax-Milgram lemma applied to (3.1) yields a unique variational solution $u^\varepsilon \in H^1(\Omega)$. Let us denote by $U$ the solution with background diffusion coefficient $D_0$:

$$\nabla \cdot D_0 \nabla U = 0, \quad \text{in } \Omega, \quad D_0 \frac{\partial U}{\partial \mathbf{n}} = g, \quad \text{on } \partial\Omega, \quad \text{with }, \int_{\partial\Omega} U d\sigma = 0 \tag{3.2}$$

and introduce the related Green function $N \in \mathcal{D}'(\Omega \times \Omega)$ satisfying, for all fixed $\mathbf{y}$ in $\Omega$,

$$\begin{cases} \nabla_{\mathbf{x}} \cdot D_0(\mathbf{x}) \nabla_{\mathbf{x}} N(\mathbf{x}, \mathbf{y}) = -\delta(\mathbf{x} - \mathbf{y}), & \text{in } \Omega, \\ \qquad D_0(\mathbf{x}) \dfrac{\partial N(\mathbf{x}, \mathbf{y})}{\partial \mathbf{n}_{\mathbf{x}}} = -\dfrac{1}{|\partial\Omega|}, & \text{on } \partial\Omega, \quad \displaystyle\int_{\partial\Omega} N(\mathbf{x}, \mathbf{y}) d\sigma(\mathbf{x}) = 0. \end{cases} \tag{3.3}$$

For all $\mathbf{x} \in \overline{\Omega}$, the Lax-Milgram lemma yields again a unique variational solution $U \in H^1(\Omega)$ and standard elliptic regularity results implies that $U \in \mathcal{C}^\infty(\Omega)$ since $D_0 \in \mathcal{C}^\infty(\overline{\Omega})$. We denote by $\Gamma$ the fundamental solution of the Laplacian, namely

$$\Gamma(\mathbf{x}) = -\frac{1}{2\pi} \log |\mathbf{x}|, \qquad d = 2, \quad \frac{1}{(d-2)|S_{d-1}|} \frac{1}{|\mathbf{x}|^{d-2}}, \qquad d \geq 3, \tag{3.4}$$

where $|S_{d-1}|$ is the measure of the $(d-1)$-dimensional unit sphere. Throughout the chapter, we use the following multi-index notations: for $i = (i_1, \cdots, i_d) \in \mathbb{N}^d$, we define $|i| = i_1 + \cdots + i_d$, $\partial^i f = \partial_1^{i_1} f \cdots \partial_d^{i_1} f$ and $\mathbf{x}^i = x_1^{i_1} \cdots x_d^{i_d}$. We also define $i! = i_1! \cdots i_d!$.

Our first result is the following:

**Theorem 3.2.1** *The solution $u^\varepsilon$ to (3.1) verifies the following asymptotic expansion, a.e. on $\partial\Omega$:*

$$u^\varepsilon(\mathbf{y})|_{\partial\Omega} = U(\mathbf{y})|_{\partial\Omega} - \sum_{|i|=1}^{d}\sum_{|j|=1}^{d} \frac{\varepsilon^{d-2+|i|+|j|}}{i!j!} M_{ij}\, \partial^j U(\mathbf{x}_0)\ \partial^i_{\mathbf{x}} N(\mathbf{x}_0,\mathbf{y})\big|_{\partial\Omega} + \mathcal{O}(\varepsilon^{2d})$$
$$-\sum_{|i|=1}^{d}\sum_{|j|=1}^{d}\sum_{|k|=0}^{d}\sum_{\substack{l=0\\ l+|k|>0}}^{d} \frac{\varepsilon^{d-2+|i|+|j|+|k|+l}}{i!j!k!l!} M^2_{ijkl}\partial^j U(\mathbf{x}_0)\left(\partial^k D_0^{-1}\right)(\mathbf{x}_0)\,\partial^i_{\mathbf{x}} N(\mathbf{x}_0,\mathbf{y})\big|_{\partial\Omega},$$

*where $M$ and $M^2$ are generalized polarization tensors given by*

$$\begin{aligned} M_{ij} &= \int_B D_1(\mathbf{x})\,\nabla(\mathbf{x}^j + \phi^0_{j\,0}(\mathbf{x}))\cdot\nabla\mathbf{x}^i d\mathbf{x}, \qquad i,j\in\mathbb{N}^d, \\ M^2_{ijkl} &= \int_B D_1(\mathbf{x})\,\nabla\phi^l_{jk}(\mathbf{x})\cdot\nabla\mathbf{x}^i d\mathbf{x}, \qquad i,j,k\in\mathbb{N}^d, \quad l\in\mathbb{N}, \end{aligned} \tag{3.5}$$

*and the functions $\phi^l_{jk}$ are the unique solutions in $H^1_{loc}(\mathbb{R}^d)\cap\mathcal{C}^\infty(\mathbb{R}^d\backslash\overline{B})$ to a set of related PDE's depending on $D_0$ and $D_1$, see [4]. Here, the notation $\mathcal{O}(\varepsilon^{2d})$ in the expansion represents a term bounded in $L^2(\partial\Omega)$ by a constant depending on $\|D_1\|_{L^\infty}$ and on $\|g\|_{L^2(\partial\Omega)}$.*

Theorem 3.2.1 has been proved in [21] by using single and double layer potential techniques when the background diffusion coefficient $D_0$ is constant on the entire domain $\Omega$ and when $D_1$ is constant on $B$. Our result generalizes that of [21] to the case of non-constant $D_0$ and $D_1$ for which layers techniques are not available. The first order of the expansion can also be obtained from the general formula proved in [44] and in [45] for $d\leq 3$, while our formula is valid in any dimension greater than 2.

The leading order in the expansion is given by

$$\varepsilon^d \sum_{|i|=|j|=1} M_{ij}\partial^i_{\mathbf{x}} N(\mathbf{x}_0,\mathbf{y})\partial^j U(\mathbf{x}_0),$$

which can be used to reconstruct $\mathbf{x}_0$ and for instance the product $D_1|B|$ if $D_1$ is constant. To be able to reconstruct $D_1$ and $|B|$ separately, one needs the next order in the expansion, see [21, 45]. The polarization tensor $M^2$ contributes only to higher orders. The polarization tensor $M$ captures the correction when the background diffusion coefficient $D_0$ is constant in $\mathbf{x}_0+\varepsilon B$, whereas $M^2$ is the correction that needs to be added when $D_0$ is not constant in $\mathbf{x}_0+\varepsilon B$. When $D_0$ is constant in $\mathbf{x}_0+\varepsilon B$, then $M^2_{ijkl} = M^2_{ijkl}\delta^0_l$ so that the expansion then reduces to the classical formula:

$$u^\varepsilon(\mathbf{y}) = U(\mathbf{y}) + \sum_{|i|=1}^{d}\sum_{|j|=1}^{d} \frac{\varepsilon^{d-2+|i|+|j|}}{i!j!} M_{ij}\partial^i_{\mathbf{x}} N(\mathbf{x}_0,\mathbf{y})\partial^j U(\mathbf{x}_0) + \mathcal{O}(\varepsilon^{2d}).$$

It is interesting to notice that the classical expansion above is valid whether or not $D_0$ is constant outside the inclusion, which a priori could not be infered from the reference works [21, 45].

Another result is given by:

**Proposition 3.2.2** *There exists a perturbation* $0 \not\equiv D_1 \in L^\infty(\Omega)$ *with spherical symmetry such that* $M_{ij} \equiv 0$.

The latter result is to be compared with the case where $D_1$ is constant for which there is always a contribution of order $\varepsilon^d$ in the expansion provided the constant is not zero. That result is interesting for applications for which the goal is to render the inclusion less detectable, like cloaking for instance. If the inclusion is carefully designed, its influence on the measurements is an order weaker than a standard inclusion.

**Elements of proof.** The starting point is the integral formula:

$$\begin{aligned} u^\varepsilon(\mathbf{y}) &= U(\mathbf{y}) - \int_{\mathbf{x}_0+\varepsilon B} D_1\left(\frac{\mathbf{x}-\mathbf{x}_0}{\varepsilon}\right) \nabla u^\varepsilon(\mathbf{x}) \cdot \nabla_{\mathbf{x}} N(\mathbf{x},\mathbf{y}) d\mathbf{x}, \\ &= U(\mathbf{y}) - \varepsilon^d \int_B D_1(\mathbf{x}) \nabla u^\varepsilon(\mathbf{x}_0+\varepsilon\mathbf{x}) \cdot \nabla_{\mathbf{x}} N(\mathbf{x}_0+\varepsilon\mathbf{x},\mathbf{y}) d\mathbf{x}. \end{aligned}$$

Then $u^\varepsilon$ is decomposed as $u^\varepsilon(\mathbf{x}) = U(\mathbf{x}) + w^\varepsilon\left(\frac{\mathbf{x}-\mathbf{x}_0}{\varepsilon}\right)$, where $U$ is the homogeneous part and $w^\varepsilon$ is a corrector. The corner stone of the proof is finding an appropriate decomposition of the Green function $N$ into singular and smooth contributions. When $D_0$ is constant, it is straightforward, see for instance [21]. When it is not, it is less clear. An attempt is made in [45], in which the decomposition is chosen to be, for $d = 3$,

$$N(\mathbf{x},\mathbf{y}) = \frac{1}{4\pi D_0(\mathbf{x}_0)|\mathbf{x}-\mathbf{y}|} - \frac{\nabla D_0(\mathbf{x}_0)\cdot(\mathbf{x}-\mathbf{y})}{8\pi D_0^2(\mathbf{x}_0)|\mathbf{x}-\mathbf{y}|} + R(\mathbf{x},\mathbf{y}),$$

where $R$ is a remainder smoother than the two first terms. $R$ is not smooth enough for deriving high order asymptotic formulas or for dimensions $d > 3$. The adequate expression is the following, and stems for the simple observation that we only need to decompose the gradient of the Green function rather than the Green function itself:

$$\nabla_{\mathbf{x}} N(\mathbf{x},\mathbf{y}) = D_0^{-1}(\mathbf{x}) \nabla_{\mathbf{x}} \Gamma(\mathbf{x}-\mathbf{y}) + \nabla_{\mathbf{x}} R(\mathbf{x},\mathbf{y}),$$

where here $R \in \mathcal{C}^\infty(\Omega\times\Omega)$. This decomposition allows to obtain high order formulas for any dimensions and to perform all the expansions needed to prove theorem 3.2.1.

The proof of proposition 3.2.2 uses bounds on the polarization tensor and is an application if the intermediate values theorem.

## 3.3 The Helmholtz equation

This section addresses the problem of small-volume inhomogeneities in the Helmholtz equation. We consider the following Helmholtz (or Schrödinger) equation posed in a bounded Lipschitz domain $\Omega$ of $\mathbb{R}^d$:

$$\left\{ \begin{array}{l} -\Delta v^\varepsilon(\mathbf{x}) + \Big(q_0(\mathbf{x}) + \dfrac{1}{\varepsilon^{2-\eta}} q_1\Big(\dfrac{\mathbf{x}-\mathbf{x}_0}{\varepsilon}\Big)\Big) v^\varepsilon(\mathbf{x}) = 0, \quad \mathbf{x} \in \Omega, \\ \dfrac{\partial v^\varepsilon}{\partial \mathbf{n}} = g \in L^2(\partial\Omega) \quad \text{on } \partial\Omega, \end{array} \right. \tag{3.6}$$

where $\mathbf{x}_0$ is a given point in $\Omega$, $q_0 \in L^\infty(\Omega)$ is the background index or potential, and $q_1 \in L^\infty(\Omega)$ is a local perturbation, with support localized in a bounded Lipschitz domain $B$. We consider the case with only one inclusion, knowing that the results below generalize to the setting with several well-separated inclusions so long as the maximal order in the expansion is sufficiently small so that the inclusions do not interact at that order. The perturbation has a magnitude of order $\varepsilon^{\eta-2}$, with $\eta \in [0,2]$. The most interesting case is $\eta = 0$, which corresponds to the strongest type of perturbation. The latter case allows to relate the asymptotic formula given in the preceding section to the one for (3.6) for a particular form of the potential $q_1$.

When $q_0$ is negative, the above system models waves propagating in a medium perturbed by a small inclusion of diameter $\varepsilon$ with a refractive index of order $\varepsilon^{\eta-2}$. We refer to [84] and [85] for the case of high-frequency waves in dimension two perturbed by small inclusions with index of order one. The case $q_0$ and $q_1$ constant with $q_0$ negative and $\eta = 2$ has been treated in [21] with Dirichlet conditions instead of Neumann conditions at the domain's boundary. When $q_0$ is positive, (3.6) models, e.g., diffusive light propagating in a medium with background absorption $q_0$ and zones of different absorption coefficients in a small volume. The case $\eta = 2$ has been investigated in dimension three in [26] for a constant background $q_0$ and a constant perturbation $q_1$.

One of our motivations here is to compare the asymptotic expansions for the solution $u^\varepsilon$ to the diffusion equation (3.1) given in theorem 3.2.1 with the one for the solution $v^\varepsilon$ to the Helmholtz equation (3.6). Relating those formulas is actually surprisingly technical as the sequel shows. To this aim, it is well-known that a solution to the diffusion equation $\nabla \cdot D\nabla u = 0$, with $D \in \mathcal{C}^2(\mathbb{R}^d)$ for instance and strictly positive, also satisfies a Helmholtz or Schrödinger equation of the form

$$\Delta\big(\sqrt{D}u\big) - \Big(\frac{\Delta\sqrt{D}}{\sqrt{D}}\Big)\big(\sqrt{D}u\big) = 0.$$

Our purpose here is to verify that the polarization tensors obtained in the diffusion and Helmholtz frameworks are indeed the same for the specific form of the potential

$q_1$ that allows us to transform one equation into the other. As in section 3.2, we define $D^\varepsilon(\mathbf{x}) = D_0(\mathbf{x}) + D_1(\frac{\mathbf{x}-\mathbf{x}_0}{\varepsilon})$ and to simplify the presentation, assume that $D_0$ is constant in $\Omega$. We assume that $D_1 \in \mathcal{C}^2(\Omega)$ with support included in $B$ and that $D_0 + D_1$ is strictly positive in $\Omega$, so that we can define

$$q_1(\mathbf{x}) := \frac{\Delta\sqrt{D_0 + D_1(\mathbf{x})}}{\sqrt{D_0 + D_1(\mathbf{x})}}. \tag{3.7}$$

Considering the function $v^\varepsilon$ which satisfies (3.6) with $q_0 = 0$, $\eta = 0$ and $q_1$ defined as above, the quantity

$$\frac{v^\varepsilon(\mathbf{x})}{\sqrt{D_0 + D_1(\frac{\mathbf{x}-\mathbf{x}_0}{\varepsilon})}}$$

solves (3.1) with $g$ replaced with $\sqrt{D_0}g$. Since $\eta = 0$, we may expect from (3.6) that the inclusion induces a correction of order $\varepsilon^{d-2}$ whereas the same inclusion induces a correction of order $\varepsilon^d$ in the diffusion equation. Some simplifications due to the particular form of the potential $q_1$ must render the correction of order $\varepsilon^d$ in the Helmholtz framework as well. This is what we will see in the sequel.

For simplicity, we present here only the expansions for $q_0 = 0$, $\eta = 0$, see [4] for the general case. We denote by $V$ the solution of the unperturbed equation

$$\Delta V = 0, \quad \mathbf{x} \in \Omega, \quad \frac{\partial V}{\partial \mathbf{n}} = g \quad \text{on } \partial\Omega, \quad \int_{\partial\Omega} V d\sigma = 0 \quad \text{and} \quad \int_{\partial\Omega} g d\sigma = 0, \tag{3.8}$$

where $\sigma$ denotes the surface measure on $\partial\Omega$. Existence and uniqueness for (3.6) uniformly in $\varepsilon$ for $\varepsilon$ small enough holds without additional condition on $q_1$ when $\eta \in ]0, 2]$. When $\eta = 0$, we add the following assumption:

**(H)** $-1$ is not an eigenvalue of the bounded operator $T$ defined as:

$$T : L^2(B) \to L^2(B), \quad \varphi \to T\varphi(\mathbf{y}) = \int_B q_1(\mathbf{x})\varphi(\mathbf{x})\Gamma(\mathbf{x} - \mathbf{y})d\mathbf{x}.$$

Here, $\Gamma$ is the fundamental solution of the Laplacian given in (3.4). **(H)** is verified for instance when $q_1 > 0$ a.e. in $B$ or when the following Rollnick type [104] norm of $q_1$ is less than one,

$$\int_B \int_B \left(\sqrt{|q_1(\mathbf{x})|}\sqrt{|q_1(\mathbf{y})|}|\Gamma(\mathbf{x}, \mathbf{y})|\right)^p d\mathbf{x}d\mathbf{y} < 1,$$

for some $p \geq 1$, or when $q_1$ is a Bohm-like potential of the form (3.7). That last case in the one of interest to us.

We then have the following theorem:

**Theorem 3.3.1** *Assume that* ***(H)*** *is satisfied when* $\eta = 0$. *Then, there exists* $\varepsilon_0 > 0$, *such that for all* $0 < \varepsilon < \varepsilon_0$, *the system (3.6) with* $q_0 = \eta = 0$ *admits a unique variational solution* $v^\varepsilon \in H^1(\Omega)$ *which satisfies the following asymptotic expansion, almost everywhere on* $\partial\Omega$:

$$\begin{aligned} v^\varepsilon(\mathbf{y})|_{\partial\Omega} &= V(\mathbf{y})|_{\partial\Omega} - \sum_{|j|=0}^{d+1}\sum_{|i|=0}^{d+1} \frac{\varepsilon^{d-2+|i|+|j|}}{i!j!}\left(Q_{ij}+Q^0_{ij}\right)\partial^j V(\mathbf{x}_0)\,\partial^i_{\mathbf{x}} N(\mathbf{x}_0,\mathbf{y})\big|_{\partial\Omega} \\ &\quad +\varepsilon^{2(d-2)} f^\varepsilon(\mathbf{y}) + \mathcal{O}(\varepsilon^{2d}), \end{aligned}$$

*where* $\mathcal{O}(\varepsilon^{2d})$ *is a term bounded in* $L^2(\partial\Omega)$ *by* $C\varepsilon^{2d}$, *and for* $(i,j) \in \mathbb{N}^d \times \mathbb{N}^d$,

$$Q_{ij} = \int_B q_1(\mathbf{x})\mathbf{x}^j\mathbf{x}^i d\mathbf{x}, \qquad Q^0_{ij} = \int_B q_1(\mathbf{x})\phi^0_j(\mathbf{x})\mathbf{x}^i d\mathbf{x},$$

*where* $\phi^0_j$ *is the unique solution in* $H^1(B)$ *to* $\phi^0_j + T\phi^0_j = -T\mathbf{x}^j$. *The operator* $T$ *is defined in* ***(H)*** *and the remainder* $\|f^\varepsilon\|_{L^2(\partial\Omega)}$ *is of order* $\mathcal{O}(1)$.

Above, $N$ is the Green function (3.3) with $D_0 = 1$. When $q_1$ is constant and not identically zero, there is a contribution of order $\varepsilon^{d-2}$ in the expansion, while for spatially varying $q_1$, the first order contribution can vanish for instance by choosing $q_1$ such that $\int_B q_1 d\mathbf{x} = 0$. More difficult is to cancel the second order to be able to recover the order $\varepsilon^d$ of the diffusion. This can be achieved with a potential of the form (3.7) as stated below, but we do not know if it is possible for other types of potentials:

**Proposition 3.3.2** *When* $q_1$ *has the form (3.7), then* $\|f^\varepsilon\|_{L^2(\partial\Omega)}$ *is of order* $\mathcal{O}(\varepsilon^4)$ *and we have*

$$\sum_{|j|=0}^{1} \frac{\varepsilon^{|j|}}{j!}\partial^j V(\mathbf{x}_0)\left(Q_{0j}+Q^0_{0j}\right) + \varepsilon\sum_{|i|=1}\partial^i_{\mathbf{x}} N(\mathbf{x}_0,\mathbf{y})\left(Q_{i0}+Q^0_{i0}\right) = 0. \tag{3.9}$$

*Here, the index* 0 *of the polarization tensors represents the vector of* $\mathbb{N}^d$ *with components all equal to zero. We have the following relation between the polarization tensor* $M$ *in the context of theorem 3.2.1 and the polarization tensor* $\widetilde{M} := \sqrt{D_0}(Q+Q^0)$ *in the context of the Helmholtz equation:*

$$M_{ij} = \widetilde{M}_{ij}, \qquad |i|+|j| \le d+1, \tag{3.10}$$

Equation (3.9) implies that the two first orders in the expansion of theorem 3.3.1 vanish so that the correction is of order $\varepsilon^d$. Equation (3.10) show the equivalence of the tensors $M_{ij}$ and $\widetilde{M}_{ij}$ for $|i|+|j| \le d+1$, which is enough to show that the expansions on $u^\varepsilon$ and $v^\varepsilon$ agree up to the order $\varepsilon^{2d}$.

**Elements of proof.** The existence and uniqueness are standard and a consequence of the Fredholm alternative. Regarding the asymptotic formula, as for the diffusion, we express $v^\varepsilon$ in terms of $V$ and the Green function $N$, to obtain, a.e. in $\Omega$:

$$v^\varepsilon(\mathbf{y}) = V(\mathbf{y}) - \varepsilon^{d-2+\eta} \int_B q_1(\mathbf{x}) \left(V(\mathbf{x}_0 + \varepsilon\mathbf{x}) + w^\varepsilon(\mathbf{x}_0 + \varepsilon\mathbf{x})\right) N(\mathbf{x}_0 + \varepsilon\mathbf{x}, \mathbf{y}) d\mathbf{x}.$$

Then one needs to decompose $N$ as singular and smooth parts and to find an appropriate equation for the corrector $w^\varepsilon$. The proof of proposition (3.3.2) is fairly technical and extensively uses the particular form of $q_1$ (3.7). We show for instance that the term $f^\varepsilon$ is of order $\varepsilon^4$, which is not obvious at the first sight, see [4] for the details.

## 3.4 Perspectives

There are different directions. A first one is to use the high order asymptotic formula of theorem 3.2.1 when the background $D_0$ is varying to perform reconstructions. We know from the expansion that the influence of the variations of $D_0$ at the location of the inclusion appears only at high orders and not the leading one, but we have not quantified such influence yet and how it affects the quality of the reconstructions. It is rather unlikely this will significantly modify the location of the inclusion since it is deduced from the leading order. Nevertheless, since the separate reconstructions of the volume and the diffusion coefficient of the inclusion uses the higher orders terms, it is expected that the correction due to the background needs to be included. Numerical simulations would help confirming this fact and quantifying the effects of a varying background. Besides, an analysis on the polarization tensor $(M^2_{ijkl})$ has still to be carried out to figure if it brings additional information on the inclusion to that of the classical tensor $(M_{ij})$.

A second direction concerns the cancellation of the high order terms in the expansion for particular inclusions to render them harder to detect. We know it is possible to cancel the leading order -not having an expression for the corresponding perturbation though-, but we actually do not know if it is possible to do so for the higher order terms. This requires a careful analysis of the properties of the polarization tensors.

Another investigation would be the effects of a varying background on closely spaced or on near boundary inclusions for which the results presented in this chapter do not apply.

# Part II

# Quantum transport in nanostructures

# Chapter 4

# The Schrödinger-Poisson system on open domains

In this chapter, we investigate the derivation of uniform bounds with respect to the scaled Planck constant $\varepsilon$ for solutions to the open transient Schrödinger-Poisson system introduced in [13]. The uniform estimates stem from a careful analysis of the non-local in time transparent boundary conditions which allow to restrict the original problem posed on an unbounded domain to a bounded domain of interest. The obtained bounds can be used to perform the semi-classical limit of the system. We also give an existence and uniqueness result of weak solutions while they were previously defined in a strong sense. The chapter is a summary of [8].

## 4.1 Introduction

The modeling of semiconductors at the quantum level has become a very active area of research during the past decades. Indeed, the design of high-performance components requires the development of simulation tools that help the engineers in finding the best configurations. This in turn demands a compromise between the accuracy of the models and the computational cost, and thus to derive models as close to physics as possible with a relatively cheap cost of resolution. The particular geometry and physics of semiconductors allow for a wide variety of models, see for instance [36]. A semiconductor can roughly be decomposed into two zones: an *access zone*, through which the particles reach the *active zone*, where basically all the main physical effects take place. Whereas the access zone is generally not the most relevant part of the component, it has usually the largest dimensions (say some hundreds of nanometers long) and thus a lot of computational time might be spent in there. On the other hand, the active zone, which could be roughly a few tens of nanometers long, represents the essential part of the semiconductor and then needs to be carefully treated. Indeed, the operation of the device is basically induced by the potential profile in the active region which presents some sharp variations -on the order of the De Broglie wavelength of the electrons- so that the dynamics requires a quantum description, more expensive than a kinetic one. It has then led to different strategies to lower the computational time spent in the access zones. One possible strategy is to prescribe adequate *transparent boundary conditions* at the interfaces access zone - active zone, so as to limit the resolution to the active zone; another strategy is to model the two zones differently -with a relatively cheap treatment of the access zone- and to couple them at the interfaces. The first strategy has already received a great interest since it is related to many wave propagation problems in unbounded domains for which the aim is to restrict the resolution to a bounded zone. There is a very abundant literature about the subject, one could cite the pioneering work of [61], [23] in the context of semiconductors and [24] for numerical considerations. Note that the concept of open systems at the quantum level cannot be straightforwardly defined as it is at the kinetic level where it suffices to prescribe the distribution function for incoming velocities. This requires the introduction of conjuguate operators which dissociate ingoing from outgoing particles as it was done elegantly in a very general framework in [98]. The second strategy is also an active area of research. Typically, the active region is treated as fully quantum, with possibly some subband decomposition, see [101], while the access zone only requires a kinetic description. The two descriptions are then connected via adequate interfaces conditions, as it was done in [51, 37].

The description chosen here is fully quantum, namely both in the access and active zones, and then falls into the first type of models. The dynamics of the

electrons is then given by the Schrödinger equation everywhere in the semiconductor and it is assumed that their energy distribution is known. The electrons being charged particles, they self-interact. The non-linear effects are taken into account at Hartree level through a potential solution to the Poisson equation, giving rise to the so-called Schrödinger-Poisson system. That system can be seen as a mean-field approximation of a system of many-interacting particles through a Coulomb potential [35]. There is as well an extensive literature about the subject, see for instance [81] for a general mathematical analysis, and [97, 98] in the context of open quantum system. In [13] a quantum transport model is introduced, and explicit boundary conditions at the interfaces access zone - active region are derived, and will be recalled further. The wavefunctions are solution to the Schrödinger equation

$$i\hbar\frac{\partial\psi_\lambda}{\partial t} = \mathcal{H}(t)\psi_\lambda, \qquad \mathcal{H}(t) = -\frac{\hbar^2}{2m_e}\,\Delta + V_e(t,\mathbf{x}) + V_s(t,\mathbf{x}), \tag{4.1}$$

where $\hbar$ is the Planck constant, $\lambda$ is a given quantum number, $m_e$ is the effective mass of the electron in the semiconductor (supposed to be constant to simplify), $V_e$ is an exterior potential, while $V_s$ is the self-consistent potential solution to the Poisson equation

$$-\Delta V_s = \int |\psi_\lambda|^2 d\mu,$$

for some measure $\mu$. In [13], the model is shown to have a unique strong solution $(\psi_\lambda, V_s)$ (say $H^2$ for the wavefunction) provided the data are regular enough. A possible way to confirm that the introduced transparent boundary conditions correctly describe the physics of the device, is to perform the *semi-classical limit* of the above system, by letting the scaled Planck constant $\varepsilon$ ($\varepsilon := \hbar := \frac{\hbar}{\sqrt{m_e}}$ in the sequel) go to zero. This limit is performed by means of Wigner transforms [110] which relates the quantum dynamics to the classical one. It is thus expected that at the limit, the boundary conditions simply reduce to standard inflow boundary conditions, as it was done in [39] for a one-dimensional stationary model. Passing rigorously to the limit requires some bounds uniform in $\varepsilon$ for the wavefunctions, which in turn provide estimates on the Wigner transform in some appropriate spaces, see [80, 94]. Our purpose here is then to address the question of uniform bounds for the open Schrödinger-Poisson system introduced in [13]. While in standard Schrödinger equations with $L^2$ initial conditions those estimates are straightforward, it is not the case when considering open systems with transparent boundary conditions. The reference [13] gives some regularity results and estimates, without precising the dependence on $\varepsilon$. This work thus provides uniform bounds in $L^2_{loc}$ which stem from a careful analysis of the non-local in time boundary conditions imposed on the interfaces active zone - access zone. In addition to this estimates, we construct as well weak solutions to the open Schrödinger-Poisson model of [13] where the solutions were defined in a strong sense. Those solutions verify the Schrödinger equation in a variational form

which could be suitable for numerical simulations since it naturally incorporates the transparent boundary conditions in the formulation.

## 4.2 Setting of the problem and main result.

The model consists in a Schrödinger-Poisson system posed on an unbounded domain, with non-vanishing conditions at the infinity modeling the electron injection in the structure. This system is then reduced to a problem posed on a bounded domain with suitable inhomogeneous transparent boundary conditions taking into account the injected particles.

**Geometry.** The unbounded domain is denoted by $\Omega$ and its dimension by $d$, with $d = 2$ or $d = 3$. The domain $\Omega$ is then split into two zones, a *bounded active zone* denoted by $\Omega_0$ and an *unbounded access zone*, consisting of $n$ wave guides $\Omega_j$, $j = 1, \cdots, n$, see figure 4.1. The interfaces between $\Omega_0$ and each $\Omega_j$ are supposed to be *flat* and are denoted by $\Gamma_j$. The wave guides $\Omega_j$ have a cylinder-like structure and can thus be written as the cartesian product $\Gamma_j \times \mathbb{R}^+$. They are equipped with a local set of coordinates $(\xi_j, \eta_j) \in \Gamma_j \times \mathbb{R}^+$. Here, $\eta_j$ is basically the variable associated with the direction of propagation in the lead $j$. The outer boundaries of the $\Gamma_j$'s are denoted by $\Gamma_{j,0}$. The remaining part of the boundary of $\Omega_0$ is denoted by $\Gamma_0$ so that $\partial\Omega_0 = \Gamma_0 \bigcup \left(\cup_{j=1}^n \Gamma_j\right)$. We also introduce $(\mu_j)_{j=1,\cdots,n}$, a partition of

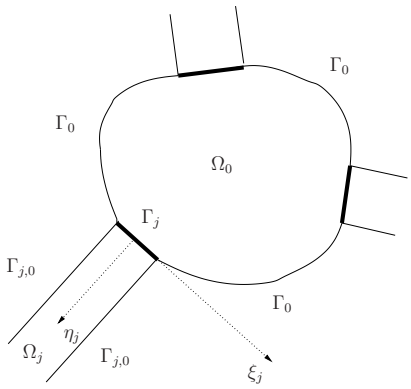


Figure 4.1: The domain $\Omega$

unity of $\Omega$, i.e., some $\mathcal{C}^\infty(\Omega)$ functions which satisfy

$$\begin{cases} 0 \leq \mu_j \leq 1, \quad \displaystyle\sum_{j=1}^{n} \mu_j = 1 \quad \text{on } \Omega, \quad \mu_j = 1 \text{ on } \Omega_j \quad j = 1, \cdots, n, \\ \mu_j = 0 \text{ on } \Omega_k \quad \text{for } k \neq 0,\ k \neq j. \end{cases}$$

**Initial conditions.** To model the electron injection, the initial conditions are supposed to be non-zero in the leads and to be scattering states of a given Hamiltonian $\mathcal{H}^0$ defined by

$$\mathcal{H}^0 = -\frac{\varepsilon^2}{2}\,\Delta + V^0,$$

where $V^0$ is an exterior potential which is assumed to depend only on the transversal coordinate in the leads $\Omega_j$, i.e., $V^0 \in L^\infty(\Omega)$ and $V^0\,\big|_{\Omega_j} = V^0(\xi_j)$. The fact that $V^0$ does not depend on $\eta_j$ is necessary to be able to construct rather simple - though not obvious- boundary conditions on the interfaces $\Gamma_j$, $j \neq 0$. When $V^0$ is linear in $\eta_j$, the analysis is more involved and the resulting boundary conditions are more complex, see for instance [60]. We then define the transversal Hamiltonian $\mathcal{H}_j^0 = -\frac{\varepsilon^2}{2}\,\Delta_{\xi_j} + V^0(\xi_j)$, equipped with Dirichlet boundary conditions on $\Gamma_{j,0}$. It admits a compact resolvent and we denote by $(\chi_m^{0,j}, E_m^j)_{m\in\mathbb{N}^*}$, $j = 1, \cdots, n$, its spectral decomposition. For two functions $f$ and $g$ in $L^2(\Gamma_j)$, we define

$$\langle f,\, g\rangle_j = \int_{\Gamma_j} f(\xi_j)\,\overline{g}(\xi_j)\,d\sigma_j, \qquad f_m^j = \int_{\Gamma_j} f(\xi_j)\,\overline{\chi}_m^j(\xi_j)\,d\sigma_j,$$

where $\sigma_j$ is the surface measure on $\Gamma_j$. We suppose without loss of generality that $E_m^j \geq 0$, $\forall m \geq 1$, $\forall j \geq 1$, it suffices in the sequel to multiply the time-dependent Schrödinger equation by the phase factor $e^{i\frac{t}{\varepsilon}\min_{j,m} E_m^j}$ to recover the general case where $V_j$ is negative and bounded from below.

The electrons are injected in the leads in given quantum states. These states follow a prescribed statistics denoted by $\mu$. $\mu$ is a non-negative measure on the state space $\Lambda$, and a pure state is denoted by $\lambda$. The wavefunctions are thus indexed by $\lambda$. Consider the following hypotheses for a family of functions $\psi_\lambda^0 \in H^1_{loc}(\Omega)$:

**(H-1)** For a.e. $\lambda \in \Lambda$, there exists a constant $E(\lambda)$ such that

$$\mathcal{H}^0\psi_\lambda^0 = E(\lambda)\psi_\lambda^0 \quad \text{in } \Omega_j, \quad \psi_\lambda^0 = 0, \quad \text{on } \Gamma_{j,0}\times\mathbb{R}_+, \quad j \neq 0.$$

**(H-2)** For any bounded set $K \subset \Omega$, there exists $C_K > 0$ finite such that

$$\int_\Lambda \|\psi_\lambda^0\|^2_{H^1(K)}\,d\mu(\lambda) \leq C_K.$$

In practice, the electrons are injected in the guide $j_0$, on the transverval mode $m_0$ and with a non-vanishing longitudinal momentum $p$. This implies that $\lambda = \{p, m_0, j_0\}$, $\Lambda = \mathbb{R}_+^* \times \mathbb{N}^* \times \{1, ..., n\}$, $E(\lambda) = \frac{1}{2}p^2 + E_{m_0}^{j_0}$ and

$$d\mu(\lambda) = \Phi(p, m_0, j_0)\,dp\,\delta(m_0)\,\delta(j_0),$$

where $\delta$ denotes the Dirac measure and the positive function $\Phi \in L^1(\mathbb{R}_+^*, \ell^1(\mathbb{N}^* \times \{1, \cdots, n\}))$ the statistics of the injected electrons, typically a Fermi-Dirac statistics. This is equivalent to writing, for any $\varphi \in L^1(\Lambda, d\mu)$,

$$\int_\Lambda \varphi(\lambda) d\mu(\lambda) = \sum_{j_0=1}^{n} \sum_{m_0=1}^{\infty} \int_{\mathbb{R}^+} \varphi(p, m_0, j_0) \Phi(p, m_0, j_0) dp.$$

The energy $\frac{1}{2}p^2$ represents the longitudinal kinetic energy of the electrons while $E_{m_0}^{j_0}$ is the transversal energy in the lead $j_0$. We add the following hypothesis on the measure $\mu$,

$$\int_\Lambda (1 + p^5) d\mu < +\infty, \tag{4.2}$$

and a local in $\lambda$ version of (**H-2**):

**(H-3)** for any bounded set $K \subset \Omega$, there exists $C'_K > 0$ finite and independent of $\lambda$ such that

$$\Phi(\lambda) \|\psi_\lambda^0\|^2_{H^1(K)} \leq C'_K.$$

A family $\psi_\lambda^0 \in H^1_{loc}(\Omega)$ indexed by $\lambda \in \Lambda$ is then said to belong to the class of initial data if hypothesis (**H-1**)–(**H-3**) are satisfied.

**Transparent boundary conditions for the initial conditions.** It is proved in [38], that wavefunctions satisfying hypothesis **(H-1)** verify some boundary conditions on $\Gamma_j$, allowing for a simplification to a boundary value problem on the bounded domain $\Omega_0$. Same kind of boundary conditions have been obtained for the one-dimensional case in [39]. These stationary boundary conditions formally read, with $\sqrt[+]{}$ being the complex square root with non-negative imaginary part,

$$\begin{aligned}
\varepsilon \left. \frac{\partial \psi_\lambda^0}{\partial \eta_j} \right|_{\Gamma_j} &= \mathbb{Z}_j[E(\lambda)](\psi_\lambda^0) + \mathbb{S}_j[E(\lambda)], \\
\mathbb{Z}_j[E(\lambda)](\psi_\lambda^0) &= i \sum_{m=1}^{\infty} \sqrt[+]{2(E(\lambda) - E_m^j)}\, \psi_m^{0,j}\, \chi_m^{0,j}(\xi_j), \qquad (4.3) \\
\mathbb{S}_j[E(\lambda)] &= -2\, i\, \delta_j^{j_0}\, p\, \chi_{m_0}^{0,j}(\xi_j), \qquad (4.4) \\
\psi_m^{0,j} &= \left\langle \psi_\lambda^0(\eta_j = 0, \cdot),\, \chi_m^{0,j} \right\rangle_j .
\end{aligned}$$

It is shown in [38] that these boundary conditions actually make sense in a weak formulation for every $\psi_\lambda^0 \in H^1(\Omega_0)$, see therein for more details and a complete analysis of the related stationary open Schrödinger-Poisson system.

**Potentials.** In [13], it is assumed that the exterior potential of the Hamiltonian (4.1) shares close properties to that of $V^0$. In order to solve exactly the Schrödinger equation in the leads for the derivation of the boundary conditions, it is supposed that the spatial dependence of the exterior potential $V_e$ is only transversal. The following class is then introduced: a given potential $V$ belongs to the class $\mathcal{V}$ if it satisfies: $V \in \mathcal{C}^1([0,T], L^\infty(\Omega))$ and for any $j = 1, \cdots, n$, there exists a function $V_j(t)$ such that for $\mathbf{x} \in \Omega_j$ we have $V(t,\mathbf{x}) = V^0(\mathbf{x}) + V_j(t)$. The regularity in time is needed to obtain energy estimates, that is $H^1(\Omega_0)$ bounds for the wavefunction. One could also consider non-regular in time potentials with some Sobolev regularity in space but in the typical application we are interested in -namely quantum transport in nanostructures- the potentials present a barrier profile which is obviously not smooth.

**The transient open Schrödinger-Poisson system.** As it was done for the stationary case in [38] and in [39], it is proven in [13], that the wavefunction $\psi_\lambda$ satisfy the boundary conditions:

$$\frac{\partial \psi_\lambda}{\partial \eta_j} = -\frac{e^{-i\pi/4}}{\sqrt{\varepsilon}}\, \mathbb{D}_j^{1/2}(\psi_\lambda) + \mathbb{A}_j^\varepsilon(\psi_\lambda^{pw}) \quad ; \quad \mathbf{x} \in \Gamma_j, \quad j = 1, ..., n, \tag{4.5}$$

where

$$\begin{aligned}
\mathbb{D}_j^{1/2} f(t,\xi_j) &= \sqrt{2} \sum_{m \geq 1} \chi_m^j(t,\xi_j)\, \partial^{1/2} \left\langle f(t,\cdot),\, \chi_m^j(t,\cdot) \right\rangle_j, \\
\chi_m^j(t,\xi_j) &= \chi_m^{0,j}(\xi_j)\, \exp\left( -\frac{i}{\varepsilon} \int_0^t (V_j(\tau) + E_m^j)\, d\tau \right), \\
\partial^{1/2} f &= \frac{1}{\sqrt{\pi}} \frac{d}{dt} \int_0^t \frac{f(\tau)}{\sqrt{t-\tau}} d\tau, \\
\psi_\lambda^{pw} &= \psi_\lambda^0 \sum_{j=1}^n \mu_j\, \theta_\lambda^j, \\
\theta_\lambda^j(t) &= \exp\left( -\frac{i}{\varepsilon} \int_0^t (E(\lambda) + V_j(s))\, ds \right), \\
\mathbb{A}_j^\varepsilon(\psi_\lambda^{pw}) &= \left. \frac{\partial\, \psi_\lambda^{pw}}{\partial \eta_j} \right|_{\Gamma_j} + \frac{e^{-i\pi/4}}{\sqrt{\varepsilon}} \mathbb{D}_j^{1/2}(\psi_\lambda^{pw}), \\
&= \frac{1}{\varepsilon} \left( \mathbb{Z}_j[E(\lambda)](\psi_\lambda^0) + \mathbb{S}_j[E(\lambda)] \right) \theta_\lambda^j + \frac{e^{-i\pi/4}}{\sqrt{\varepsilon}}\ \mathbb{D}_j^{1/2}(\psi_\lambda^{pw}).
\end{aligned} \tag{4.6}$$

Then, the Schrödinger-Poisson system reads:

$$i\,\varepsilon\, \partial_t \psi_\lambda = \mathcal{H}(t)\psi_\lambda \quad ; \quad \psi_\lambda(0,\cdot) = \psi_\lambda^0 \quad ; \quad \mathbf{x} \in \Omega_0 \quad ; \quad \lambda \in \Lambda, \tag{4.7}$$

$$-\Delta V_s = \int_\Lambda |\psi_\lambda|^2 d\mu(\lambda) \quad ; \qquad \mathbf{x} \in \Omega_0 \quad ; \quad V_s\,|_{\partial\Omega_0} = 0. \tag{4.8}$$

with the boundary conditions (4.5), $\psi_\lambda = 0$ for $\mathbf{x} \in \Gamma_0$, and where $V_e$ belongs to the class of potentials $\mathcal{V}$ and $\psi_\lambda^0$ belongs to the class of initial conditions. The existence result of [13] provides strong solutions to (4.7)–(4.8). The theorem does not provide any information about the dependence on $\varepsilon$ of the different bounds on $\psi_\lambda$ and $V_s$, which is paramount for the semi-classical limit.

We present now the weak formulation of (4.7)–(4.8) and the main result. The solutions to (4.7) are sought under the following weak form: let $u \in \mathcal{C}^1([0,T), H^1(\Omega_0))$ be a test function, where $T$ is an arbitrary non-negative constant; denoting by $(\cdot,\cdot)$ the $L^2(\Omega_0)$ inner product and using the Green formula, the boundary conditions (4.5), we find $\lambda$ a.e.,

$$-i\,\varepsilon \int_0^T (\psi_\lambda, \partial_s u) ds = i\,\varepsilon\,(\psi_\lambda^0, u(0,\cdot)) + \frac{1}{2}\varepsilon^2 \int_0^T (\nabla\psi_\lambda, \nabla u) ds + \int_0^T (V\,\psi_\lambda, u) ds$$

(4.9)

$$+\frac{1}{2}\sum_{j=1}^{n}\left[\varepsilon^{3/2}\,e^{-i\pi/4}\int_0^T \langle \mathbb{D}_j^{1/2}(\psi_\lambda),\, u\rangle_j\, ds - \varepsilon^2 \int_0^T \langle \mathbb{A}_j^\varepsilon(\psi_\lambda^{pw}),\, u\rangle_j\, ds\right].$$

When the potential $V_e$ belongs to the class $\mathcal{V}$, it is rather natural to consider wave-functions $\psi_\lambda$ solution to (4.9) belonging to $L^2((0,T), H^1(\Omega_0)) \cap \mathcal{C}^0([0,T], L^2(\Omega_0))$. Yet, this regularity is not enough since the boundary terms need more integrability in time to make sense. To define the convenient functional space, we introduce the following family of unitary transformations: for any $f \in L^2((0,T), L^2(\Gamma_j))$, let

$$\mathcal{T}_j f(t,\xi_j) = \sum_{m\geq 1} e^{\frac{i}{\varepsilon}\int_0^t (E_m^j + V_j(s))ds}\,\left\langle f(t,\cdot),\,\chi_m^{0,j}\right\rangle_j\,\chi_m^{0,j}(\xi_j), \tag{4.10}$$

and let $(\mathcal{T}_j\, f)_m = \langle \mathcal{T}_j\, f, \chi_m^{0,j}\rangle_j$. Consider now the functional space

$$\begin{aligned}\mathsf{E} = \{\varphi \in L^2((0,T), H^1(\Omega_0)) \cap \mathcal{C}^0([0,T], L^2(\Omega_0)), \quad &\text{such that}\\ \mathcal{T}_j\varphi \in H^{1/4}((0,T), L^2(\Gamma_j)), \qquad &j = 1,\cdots,n\big\}\,,\end{aligned}$$

and let $\mathsf{E}^0$ be the space of functions belonging to $\mathsf{E}$ with a vanishing trace on $\Gamma_0$. Above, $H^{1/4}((0,T))$ is a fractional Sobolev space. In the weak formulation (4.9), the boundary term $\int_0^T \langle \mathbb{D}_j^{1/2}(\psi_\lambda),\, u\rangle\, ds$ has to be understood in the following weak sense, which uses the expression of the half-derivative in the Fourier space:

$$\int_0^T \langle \mathbb{D}_j^{1/2}(\psi_\lambda),\, u\rangle\, ds = \frac{e^{i\pi/4}}{2\pi}\sum_{m\geq 1}\int_{\mathbb{R}} \bar{\sqrt{}}\xi\, \mathcal{F}(\widetilde{\mathcal{T}_j\,\psi_\lambda})_m\, \overline{\mathcal{F}(\widetilde{\mathcal{T}_j\,u})_m}\, d\xi. \tag{4.11}$$

Above, the $\widetilde{\ }$ sign is the extension by 0 outside $[0,T]$, $\mathcal{F}$ stands for the Fourier transform with respect to time and $\bar{\sqrt{}}$ is the complex square root with non-positive imaginary part. The dual variable of $t$ is denoted by $\xi$. This expression is well-defined for any $\psi_\lambda \in \mathsf{E}$ and $u \in \mathcal{C}^1([0,T], H^1(\Omega_0))$. Our main result is the following:

**Theorem 4.2.1** *Let $\psi_\lambda^0$ belongs to the class of initial data, let $V_e \in \mathcal{V}$ and assume $\mu$ verifies* (4.2)*. Let*

$$\begin{aligned} n(t) &= \int_\Lambda \|\psi_\lambda(t,\cdot)\|^2_{L^2(\Omega_0)} d\mu, \\ \mathcal{E}(t) &= \frac{\varepsilon^2}{2}\int_\Lambda \|\nabla\psi_\lambda(t,\cdot)\|^2_{L^2(\Omega_0)} d\mu + \frac{1}{2}\|\nabla V_s(t,\cdot)\|^2_{L^2(\Omega_0)}. \end{aligned}$$

*Then, the Schrödinger-Poisson system* (4.8)-(4.9) *admits a unique weak solution, for $d = 2$ or $d = 3$, such that, $\lambda$ a.e.,*

$$V_s \in L^2((0,T), W^{3,r}(\Omega_0)) \cap H^1((0,T), W^{1,r}(\Omega_0)) \qquad ; \qquad \psi_\lambda \in \mathsf{E}^0,$$

*with $r < 2$ when $d = 2$ and $r = \frac{3}{2}$ when $d = 3$. Moreover, assuming that*

$$n(0) + \mathcal{E}(0) + \varepsilon \left| \sum_{j=1}^{n} \int_\Lambda \left\langle \mathbb{Z}_j[E(\lambda)](\psi_\lambda^0),\, \psi_\lambda^0 \right\rangle_j d\mu \right| \leq C_0, \tag{4.12}$$

*where $C_0$ is independent of $\varepsilon$, there exists $C_1$, depending on $C_0$, on $\|V_e\|_{\mathcal{C}^1([0,T],L^\infty(\Omega))}$, on $\|p\|_{L^5(\Lambda,d\mu)}$, on $r$, and independent of $\varepsilon$ as well such that,*

$$\|n\|_{L^\infty(0,T)} + \|\mathcal{E}\|_{L^1(0,T)} + \|\partial_t V_s\|_{L^2((0,T),L^r(\Omega_0))} \leq C_1, \tag{4.13}$$

*where $r < 2$ when $d = 2$ and $r < \frac{3}{2}$ when $d = 3$.*

(4.13) provides uniform bounds with respect to $\varepsilon$.

## 4.3 Outline of the proof

The existence part is very standard and is obtained after regularization of the problem in order to use the existence result of strong solutions of [13]. Some estimates then give compactness and allow to pass to the limit in weak formulation. The proof of the $\varepsilon$-independent estimates is more involved and requires a careful analysis of the boundary term $\mathbb{A}_j^\varepsilon(\psi_\lambda^{pw})$, the term involving $\mathbb{D}_j^{1/2}$ presenting no difficulty since it is dissipative, as can be infered from (4.11). Indeed, in the weak formulation (4.9), in order to obtain a $L^2$ bound on the wavefunction for instance, the term $\varepsilon\langle \mathbb{A}_j^\varepsilon(\psi_\lambda^{pw}), \psi_\lambda\rangle_j$ needs to be uniformly bounded with respect to $\varepsilon$. A straightforward bound is given by $C_0\|\psi_\lambda\ \|_{L^2(\Gamma_j)}\|\psi_\lambda^0\ \|_{H^{1/2}(\Gamma_j)}$ for some positive constant $C_0$ independent of $\varepsilon$ (recall that $\mathbb{A}_j^\varepsilon$ is of order $\varepsilon^{-1}$); and by means of trace theorems, this bound turns into $\varepsilon^{-1/2}C_1\|\psi_\lambda\ \|^{1/2}_{L^2(\Omega_0)}\|\varepsilon\nabla\psi_\lambda\ \|^{1/2}_{H^1(\Omega_0)}\|\psi_\lambda^0\ \|_{H^{1/2}(\Gamma_j)}$ which has a wrong homogeneity in $\varepsilon$ whatever the available bound on $\psi_\lambda^0$. We thus expect in the

definition of $\mathbb{A}_j^\varepsilon$ (4.6) some compensations between the homogeneous stationary BC given by $\mathbb{Z}_j$ and the homogeneous time-dependent BC involving the operator $\mathbb{D}_j^{1/2}$. More precisely, we prove that, using previous notations,

$$\int_0^t \langle \mathbb{A}_j^\varepsilon(\psi_\lambda^{pw}),\, \psi_\lambda \rangle_j \, ds = \frac{1}{\varepsilon} \int_0^t \langle \mathbb{S}_j[E(\lambda)]\, \theta_\lambda^j, \psi_\lambda \rangle_j \, ds,$$

so that the contributions of $\mathbb{Z}_j$ and $\mathbb{D}_j^{1/2}$ cancel each other. Defining $\Phi_{m,T}^j(s) = \widetilde{(\mathcal{T}_j \psi_\lambda)}_m(s)$, with the notations of (4.11), using the expression of $\mathbb{S}_j$ given by (4.4) and the fact that the electrons are injected with a momentum $p$, in the lead $j_0$ and in the transversal mode $m_0$, we have $E(\lambda) = \frac{1}{2}p^2 + E_{m_0}^{j_0}$ and therefore,

$$\int_0^T \langle \mathbb{A}_j^\varepsilon(\psi_\lambda^{pw}),\, \psi_\lambda \rangle_j \, ds = -\delta_{j_0}^j \frac{2ip}{\varepsilon} \int_0^T \theta_\lambda^{j_0}(s)\, \overline{\psi_{m_0}^{j_0}(s)}\, ds = -\delta_{j_0}^j \frac{2ip}{\varepsilon} \mathcal{F}\, \overline{\Phi_{m_0,T}^{j_0}}(p^2/2\varepsilon).$$

Using the following the interpolation estimate, we have

$$\left| \mathcal{F}\, \overline{\Phi_{m_0,t}^{j_0}}(p^2/2\varepsilon) \right| \;\leq\; C \left( \frac{\varepsilon}{p^2} \right)^{1/4} \| \xi^{1/4}\, \mathcal{F}\, \overline{\Phi_{m_0,t}^{j_0}} \|_{L^2(\mathbb{R}^+)} + C \left( \frac{\varepsilon}{p^2} \right)^{1/2} \| \mathcal{F}\, \overline{\Phi_{m_0,t}^{j_0}} \|_{L^2(\mathbb{R})}.$$

The first term on the right above can then be estimated thanks to the operator $\mathbb{D}_j^{1/2}$ and relation (4.9) with $u = \psi_\lambda$ and the second by trace theorems using the fact the interfaces $\Gamma_j$ are flat. Both terms have the correct homogeneity in $\varepsilon$. To obtain estimate (4.13), one then needs to follow the same route to get an $H^1$ bound for $\psi_\lambda$ and to combine it with the $L^2$ estimate.

## 4.4 Perspectives

The derived uniform bounds allow us to perform the semi-classical limit of the system and to recover the classical inflow boundary conditions for kinetic models as in [39] for the stationary case. Whereas the one-dimensional case seems tractable, the case $d \geq 2$ is much more involved since one has to deal with reflecting boundary conditions on $\Gamma_0$ for the Wigner transform, which is known to be a difficult task, see for instance [70, 96].

# Chapter 5

# The moment problem in quantum statistical physics

In this chapter, we address the following inverse problem in quantum statistical physics: does the quantum free energy (von Neumann entropy + kinetic energy) admit a unique minimizer among the density operators having a given local density $n(x)$? We give a positive answer to that question, in dimension one. This enables to define rigourously the notion of local quantum equilibrium, or quantum Maxwellian, which is at the basis of recently derived quantum hydrodynamic models and quantum drift-diffusion models. We also characterize this unique minimizer, which takes the form of a global thermodynamic equilibrium (canonical ensemble) with a quantum chemical potential. This chapter is a summary of the article [1].

## 5.1 Introduction

We deal with a question which is at the core of recently derived quantum hydrodynamic models based on an entropy minimization principle [55, 54]. Let a given density of particles $n(x) \geq 0$, can we find a minimizer of the quantum free energy among the density operators $\varrho$ having $n(x)$ as local density, i.e., satisfying the constraint $\rho(x,x) = n(x)$, where $\rho(x,y)$ denotes the integral kernel of $\varrho$?

This question arises in the moment closure strategy initially introduced by Degond and Ringhofer in [55] in order to derive quantum hydrodynamic models from first principles. Let us briefly review this theory (for more details, one can refer to the review [53]). The quest of macroscopic quantum models is motivated by applications such as nanoelectronics, where affordable numerical simulations of the electronic transport are necessary while the miniaturization of devices now imposes to take into account quantum mechanical effects in the models, resulting in a higher simulation cost. At the microscopic level of description, the Schrödinger equation and the quantum Liouville equation are numerically too expensive, which motivates the derivation of models at a more macroscopic level. In the classical setting, the relationships between microscopic (kinetic) and macroscopic (fluid) levels of description are fairly well understood by means of asymptotic analysis, see for instance [83, 82]. In particular, it is known that the understanding of the structure of the fluid model relies on the properties of the collision operator at the underlying kinetic level. Indeed, collisions are the source of entropy dissipation, which induces the relaxation of the system towards local thermodynamical equilibria. The free parameters of these local equilibria are the moments of the system (e.g. local density, momentum and energy) and are driven by the fluid equations. Arguing that the derivation of precise quantum collision operators is a very difficult task, while only the macroscopic properties of such operators is needed in our context, Degond and Ringhofer have grounded their theory on a notion of quantum local equilibria. To do so, they have generalized Levermore's moment approach [93] to the quantum setting. The idea consists in closing the system of moment equations by defining a local equilibrium as the minimizer of an entropy functional (say, the von Neumann entropy) under moment constraints.

In [54], this approach was adapted so as to describe systems in strong interaction with their surrounding media and obtain quantum macroscopic models by applying a diffusive asymptotics. The most simple of these models, the quantum drift-diffusion model, was studied numerically for instance in [73] and the simulation results for one-dimensional devices such as resonant tunneling diodes were encouraging. This model is based on the most elementary constrained entropy minimization problem. Indeed, in this case, the local quantum equilibrium at a given temperature, also called quantum Maxwellian, is defined as the minimizer of the quantum free energy

subject to a local constraint of prescribed density. Note that not only the total number of particles is fixed, as in the usual quantum statistics theory (for the so-called canonical ensemble), but also the local density $n(x)$ is imposed at any point $x$ of the physical space. This problem has been studied formally in [54] and the Lagrange multipliers theory lead to the existence of a quantum chemical potential $A(x)$ such that the solution of the minimization problem is a density operator of the form

$$\varrho = \exp\left(-\frac{-\Delta + A(x)}{T}\right). \tag{5.1}$$

Remark that the difficulty in this problem lies in the fact that its solution will depend on its data in a global way. The similar problem in classical physics, i.e., reconstructing $f(x,v) = \exp(-(\frac{|v|^2}{2} + A(x)))$ from its density $n(x) = \int f(x,v)dv$, is very simple and the chemical potential, given by $A(x) = -\log n(x) + \frac{3}{2}\log(2\pi)$, depends on $n(x)$ in a local way. Here, due to the operator formalism of quantum mechanics, which is not commutative, the density and the associated chemical potential are linked together by a non-explicit formula, and in a global manner.

Our aim here is to make a first step towards the rigorous justification of quantum hydrodynamics models, by studying the quantum entropy minimization principle in the most simple situation, in the case of a density constraint. We work in dimension one, in a finite box with periodic boundary conditions and show that, in an appropriate functional framework, the quantum Maxwellian is properly defined, i.e., that to any density $n(x) > 0$ corresponds a unique density matrix $\varrho$ minimizing the free energy. Moreover, we prove that $\varrho$ actually takes the form (5.1), where $A(x)$ is the quantum chemical potential. In the sequel, the temperature $T$ will be set to 1.

## 5.2 Notations and main result

The physical space that we consider is monodimensional and bounded. The particles are supposed to be confined in the torus $[0,1]$, i.e., with periodic boundary conditions. We consider the Hamiltonian $H = -\frac{d^2}{dx^2}$ on the space $L^2(0,1)$ of complex-valued functions, equipped with the domain

$$D(H) = \left\{ u \in \mathrm{H}^2(0,1) :\ u(0) = u(1),\ \frac{du}{dx}(0) = \frac{du}{dx}(1) \right\}.$$

The domain of the associated quadratic form is

$$\mathrm{H}^1_{per} = \left\{ u \in \mathrm{H}^1(0,1) :\ u(0) = u(1) \right\}.$$

Its dual space will be denoted $\mathrm{H}^{-1}_{per}$. We shall denote by $\mathcal{J}_1$ the space of trace class operators on $L^2(0,1)$ [103, 108] and by $\mathcal{J}_2$ the space of Hilbert-Schmidt operators

on $L^2(0,1)$. We denote by $\mathcal{K}$ the space of compact operators on $L^2(0,1)$. A density operator is defined as a nonnegative trace class self-adjoint operator on $L^2(0,1)$. Let us define the following space:

$$\mathcal{E} = \left\{ \varrho \in \mathcal{J}_1,\ \varrho = \varrho^* \text{ and } \sqrt{H}|\varrho|\sqrt{H} \in \mathcal{J}_1 \right\}.$$

This is a Banach space endowed with the norm

$$\|\varrho\|_{\mathcal{E}} = \operatorname{Tr}|\varrho| + \operatorname{Tr}(\sqrt{H}|\varrho|\sqrt{H}).$$

For any $\varrho \in \mathcal{E}$, the associated density $n[\varrho]$ is formally defined by

$$n[\varrho](x) = \rho(x,x), \qquad \text{with } \forall \phi \in L^2(0,1), \quad \varrho(\phi)(x) = \int_0^1 \rho(x,y)\phi(y)dy.$$

The density $n[\varrho]$ is in fact defined by the following weak formulation:

$$\forall \Phi \in L^\infty(0,1), \quad \operatorname{Tr}(\Phi\varrho) = \int_0^1 \Phi(x) n[\varrho](x)dx,$$

where, in the left-hand side, $\Phi$ denotes the multiplication operator by $\Phi(x)$, which belongs to $\mathcal{L}(L^2(0,1))$. The energy space will be the following closed convex subspace of $\mathcal{E}$:

$$\mathcal{E}_+ = \{\varrho \in \mathcal{E} :\ \varrho \geq 0\}.$$

On $\mathcal{E}_+$ we define the following free energy:

$$F(\varrho) = \operatorname{Tr}(\varrho\log(\varrho) - \varrho) + \operatorname{Tr}(\sqrt{H}\varrho\sqrt{H}). \tag{5.2}$$

We will see that $F$ is well-defined continuous on $\mathcal{E}_+$. The entropy term is well-defined thanks to the following logarithmic Sobolev inequality for systems, proved in [57] and adapted to bounded domains in [58]: for all $\varrho \in \mathcal{E}_+$ we have

$$\operatorname{Tr}\varrho\log\varrho + \operatorname{Tr}(\sqrt{H}\varrho\sqrt{H}) \geq \int_0^1 n[\varrho]\log n[\varrho]dx + \frac{\log(4\pi)}{2}\operatorname{Tr}\varrho. \tag{5.3}$$

This inequality, coupled to the fact that if $\varrho \in \mathcal{E}_+$, then $\sqrt{n[\varrho]} \in \mathrm{H}^1$, so that $n[\varrho]\log n[\varrho] \in L^1(0,1)$ and $\operatorname{Tr}\varrho\log\varrho$ is bounded for all $\varrho \in \mathcal{E}_+$.

Our main result is stated in the following theorem.

**Theorem 5.2.1** *Consider a density $n \in \mathrm{H}^1_{per}$ such that $n > 0$ on $[0,1]$. Then the following minimization problem with constraint:*

$$\min F(\varrho) \text{ for } \varrho \in \mathcal{E}_+ \text{ such that } n[\varrho] = n,$$

*where $F$ is defined by* (5.2)*, is attained for a unique density operator $\varrho[n]$, which has the following characterization. We have*

$$\varrho[n] = \exp\left(-(H + A)\right), \tag{5.4}$$

*where $A$ belongs to the dual space $\mathrm{H}^{-1}_{per}$ of $\mathrm{H}^{1}_{per}$ and the operator $H + A$ is taken in the sense of quadratic forms.*

The functional space $\mathrm{H}^{-1}_{per}$ for the quantum chemical potential $A(x)$ is optimal, meaning that if $n$ belongs to $\mathrm{H}^1$ but does not belong to any $\mathrm{H}^s$, $s > 1$, then we have $A \in \mathrm{H}^{-1}_{per}$ and $A$ cannot be more regular.

## 5.3 Elements of proof

We state first some basic results on the space $\mathcal{E}_+$ and the entropy functional $F$, see [1] for the proofs:

**Lemma 5.3.1** *Let $(\varrho_k)_{k\in\mathbb{N}}$ be a bounded sequence of $\mathcal{E}_+$. Then, up to an extraction of a subsequence, there exists $\varrho \in \mathcal{E}_+$ such that*

$$\varrho_k \to \varrho \text{ in } \mathcal{J}_1 \quad \text{as } k \to +\infty \tag{5.5}$$

*and*

$$\mathrm{Tr}(\sqrt{H}\varrho\sqrt{H}) \leq \liminf_{k\to+\infty} \mathrm{Tr}(\sqrt{H}\varrho_k\sqrt{H}). \tag{5.6}$$

*Furthermore, if one has*

$$\mathrm{Tr}(\sqrt{H}\varrho\sqrt{H}) = \lim_{k\to+\infty} \mathrm{Tr}(\sqrt{H}\varrho\sqrt{H})$$

*then one can conclude in addition that*

$$\sqrt{H}\sqrt{\varrho_k} \to \sqrt{H}\sqrt{\varrho_k} \text{ in } \mathcal{J}_2 \quad \text{as } k \to +\infty. \tag{5.7}$$

**Lemma 5.3.2** *The application $\varrho \mapsto \mathrm{Tr}(\varrho\log\varrho - \varrho)$ possesses the following properties.*
*(i) There exists a constant $C > 0$ such that, for all $\varrho \in \mathcal{E}_+$, we have*

$$\mathrm{Tr}(\varrho\log\varrho - \varrho) \geq -C\left(\mathrm{Tr}\,\sqrt{H}\varrho\sqrt{H}\right)^{1/2}. \tag{5.8}$$

*(ii) Let $\varrho_k$ be a bounded sequence of $\mathcal{E}_+$ such that $\varrho_k$ converges to $\varrho$ in $\mathcal{J}_1$, then $\varrho_k\log\varrho_k - \varrho_k$ converges to $\varrho\log\varrho - \varrho$ in $\mathcal{J}_1$.*
*(iii) The application $\varrho \mapsto \mathrm{Tr}(\varrho\log\varrho - \varrho)$ is strictly convex on $\mathcal{E}_+$.*

**Existence and uniqueness.** They are given by the following proposition:

**Proposition 5.3.3** *Consider a density $n(x)$ such that $n > 0$ on $[0,1]$ and $n \in \mathrm{H}^1_{per}$. Then the minimization problem with constraint*

$$\min F(\varrho) \text{ for } \varrho \in \mathcal{E}_+ \text{ such that } n[\varrho] = n, \tag{5.9}$$

*where $F$ is defined by* (5.2)*, is attained for a unique density operator $\varrho[n]$.*

The proof is a consequence of the two previous lemmas. We denote

$$\mathcal{A} = \{\varrho \in \mathcal{E}_+ \text{ such that } n[\varrho] = n\}.$$

It can be seen that $\mathcal{A}$ is not empty. Besides, using (5.8), one finds that $F$ is bounded on $\mathcal{A}$ so that one can consider a minimizing sequence $(\varrho_k)_{k\in\mathbb{N}}$ for (5.9), i.e., a sequence $\varrho_k \in \mathcal{A}$ such that $\lim_{k\to+\infty} F(\varrho_k) = \inf_{\sigma\in\mathcal{A}} F(\sigma) > -\infty$. Such a sequence being bounded in $\mathcal{E}_+$, we can extract a subsequence and pass to the limit in the entropy functional and in the constraint using lemma 5.3.1 to obtain the existence of a minimizer. The uniqueness is a consequence of the strict convexity of $F$, see Item *(iii)* of lemma 5.3.2.

**Characterization.** In order to characterize the minimizer $\varrho[n]$ of (5.2.1), we need to write the Euler-Lagrange equation for this minimization problem. This task is difficult because the constraint $n[\varrho] = n$ is not easy to handle when perturbing a density operator. We circumvent this difficulty by defining a new minimization problem with penalization, whose minimizer converges to $\varrho[n]$. Consider a density $n(x)$ such that $n > 0$ on $[0,1]$ and $n \in \mathrm{H}^1_{per}$. For all $\varepsilon \in (0,1]$ we define the penalized free energy functional, for all $\varrho \in \mathcal{E}_+$,

$$F_\varepsilon(\varrho) = \mathrm{Tr}(\varrho\log\varrho - \varrho) + \mathrm{Tr}(\sqrt{H}\varrho\sqrt{H}) + \frac{1}{2\varepsilon}\|n[\varrho] - n\|^2_{L^2},$$

for which we prove it admits a unique minimizer of the form

$$\varrho_\varepsilon[n] = \exp\left(-(H + A_\varepsilon)\right). \tag{5.10}$$

This done is two steps: (i) regularization of the entropy function since it is not clear whether or not $\mathrm{Tr}(\varrho\log\varrho - \varrho)$ is differentiable on $\mathcal{E}_+$ by introducing for all $\eta \in [0,1]$ and $s \in \mathbb{R}_+$,

$$\beta_\eta(s) = (s+\eta)\log(s+\eta) - s - \eta\log\eta,$$

and (ii) by passing to the limit $\eta \to 0$ in the Euler-Lagrange equation defining the corresponding minimizer $\varrho_{\varepsilon,\eta}[n]$. A crucial step for the identification (5.10) is proving that the kernel of $\varrho_\varepsilon[n]$ is reduced to zero. Remains then to send $\varepsilon$ to

zero in (5.10). Showing the convergence of $\varrho_\varepsilon[n]$ to the minimizer of $F$ is fairly straightforward, more difficult is the convergence of $A_\varepsilon$. For this, we use the Euler-Lagrange equation solved by $\varrho_\varepsilon[n]$ to obtain a bound in $\mathrm{H}^{-1}_{per}$ for $A_\varepsilon$ and to prove that $A_\varepsilon$ converge strongly in $\mathrm{H}^{-1}_{per}$ to a chemical potential $A$. This allows to show the convergence of the spectral elements of $H + A_\varepsilon$ to that of $H + A$ and to end the proof of the theorem.

## 5.4 Perspectives

This work can be extended in several directions. A first one would be the generalization of the existence result to higher dimensions, other types of boundary conditions, to the whole-space case, to other types of entropy function, like e.g. Fermi-Dirac entropy, or to Hamiltonians including spin effects. The extension of the characterization seems to be a more difficult problem for such configurations. A second investigation would concern the entropy minimization problem with constraints of higher order moments, as in [89] for the classical case. An other direction is related to the existence of solutions and the long-time behavior for different models based on the local equilibria defined in the chapter: for instance quantum Liouville equations with a BGK-relaxation operator, as for instance in [22], or quantum drift diffusion / quantum energy transport models, see [54, 73].

# Bibliography

## Works presented in the habilitation


[1] F. Méhats and O. Pinaud, *An inverse problem in quantum statistical physics*, 35 pages, accepted in J. of Stat. Phys. (2010).

[2] G. Bal and O. Pinaud, *Imaging using transport models for wave-wave correlations*, 22 pages, accepted in M3AS (2010).

[3] G. Bal and O. Pinaud, *Dynamics of wave scintillation in random media*, 52 pages, to appear in Communications in Partial Differential Equations (2010).

[4] G. Bal and O. Pinaud, *Small volume expansions for elliptic equations*, 36 pages, to appear in Asymptotic Analysis (2010).

[5] G. Bal, I. Langmore, and O. Pinaud, *Single scattering estimates for the scintillation function of waves in random media*, 21 pages, to appear in Journal of Mathematical Physics (2010).

[6] G. Bal and O. Pinaud, *Self-averaging of kinetic models in random media*, Kinetic and Related Models, 1(1) (2008), pp. 85–100.

[7] G. Bal and O. Pinaud, *Kinetic models for imaging in random media*, SIAM Multiscale Model. Simul., 6 (2007), pp. 792–819.

[8] O. Pinaud, *Uniform bounds and weak solutions to an open Schrödinger-Poisson system*, Commun. Math. Sci., 5 (2007), pp. 697–722.

[9] G. Bal and O. Pinaud, *Accuracy of transport models for waves in random media*, Wave Motion, 43(7) (2006), pp. 561–578.

[10] G. Bal and O. Pinaud, *Time-reversal-based detection in random media*, Inverse Problems, 21 (2005), pp. 1593–1619.


Preprints available at http://math.univ-lyon1.fr/~pinaud/

## Other works


[11] N. Ben Abdallah and O. Pinaud, *Multiscale simulation of transport in an open quantum system: Resonances and WKB interpolation*, J. Comp. Physics, 213 (2006), pp. 288–310.

[12] N. Ben Abdallah, F. Méhats, and O. Pinaud, *Adiabatic approximation of the Schrödinger-Poisson system with a partial confining*, SIAM J. Math. Anal., 36 (2005), pp. 986–1013.

[13] N. Ben Abdallah, F. Méhats, and O. Pinaud, *On a open transient Schrödinger-Poisson system*, Math. Meth. Mod. in App. Sci., 15 (2005), pp. 667–688.

[14] O. Pinaud, *Adiabatic approximation of the Schrödinger-Poisson system with a partial confining: the Stationary Case*, J. Math. Phys., 45 (2005), pp. 2029–2048.

[15] O. Pinaud, *Transient simulations of a resonant tunneling diode*, J. App. Phys., 92 (2002), pp. 1987–1994.

[16] N. Ben Abdallah, O. Pinaud, C. Gardner, and C. Ringhofer, *A comparison of resonant tunneling based on Schrödinger's equation and quantum hydrodynamics*, VLSI Design, 15 (2002), pp. 695–700.

[17] N. Ben Abdallah and O. Pinaud, *A mathematical model for the transient evolution of a resonant tunneling diode*, C. R. Math. Acad. Sci. Paris, 334 (2002), pp. 283–288.

[18] E. Dauce, O. Moynot, O. Pinaud, and M. Samuelides, *Mean-field theory and synchronization in random recurrent neural networks*, Neural Processing Letters, 14 (2001), pp. 115–126.

[19] O. Moynot, E. Daucé, and O. Pinaud, *Equations de champ moyen dans les réseaux de neurones à deux populations*, In Cognito, 15 (1999), pp. 41–46.

# Other references

[20] G. Alessandrini, *Singular solutions of elliptic equations and the determination of conductivity by boundary measurements*, J. Differ. Equ., 84 (1990), pp. 252–273.

[21] K. Ammari and H. Kang, *Reconstruction of Small Inhomogeneities from Boundary Measurements*, Lecture Notes in Mathematics, Springer, Berlin, 2004.

[22] A. Arnold, *Self-consistent relaxation-time models in quantum mechanics*, Comm. Partial Differential Equations, 21 (1996), pp. 473–506.

[23] A. Arnold, *Mathematical concept of open quantum boundary conditions*, Transp. Theory. Stat. Phys., 6 (2001), pp. 561–584.

[24] A. Arnold, M. Ehrhardt, and I. M. Sofronov, *Approximation, stability and fast calculations of non-local boundary conditions for the Schrödinger equstion*, Comm. in Math. Sciences, 1 (2003), pp. 501–556.

[25] F. Bailly, J. F. Clouet, and J.-P. Fouque, *Parabolic and gaussian white noise approximation for wave propagation in random media*, SIAM J. Appl. Math, 56(5) (1996), pp. 1445–1470.

[26] G. Bal, *Optical tomography for small volume absorbing inclusions*, Inverse Problems, 19 (2003), pp. 371–386.

[27] ——, *On the self-averaging of wave energy in random media*, SIAM Mult. Mod. Simul., 2(3) (2004), pp. 398–420.

[28] G. Bal, *Homogenization in random media and effective medium theory for high frequency waves*, Discrete Contin. Dyn. Syst. Ser. B, 8 (2007), pp. 473–492 (electronic).

[29] G. Bal, T. Komorowski, and L. Ryzhik, *Self-averaging of Wigner transforms in random media*, Comm. Math. Phys., 242(1-2) (2003), pp. 81–135.

[30] G. Bal, T. Komorowski, and L. Ryzhik, *Asymptotics of the phase of the solutions of the random schrödinger equation*, submitted, (2009).

[31] G. Bal, G. Papanicolaou, and L. Ryzhik, *Radiative transport limit for the random Schrödinger equation*, Nonlinearity, 15 (2002), pp. 513–529.

[32] ——, *Self-averaging in time reversal for the parabolic wave equation*, Stochastics and Dynamics, 4 (2002), pp. 507–531.

[33] G. Bal and K. Ren, *Transport-based imaging in random media*, SIAM Applied Math., 68(6) (2008), pp. 1738–1762.

[34] G. Bal and L. Ryzhik, *Time Reversal and Refocusing in Random Media*, SIAM J. Appl. Math., 63(5) (2003), pp. 1475–1498.

[35] C. Bardos, F. Golse, and N. Mauser, *Weak coupling limit of the $N$-particle Schrödinger equation*, Methods Appl. Anal., 7 (2000), pp. 275–293.

[36] G. Bastard, *Wave mechanics applied to semiconductor heterostructures*, Halsted Press, 1988.

[37] N. Ben Abdallah, *A hybrid kinetic-quantum model for stationary electron transport in a resonant tunneling diode*, J. Stat. Phys., 90 (1998), pp. 627–662.

[38] ——, *On a muldidimensional Schrödinger-Poisson scattering model for semiconductors*, J. Math. Phys., 41 (2000), pp. 4241–4261.

[39] N. Ben Abdallah, P. Degond, and P. A. Markowich, *On a one-dimensional Schrdinger-Poisson scattering model*, ZAMP, 48 (1997), pp. 135–155.

[40] P. Blomgren, G. Papanicolaou, and H. Zhao, *Super-Resolution in Time-Reversal Acoustics*, J. Acoust. Soc. Am., 111(1) (2002), pp. 230–248.

[41] B. Borcea, G. Papanicolaou, and C. Tsogka, *Theory and applications of time reversal and interferometric imaging*, Inverse Problems, 19 (2003), pp. S139–S164.

[42] B. Borcea, G. Papanicolaou, C. Tsogka, and J. Berryman, *Imaging and time reversal in random media*, Inverse Problems, 18 (2002), pp. 1247–1279.

[43] L. Borcea, G. Papanicolaou, and C. Tsogka, *Interferometric array imaging in clutter*, Inverse Problems, 21 (2005), pp. 1419–1460.

[44] Y. Capdeboscq and M. S. Vogelius, *A general representation formula for boundary voltage perturbations caused by internal conductivity inhomogeneities of low volume fraction*, Mathematical Modeling and Numerical Analysis, 37(1) (2003), pp. 159–174.

[45] D. J. Cedio-Fengya, S. Moskow, and M. S. Vogelius, *Identification of conductivity imperfections of small diameter by boundary measurements. Continuous dependence and computational reconstruction*, Inverse Problems, 14 (1998), pp. 553–594.

[46] S. Chandrasekhar, *Radiative Transfer*, Dover Publications, New York, 1960.

[47] T. Chen, *Convergence in higher mean of a random Schrödinger to a linear Boltzmann evolution*, Comm. Math. Phys., 267 (2006), pp. 355–392.

[48] J. F. Claerbout, *Fundamentals of Geophysical Data Processing: With Applications to Petroleum Prospecting*, Blackwell scientific, Palo Alto, 1985.

[49] J. F. Clouet and J.-P. Fouque, *A time-reversal method for an acoustical pulse propagating in randomly layered media*, Wave Motion, 25 (1997), pp. 361–368.

[50] D. A. Dawson and G. C. Papanicolaou, *A random wave process*, Appl. Math. Optim., 12 (1984), pp. 97–114.

[51] P. Degond and A. El Ayyadi, *A coupled Schrödinger drift-diffusion model for quantum semiconductor device simulations*, J. Comp. Phys., 181 (2002), pp. 222–259.

[52] ——, *On quantum hydrodynamic and quantum energy transport models*, Commun. Math. Sci., 5 (2007), pp. 887–908.

[53] P. Degond, S. Gallego, F. Méhats, and C. Ringhofer, *Quantum hydrodynamic and diffusion models derived from the entropy principle*, in Quantum transport, vol. 1946 of Lecture Notes in Math., Springer, Berlin, 2008, pp. 111–168.

[54] P. Degond, F. Méhats, and C. Ringhofer, *Quantum energy-transport and drift-diffusion models*, J. Stat. Phys., 118 (2005), pp. 625–667.

[55] P. Degond and C. Ringhofer, *Quantum moment hydrodynamics and the entropy principle*, J. Statist. Phys., 112 (2003), pp. 587–628.

[56] A. Derode, A. Tourin, J. de Rosny, M. Tanter, S. Yon, and M. Fink, *Taking advantage of multiple scattering to communicate with time reversal antennas*, Phys. Rev. Lett., 90 (2003), p. 014301.

[57] J. Dolbeault, P. Felmer, M. Loss, and E. Paturel, *Lieb-Thirring type inequalities and Gagliardo-Nirenberg inequalities for systems*, J. Funct. Anal., 238 (2006), pp. 193–220.

[58] J. Dolbeault, P. Felmer, and J. Mayorga-Zambrano, *Compactness properties for trace-class operators and applications to quantum mechanics*, Monatshefte für Mathematik, 155 (2008), pp. 43–66.

[59] G. F. Edelmann, T. Akal, W. S. Hodgkiss, S. Kim, W. A. Kuperman, and H. C. Song, *An Initial Demonstration of Underwater Acoustic Communication Using Time Reversal*, IEEE J. Oceanic Eng., 27 (2002), pp. 602–609.

[60] M. Ehrhardt and R. E. Mickens, *Solutions to the Discrete Airy Equation: Application to Parabolic Equation Calculations*, J. Comput. Appl. Math., 172 (2004), pp. 183–206.

[61] B. Engquist and A. Majda, *Absorbing boundary conditions for the numerical simulation of waves*, Math. Comp., 31 (1971), pp. 629–651.

[62] L. Erdös, M. Salmhofer, and H.-T. Yau, *Quantum diffusion of the random Schrödinger evolution in the scaling limit. II. The recollision diagrams*, Comm. Math. Phys., 271 (2007), pp. 1–53.

[63] ——, *Quantum diffusion of the random Schrödinger evolution in the scaling limit*, Acta Math., 200 (2008), pp. 211–277.

[64] L. Erdös and H. T. Yau, *Linear Boltzmann equation as the weak coupling limit of a random Schrödinger Equation*, Comm. Pure Appl. Math., 53(6) (2000), pp. 667–735.

[65] A. C. Fannjiang, *Self-averaging scaling limits for random parabolic waves*, Arch. Ration. Mech. Anal., 175 (2005), pp. 343–387.

[66] ——, *White-noise and geometrical optics limits of Wigner-Moyal equation for wave beams in turbulent media*, Comm. Math. Phys., 254 (2005), pp. 289–322.

[67] ——, *White-noise and geometrical optics limits of Wigner-Moyal equation for beam waves in turbulent media. II. Two-frequency formulation*, J. Stat. Phys., 120 (2005), pp. 543–586.

[68] M. Fink, *Chaos and time-reversed acoustics*, Physica Scripta, 90 (2001), pp. 268–277.

[69] M. Fink and C. Prada, *Acoustic time-reversal mirrors*, Inverse Problems, 17(1) (2001), pp. R1–R38.

[70] E. Fouassier, *High frequency limit of Helmholtz equations: refraction by sharp interfaces*, J. Math. Pures Appl. (9), 87 (2007), pp. 144–192.

[71] J.-P. Fouque, J. Garnier, G. Papanicolaou, and K. Sølna, *Wave propagation and time reversal in randomly layered media*, vol. 56 of Stochastic Modelling and Applied Probability, Springer, New York, 2007.

[72] A. Friedman and M. S. Vogelius, *Identification of small inhomogeneities with of extreme conductivity by boundary measurements: a theorem of continous dependence*, Arch. Rat. Mech. Anal., 105 (1989), pp. 299–326.

[73] S. Gallego and F. Méhats, *Entropic discretization of a quantum drift-diffusion model*, SIAM J. Numer. Anal., 43 (2005), pp. 1828–1849.

[74] J. Garnier, *Imaging in randomly layered media by cross-correlating noisy signals*, Multiscale Model. Simul., 4 (2005), pp. 610–640 (electronic).

[75] J. Garnier and G. Papanicolaou, *Pulse propagation and time reversal in random waveguides*, SIAM J. Appl. Math., 67 (2007), pp. 1718–1739 (electronic).

[76] ———, *Passive sensor imaging using cross correlations of noisy signals in a scattering medium*, SIAM J. Imaging Sci., 2 (2009), pp. 396–437.

[77] J. Garnier and K. Sølna, *Effective transport equations and enhanced backscattering in random waveguides*, SIAM J. Appl. Math., 68 (2008), pp. 1574–1599.

[78] ———, *Random backscattering in the parabolic scaling*, J. Stat. Phys., 131 (2008), pp. 445–486.

[79] ———, *Coupled paraxial wave equations in random media in the white-noise regime*, Ann. Appl. Probab., 19 (2009), pp. 318–346.

[80] P. Gérard, P. A. Markowich, N. J. Mauser, and F. Poupaud, *Homogenization limits and Wigner transforms*, Comm. Pure Appl. Math., 50 (1997), pp. 323–380.

[81] J. Ginibre and G. Velo, *On a class of nonlinear Schrödinger equations with non-local interaction*, Math. Z., 170 (1980), pp. 109–136.

[82] F. Golse, *The Boltzmann equation and its hydrodynamic limits*, in Evolutionary equations. Vol. II, Handb. Differ. Equ., Elsevier/North-Holland, Amsterdam, 2005, pp. 159–301.

[83] F. Golse and L. Saint-Raymond, *Hydrodynamic limits for the Boltzmann equation*, Riv. Mat. Univ. Parma (7), 4** (2005), pp. 1–144.

[84] D. Hansen and M. Vogelius, *High frequency perturbation formulas for the effect of small inhomogeneities*, Preprint, (2006).

[85] D. J. Hansen, C. Poignard, and M. S. Vogelius, *Asymptotically precise norm estimates of scattering from a small circular inhomogeneity*, Appl. Anal., 86 (2007), pp. 433–458.

[86] W. Hodgkiss, H. Song, W. Kuperman, T. Akal, C. Ferla, and D. Jackson, *A long-range and variable focus phase-conjugation experiment in shallow water*, J. Acoust. Soc. Am., 105 (1999), pp. 1597–1604.

[87] V. Isakov, *Inverse Problems for Partial Differential Equations*, Springer Verlag, New York, 1998.

[88] A. Ishimaru, *Wave Propagation and Scattering in Random Media*, New York: Academics, 1978.

[89] M. Junk, *Domain of definition of Levermore's five-moment system*, J. Statist. Phys., 93 (1998), pp. 1143–1167.

[90] W. Kohler and G. C. Papanicolaou, *Power statistics for wave propagation in one dimension and comparison with radiative transport theory*, J. Mathematical Phys., 14 (1973), pp. 1733–1745.

[91] T. Komorowski, S. Peszat, and L. Ryzhik, *Limit of fluctuations of solutions of Wigner equation*, Comm. Math. Phys., 292 (2009), pp. 479–510.

[92] E. W. Larsen and J. B. Keller, *Asymptotic solution of neutron transport problems for small mean free paths*, J. Math. Phys., 15 (1974), pp. 75–81.

[93] C. D. Levermore, *Moment closure hierarchies for kinetic theories*, J. Statist. Phys., 83 (1996), pp. 1021–1065.

[94] P.-L. Lions and T. Paul, *Sur les mesures de Wigner*, Rev. Mat. Iberoamericana, 9 (1993), pp. 553–618.

[95] J. Lukkarinen and H. Spohn, *Kinetic limit for wave propagation in a random medium*, Arch. Ration. Mech. Anal., 183 (2007), pp. 93–162.

[96] L. Miller, *Refraction of high-frequency waves density by sharp interfaces and semiclassical measures at the boundary*, J. Math. Pures Appl. (9), 79 (2000), pp. 227–269.

[97] F. Nier, *Schrödinger-Poisson systems in dimension $d \leq 3$: the whole space case*, Proc. Roy. Soc. Edinburgh Section A, 23 (1993), pp. 489–510.

[98] ——, *The dynamics of some open systems with short-range non-linearity*, Nonlinearity, 11 (1998), pp. 27–72.

[99] G. Papanicolaou, L. Ryzhik, and K. Sølna, *Statistical stability in time reversal*, SIAM J. App. Math., 64(4) (2004), pp. 1133–1155.

[100] G. Papanicolaou, L. Ryzhik, and K. Sølna, *Self-averaging from lateral diversity in the Itô-Schrödinger equation*, Multiscale Mod. and Simulation, 6 (2007), pp. 468–492.

[101] E. Polizzi and N. Ben Abdallah, *Subband decomposition approach for the simulation of quantum electron transport in nanostructures*, J. Comput. Physics, 202 (2004), pp. 150–180.

[102] F. Poupaud and A. Vasseur, *Classical and quantum transport in random media*, J. Math. pures Appl., 6 (2003), pp. 711–748.

[103] M. Reed and B. Simon, *Methods of modern mathematical physics. I. Functional analysis*, Academic Press, Inc., New York, second ed., 1980.

[104] ——, *Methods of modern mathematical physics. IV. Analysis of operators*, Academic Press, Inc., New York, second ed., 1980.

[105] L. Ryzhik, G. Papanicolaou, and J. B. Keller, *Transport equations for elastic and other waves in random media*, Wave Motion, 24 (1996), pp. 327–370.

[106] P. Sheng, *Introduction to Wave Scattering, Localization and Mesoscopic Phenomena*, Academic Press, New York, 1995.

[107] P. J. Shull, *Nondestructive evaluation. Theory, Techniques and Applications*, Marcel Dekker, New York, 2002.

[108] B. Simon, *Trace ideals and their applications*, vol. 120 of Mathematical Surveys and Monographs, American Mathematical Society, Providence, RI, second ed., 2005.

[109] H. Spohn, *Derivation of the transport equation for electrons moving through random impurities*, J. Stat. Phys., 17 (1977), pp. 385–412.

[110] E. Wigner, *On the quantum correction for thermodynamic equilibrium*, Phys. Rev. 40, (1932), pp. 742–749.